ESTIMATED INCREASE IN INUNDATION PROBABILITY WITH CONFIDENCE INTERVALS FOR THE GULF OF MEXICO

A Dissertation

by

NATALYA N. WARNER

MS, I.I.Mechnikov State University of Odessa, Ukraine, 1985

Submitted in Partial Fulfillment of the Requirements for the Degree of

DOCTOR OF PHILOSOPHY

in

COASTAL MARINE SYSTEM SCIENCE

Texas A&M University-Corpus Christi
Corpus Christi, Texas

March 2013

ESTIMATED INCREASE IN INUNDATION PROBABILITY WITH CONFIDENCE INTERVALS FOR THE GULF OF MEXICO

A Dissertation

by

NATALYA N. WARNER

This dissertation meets the standards for scope and quality of Texas A&M University-Corpus Christi and hereby approved.

Dr. Philippe E. Tissot, Chair **Dr. Gary Jeffress, Member**

Dr. Pablo Tarazaga, Member **Dr. Blair Sterba-Boatwright, Member**

Dr. Cherie McCollough, Faculty Graduate Representative

JoAnn Canales, Ph.D.
Interim Dean, College of Graduate Studies

March, 2013

March 2013

ABSTRACT

Estimated Increase in Inundation Probability with Confidence Intervals for the Gulf of Mexico

(March, 2013)

Natalya Warner

M.S., I.I.Mechnikov State University of Odessa, Ukraine

Chair of Advisory Committee: Dr. P. E. Tissot

The main objective of this research is to study the impact of sea level rise on the relative increase in frequency of inundation for the low-lying coastal zones of the Gulf of Mexico caused by storms of different sizes. The research is based on locations around the Gulf of Mexico that benefit from existing long term sea level records and are located near population centers: Galveston Pier 21, Galveston Pleasure Pier, Port Isabel, Rockport, Texas, Grand Isle, La, and Pensacola, Key West, and St Petersburg, Florida stations.

The stations' long-term water level records are divided into a long term sea level trend, a tidal component and a stationary surge component. Several extreme value distributions, such as three and four parameters Burr, Dagum, log-logistic, and generalized extreme value distribution (GEV), are compared using multiple statistical measures for the modeling of maximum annual storm surges. While differences are small the GEV and log logistic distributions are selected for this work based on performance, sensitivity to the series outliers and ease of implementation. Increases in inundation frequencies are computed by combining the stations' respective annual maximum surge

models with two possible sea level rise scenarios, a conservative linear continuation of the past century trend and a scenario based on the upper limit of the sea level range in the IPCC (Intergovernmental Panel on Climate Change) AR4 report (Assessment Report 4), i.e. the A1FI scenario. Differences in oceanographic setting are discussed and affect vulnerability to sea level rise. To compare vulnerability to sea level rise, the ratios of future and present exceedance probabilities are computed for a range of water levels. The locations' respective vulnerabilities to sea level rise are assessed by comparing the maximum ratios of future to present water level exceedance probabilities and the corresponding water levels. Water levels at maximum ratios have a strong correlation with most common moment- and quantile - based statistics of surges, except the maximum annual surges. This indicates that the results of this study are not overly sensitive to the most extreme values or largest surge on the record provided that the record includes at least one large surge.

Statistical bootstrap methods are used to estimate 90% and 95% confidence intervals for increases in inundation probability. For most cases the confidence intervals show a substantial decrease in interval width for stations with lengths of datasets of 50 years or longer indicating a preferred data length provided that a large surge event is included. For all locations the lower bounds of the confidence intervals imply significant increase in exceedance probabilities for both sea level rise scenarios.

While expected increases in inundation frequencies are substantial for all stations, the results show considerable variation depending on the sizes of the surges, the station locations and the sea level rise scenarios. Annual maximum water levels resulting from small storms/surges will have higher frequencies, typically by a factor of 3 or more, than

the historical frequency of water levels resulting from large hurricanes. As a result more frequent, smaller storm surges may have a larger impact on coastal communities than the effects of the less frequent, larger storm surges.

Ratios of the exceedance probabilities depend mostly on sea level trends and the shape of the curves of the exceedance probabilities. The relative importance of these parameters depends on the sea level rise scenario. For a continued linear sea level rise maximum ratios are strongly correlated to the sea level trends or vertical land motion. For the conservative sea level rise scenario the study's highest increase in water level exceedance probability of 17 times is computed for a water level of 1.23m above present mean sea level for Grande Isle, Louisiana. For higher rates of global sea level rise local subsidence becomes less important and the dominant factor becomes the range of the locations' surges. For the study's A1FI based sea level rise scenario, the highest increase in water level exceedance probability is over 100 times for a water level of 0.83m above present mean sea level for Key West, Florida.

The results of this research provide coastal decision makers quantitative estimates of future inundation risks for two sea level rise scenarios and a calibrated method to compute such risks for more sea level rise scenarios. This research is relevant for engineers, planners, insurance executives, and others to take into account the increasing impacts of storm surges of various sizes as sea level rises. The results will help develop better insurance rates, plan structures, land-use zoning, and others as the century progresses. The models, methodology and estimates developed as part of this research may be used to estimate the time before specific locations may become economically uninhabitable due to surge inflicted damages as sea level rises. Particularly, it is expected

that this work will allow better to quantify coastal vulnerability to sea level rise along the Gulf of Mexico.

CONTENTS

PAGE

FIGURES

PAGE

PAGE

PAGE

PAGE

TABLES

PAGE

CHAPTER 1

Storm Flooding Sensitivity to Sea Level Rise for Galveston Bay, Texas

ABSTRACT

The combination of sea level rise and population growth in coastal regions makes it essential to continue improving flood management strategies. Flooding estimates must take into account both local vertical land motion and estimated rates of sea level rise linked to global climate change. Several extreme value distributions are compared using multiple statistical measures for the modeling of maximum annual storm surges based on the 105-year record of Galveston Pier 21, Texas. Increases in inundation frequencies are computed based on two possible sea level rise scenarios, a conservative linear continuation of the past century trend and a scenario based on the upper limit of the sea level range in the IPCC AR4 report, i.e. the A1FI scenario. The research shows that by year 2100 exceedance probabilities may double for the impact of the largest storms such as Hurricane Ike, but may increase by 6-7 times for the smaller surges associated locally with the impact of storms such as Hurricanes Cindy, Alicia and Rita. While individually not as devastating or costly as large hurricanes, the cumulative and regular cost of smaller surge events could well be a bigger threat to coastal communities as sea level rises.

INTRODUCTION

Floods are the most common natural disasters that affect the United States. According to the United States Federal Emergency Management Agency (FEMA) almost 2.03 million properties were affected by floods from January 1978 to November 2012 in the United States with total monetary loss of approximately 42 billion dollars (NFIP, 2013). Floods have two major sources. River floods develop slowly and primarily impact communities in the vicinity of the streams, while floods generated by storm surges happen less frequently, more rapidly, and impact only coastal areas. Storm surge flooding can have a devastating impact on coastal locations, in some cases threatening the overall economic viability of coastal regions. Examples include the human and economic losses caused by recent events such as the Louisiana Flood in 1995, Hurricane Floyd in 1999, tropical storm Allison in 2001, Hurricanes Ivan in 2004, Katrina and Rita in 2005, Ike in 2008, and Irene in 2011.

Significant storms also generate large numbers of insurance claims placing unprepared insurance companies at risk. For example at least 11 insurance companies became insolvent after the passage of Hurricane Andrew in 1992 (Teugels and Sundt, 2004). More recently the landfall of Hurricane Ike in Galveston and other recent storms in Texas prompted the Texas legislature to update the state's windstorm insurance program (Ramsey, 2011). In addition, estimates for the rate of occurrence of storm surges and for the impact of storm surge flooding are important input in the establishment of governmental policies. For example, the policies of the US National Flood Insurance Program are based on the occurrence rate and impact of future floods: "households with

two flood-related claims are now required to be elevated by 2.5 cm above the 100-year flood level, or to relocate" (Bates et al., 2008). It is therefore of great interest to estimate as accurately as possible the rate at which storm surge flood events can be expected to occur and their likely impact (Beirlant et al., 2005).

Sea level rise, whether caused by downward vertical land motion or global sea level rise, will cause storm surge floods to progress further inland, thereby increasing flood damage and reducing the recurrence interval of present 20- or 100-year floods. Recent research results indicate that effects of sea level rise on storm surge impact and occurrence rate estimates may not be adequately accounted for. Research by Purvis et al. (2008) examined the probability of future coastal flooding in the United Kingdom, given the uncertainty over possible sea level rise. They concluded that focusing only on most the plausible sea level rise may significantly underestimate monetary losses as it fails to account for the impact of low probability, high consequence events. Another study by Frazier et al. (2010) concludes that the impact of storm surges in Sarasota County, Florida, caused by small hurricanes will increase due to sea level rise.

A number of studies have been conducted to model flood resulting from river flooding and storm surges using a variety of extreme value distributions. The generalized extreme value (GEV) distribution is recommended by FEMA (FEMA, 2007) and is the most widely used distribution in the field (Kotz and Nadarajah, 2000; Nadarajah and Shiau, 2005; ÖnÖz and Bayazit, 1995). However Huang et al. (2008) suggested caution when applying the GEV after studying its application to locations along the East and Southeast Atlantic coast of the US and the Gulf of Mexico. Substantial differences between model and measurements were observed when comparing 100-year annual

maximum water levels with historical data for these locations. While the modeled return periods exhibited less than 5% difference with observed data for locations along the Pacific and North East Coastal areas, a difference of over 21% was computed for Galveston Pier 21, Texas. Letetrel et al. (2010) used the generalized Pareto distribution to analyze the return periods of the sea level extremes in Marseille, France. Other distributions that have been used by prior researchers include the logistic and the log-logistic distribution (Ahmad et al., 1988; Rao and Hamed, 2000).

Ahmad et al. (1988) compared the log-logistic, GEV, three parameter log-normal and three parameter Pearson distributions. Datasets for their study were obtained for sites in Scotland with annual flood series varying in length from 5 to 66 years. The authors recommended "that the ideal distribution for flood frequency analysis should (a) reproduce at least as much variability in flood characteristics as observed in the empirical data sets; (b) be insensitive to extreme outliers especially in the upper tail; (c) must have a distribution function and an inverse distribution function that can be explicitly expressed in closed form; and (d) must not be computationally complex nor involve the estimation of a large number of parameters". For their study, the log-logistic distribution satisfied the above requirements better than other evaluated distributions. The goal of this study was to (1) identify the best performing distribution(s) for modeling extreme surges along the northern part of the Gulf of Mexico and (2) use the identified distribution to determine sensitivity of storm surge impact to sea level rise estimates. To this end, the study first compares performance of several distributions for the modeling of extreme surges at the US National Ocean Service station of Galveston Pier 21, Texas. This station was chosen because it has the longest water level record in the Gulf of Mexico starting in

1904 and because it is located in the economically important greater Houston area. The distribution that best models this data is then used to model future impact of storm surges for a broad range of storm sizes and for two distinct sea level rise scenarios.

DATA AND METHODS

Study site and data

The study site, the station of Galveston Pier 21 (Latitude 29° 18.6' N, Longitude 94° 47.6' W), is part of the US National Water Level Observation Network and is located on the north-east side of Galveston Island, Texas (Figure 1.1).

Figure 1.1. ***Map of the study area, the entrance of Galveston Bay, Texas.***

The station is positioned on a ship channel about 4 km away from the main Galveston Ship Channel and the mouth of Galveston Bay. The station's records are available starting in January 1904 and include water levels measured hourly with only a few interruptions. This high quality 105 year time series is well suited for the comparison

of statistical distributions of extreme events, and has been used for prior similar studies (Huang et al., 2008; Turner, 1991).

The 105 years of verified hourly water levels were obtained from NOAA's Tides and Currents data repository (NOAA, 2011a), and were further processed as follows. Monthly maximum water levels were obtained from the same site and compared to the maxima identified in the hourly time series. Most differences were within a range of 0.31 m, the station's Mean Range of Tide (NOAA, 2011b). Substantial differences of 0.45 m and 1.22 m were found for Hurricane #6 of August 1909 and Hurricane #2 of September 1919. For these two storms NOAA maximum water level records are based on water marks such as marks on buildings. The monthly tide gauge records during these two storms are different likely because of unidentified equipment malfunction during these storms (personal communications with Chris Zervas, NOAA CO-OPS). As the hourly water levels are inconsistent with building marks and the damage caused by the storms, the maximum water levels taken from building marks were retained for this study, i.e. 2.07 m for September 1919 and 0.39 m for August 1909. The mean sea level trend of 6.39 mm/year (NOAA, 2011c) was removed from the hourly time series with the zero mean sea levels set for year 1999 to match tidal predictions (NOAA, 2011d). The harmonically predicted water levels were also obtained from (NOAA, 2011a). They were subtracted from water level series to remove tidal variability and to compute surges. The tidal component for the two cases described above (August 1909 & September 1919) was not removed as the timing of the maximum water levels could not be reliably identified. Overall missing data accounted for 2.35% of the hourly time series. Two gaps represented a significant portion of the missing data: 178 days from March through

October 1984 and 120 days from February through May 1916. Neither of these periods was affected by significant storms. For months that did not include any data, data was imputed by the means of the maximum surges for the corresponding months. The maximum annual surges were then identified using the imputed data. The timing of the missing data did not coincide with hurricanes or tropical storms impacting the Texas coast with two exceptions, the category 4 Hurricane #2 of August 1915 and the category 1 Hurricane #1 of July 1943. Reliable water level data was not found for these two events. The extreme event distribution sensitivity to the absence of these two events will be addressed in a later section by computing the variability in the distribution parameters for a range of likely surges.

The resulting surge time series is presented in Figure 1.2a and compared to the water level maxima time series (Figure 1.2b) where the sea level rise is clearly discernable. The surge time series is the basis for the statistical analysis of this research.

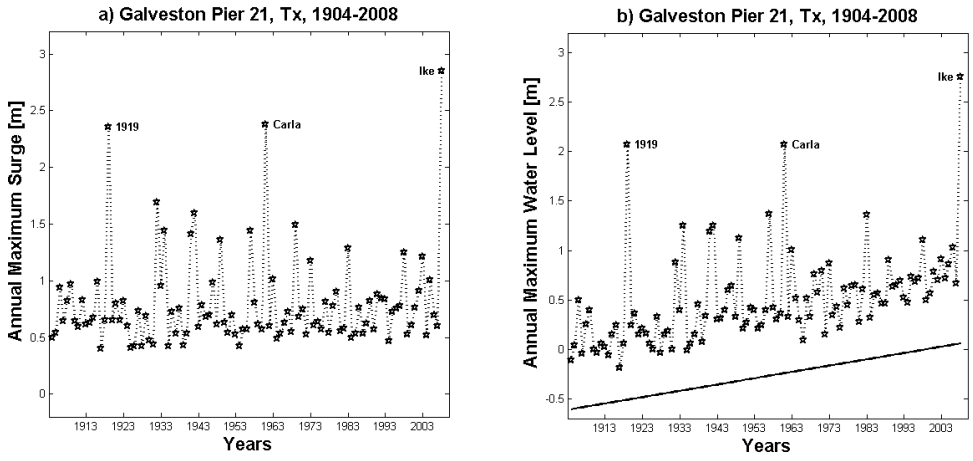

Figure 1.2. ***(a) Annual maximum surge time series (b) Annual maximum water level time series.***

Extreme Value Statistical Distributions

The extreme value distributions selected for this study included the GEV recommended by (FEMA, 2007), the log-logistic recommended by (Ahmad et al., 1988), the Dagum, and the three and four-parameter Burr models recommended by (Kleiber and Kotz, 2003; Reiss and Thomas, 2007). While results are presented for these distributions, a number of other distributions available within the EasyFit Professional Software (EasyFit, 2004-2010) were compared, including the Pearson, Wakeby, lognormal, Pareto, and other distributions. The selected distributions were both among the best performing based on the statistics below and were previously used to model riverine floods or storm surges.

EasyFit was used to fit all models for this study. EasyFit uses maximum likelihood estimation of model parameters.

Two goodness-of-fit tests were used to evaluate the suitability of the five selected probability distributions: the Kolmogorov-Smirnov (KS) and the Anderson-Darling (AD) tests. The statistic *Dn* of the KS test computes the maximum absolute value of the difference between the empirical and theoretical cumulative distribution functions over the relevant range of inputs. A smaller value of this statistic implies a better fit between the distributions (Rao and Hamed, 2000):

$$D_n = \max_x |F_n(x) - F(x)| \quad (1)$$

One of the AD tests is the *An* statistic. It is defined as the integral of the squared difference between the empirical and theoretical distribution functions multiplied by a weight function that emphasizes discrepancies in the tails. It is considered one of the

most powerful tests for this type of distribution and can provide better discrimination between distributions and particularly their ability to model extreme events (ÖnÖz and Bayazit, 1995; Sinclair et al., 1990):

$$A_n^2 = n\int_{-\infty}^{\infty} \frac{(F_n(x) - F(x))^2}{F(x)[1-F(x)]}\, dF, \tag{2}$$

In the above expression n is the sample size, $F_n(x)$ is the empirical cumulative distribution function and $F(x)$ is the theoretical cumulative distribution function. Sinclair et al. (1990) proposed a modified form of this test to emphasize the difference between the empirical distribution and theoretical distribution in one specific tail. One of the modifications of the test presented in their work, the AU_n statistic, gives a larger weight to the upper tail and is therefore well suited for our flood frequency analysis as the largest events have the biggest impact:

$$AU_n^2 = n\int_{-\infty}^{\infty} \frac{(F_n(x) - F(x))^2}{[1-F(x)]}\, dF \tag{3}$$

The following equivalent expression obtained after integration and simplification (Sinclair et al., (1990) was used for the AU_n statistic:

$$AU_n^2 = \frac{n}{2} - 2\sum_{j=1}^{n} F(x(j)) - \sum_{j=1}^{n} [2 - \frac{(2j-1)}{n}] \log[1 - F(x(j))] \tag{4}$$

Again, a smaller value of this statistic implies a better fit between the distributions.

Rates of the sea level rise

Various studies (Bindoff et al., 2007; Domingues et al., 2008; Edwards, 2007; Gregory, 2008; Vermeer and Rahmstorf, 2009) indicate a large uncertainty in projections of the sea level rise by the end of the century. The difficulties in accurate estimation of sea level rise are due to uncertainty related to future changes in global atmospheric temperatures and still ongoing research on all possible contributions of melting ice sheets from Greenland and Antarctica (Gregory, 2008; Hansen, 2007; Meehl et al., 2007; Shum et al., 2008). For example the latest IPCC Fourth Assessment Report (AR4) (Meehl et al., 2007) projections do not include likely acceleration of future glacial contributions (Shum et al., 2008). While the higher end of the IPCC AR4 sea level rise estimates are used for this work, substantially higher sea level rise predictions can be found in recent work, e.g. in (Vermeer and Rahmstorf, 2009). Note that for the Gulf of Mexico only small regional deviations due to ocean density and circulation change relative to the global average sea level rise have been observed or predicted (Meehl et al., 2007) and such potential regional variability is not considered in this work.

For the purpose of this study, two sea level rise scenarios were selected:

- A very conservative continued linear sea level rise of 6.39 mm/year, based on the 20th century trend for Galveston Pier 21 station (NOAA, 2011c), resulting in a 0.65 m increase in sea level by year 2100 as compared to 1999 mean sea level;
- A quadratic sea level rise rate, resulting in a total 1.08 m increase in sea level by year 2100 as compared to 1999 mean sea level. For this second scenario the local vertical land motion of 4.69 mm/year was estimated by comparing last

century's local sea level rise rate (6.39 mm/year) with a global sea level rise rate of 1.7 mm/year (Bindoff et al., 2007). A quadratic sea level rise rate was then added to the vertical land motion rate to bridge the years between the last water level measurements and the global increase in sea levels as estimated for the A1FI 2090-2099 upper bound level (Meehl et al., 2007).

Analysis of the surge distribution for Galveston Pier 21

Water levels are driven by high frequency forcing, tidal and meteorological, and by longer term factors such as local subsidence and global sea level rise (CCSP, 2009). For the study location these events are driven by meteorological forcing such as tropical and extra tropical storms with possible impact from precipitation and riverine input. While recent studies (Bender et al., 2010) suggest that climate change will modify both the overall frequency of tropical storms and the intensity distribution of storms in the Atlantic basin, records of past storm activity including recent events are yet to indicate any significant trend for the Atlantic Basin (Landsea, 2007) and Gulf of Mexico in particular (Levinson et al., 2010). Also, storm surge is not well correlated with the intensity of tropical storms. Estimates of changes in other storm characteristics such as size (Irish et al., 2008) and forward speed (Rego and Li, 2009) would have to be combined with possible changes in storm frequency to attempt estimates of changes in future storm surges. The meteorological forces driving storm surges, including the frequency and life cycle of tropical storms as well as the distribution of storm characteristics, are assumed stationary throughout the study period. To assess the validity of this assumption the parameters of each of the selected distributions were computed for

a succession of 15 periods each 7 years long using the EasyFit Professional Software (EasyFit, 2004-2010). Monthly surge maxima rather than annual maxima were used for this test. While switching to monthly maxima increases the relative importance of smaller events the size of the data set is increased by an order of magnitude allowing for a more statistically robust assessment. The results of this fit are presented in results section for the case of the log-logistic distribution.

RESULTS

Stationarity of the surge distribution for station Galveston Pier 21, Texas

The stationarity of the surge time series was verified based on the monthly water level time series as described in section 2.4. The parameters of the log-logistic distributions fitted for each of the 15 periods are presented in Figure 1.3. The absence of significant trends supports the assumption of the stationarity of the surge distribution for the past century. For the past 105 years the only substantial difference in parameters is found for the 4^{th} period (1925-1931). This discrepancy can be explained by the smallest mean of the surge levels and the absence of hurricanes during that period. The results of this stationarity test were equivalent for the other distributions. The lack of trend for the distributions parameters also addresses the potential importance of increased mean water levels at the study location. Higher water levels in shallow bays should eventually lead to larger storm induced surges in the bays. The absence of impact from the mean sea level rise of 0.67 m from 1904 to 2008 is likely due in part to the proximity of the Pier 21 station to the Gulf of Mexico. The station is located on a ship channel about four kilometers away from the main Galveston ship channel and near the mouth of Galveston Bay, a location for which sea level rise relative to water depth is much smaller than for the inland side or back bay of Galveston Bay.

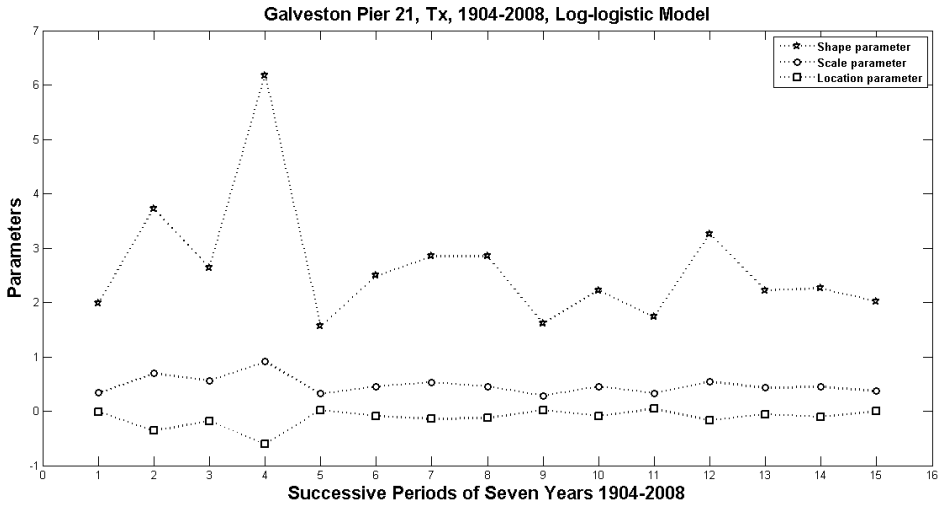

Figure 1.3. ***Log-logistic distribution parameters computed on a series of monthly maxima (shape parameter is divided by 2).***

Comparison of five extreme value distributions

The parameters for the five selected extreme value distributions were estimated and their cumulative distribution functions (CDF) compared against the empirical distribution using the 105 years maximum surge time series. The fitted values of the parameters for each distribution are presented in Table 1.1. Their goodness of fit as estimated by the KS statistic and the AD statistics with weights on both tails as well as the upper and lower tails alone are presented in Table 1.2. Comparisons of models using the same statistic are valid, but comparisons between two different statistics are not.

	Shape	Shape	Scale	Location
Four-parameter Burr	1.26	1.92	0.34	0.38
Dagum	0.59	2.35	0.39	0.39
Three-parameter Burr	0.27	10.19	0.52	
GEV	0.35		0.17	0.60
Log-logistic	2.19		0.30	0.37

Table 1.1. ***Parameters for each of the 5 selected distributions.***

	Three-parameter Burr	Log-logistic	GEV	Four-parameter Burr	Dagum
KS statistic	0.041	0.057	0.059	0.064	0.073
AD Upper statistic	0.081	0.107	0.120	0.133	0.161
AD Normal statistic	0.212	0.316	0.338	0.377	0.442

Table 1.2. ***Statistics of the KS test, AD test and modified AD test for upper tail and lower tail.***

Comparing the results in Table 1.2, the three-parameter Burr distribution has the lowest statistics, i.e. the best performance for all measures, followed by the log-logistic, the GEV, the four-parameter Burr, and Dagum distributions. The performance of the respective distributions is further evaluated graphically in Figure 1.4 for the KS statistics, i.e. the absolute differences between the empirical and theoretical CDFs for surges above 0.7 m. The largest discrepancy for this range of surge is observed around 0.85 m surges with differences in exceedance probabilities ranging from just below 0.03 for the three-parameter Burr to just below 0.04 for the four-parameter Burr distribution. For surges above 0.9 m the three-parameter Burr and log-logistic distributions perform slightly better than the other distributions.

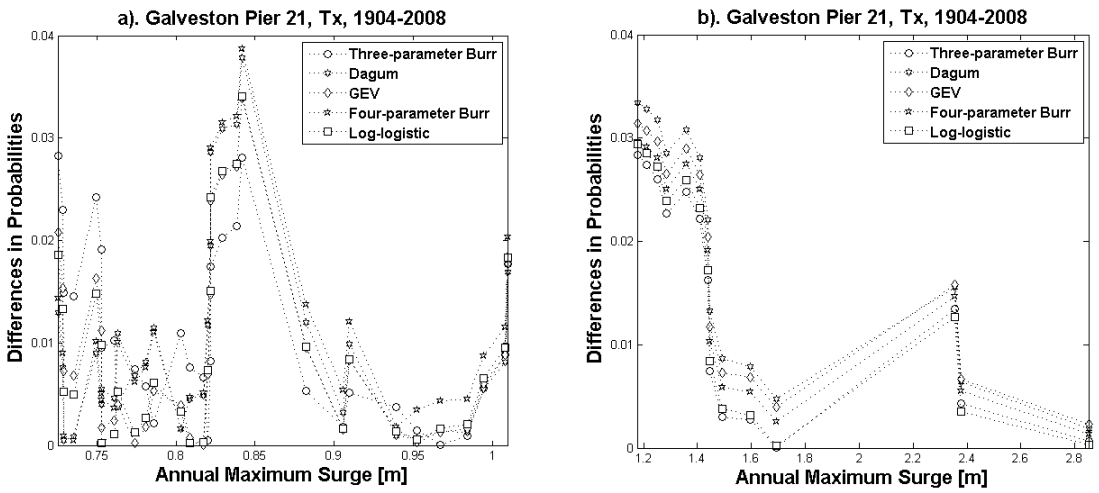

Figure 1.4. ***Differences between the modeled and empirical CDFs as functions of surge for (a) 0.73-1.01 m surges and (b) 1.18-2.85 m surges.***

To further compare the distributions, the related return periods are computed for surges of increasing size and the results compared to the return periods computed directly from the observed data, similar to the method used by Huang et al. (2008). The results are illustrated in Figure 1.5. The observational return periods are computed by tallying the number of events up to a given surge without any smoothing contributing to the higher variability for long return period events. The difference between empirical and estimated return periods for the largest event in the data set, the surge generated by 2008 Hurricane Ike, are 1.2% for the log-logistic distribution, 2.5% for the three-parameter Burr, 5.4% for the four-parameter Burr, 7.6% for the Dagum Model, and 9.0% for GEV model

.

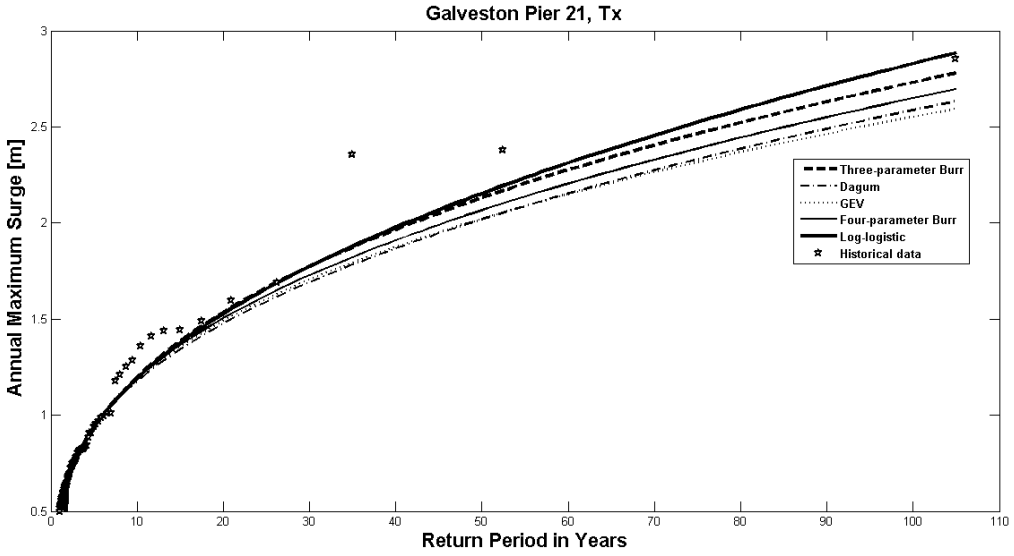

Figure 1.5. ***Comparison of estimated return periods computed based on the observed data.***

To test the robustness of the respective models the parameters of the distributions were recomputed for the first 104 years of the time series, omitting the 2008 surge generated by Ike (resulting parameters are not shown in this publication). Return periods of 128, 146, 201, 176, and 212 years are obtained for the log-logistic, three-parameter Burr, four-parameter Burr, Dagum and GEV distributions respectively. The return period of 128 years estimated by the log-logistic distribution shows the best agreement with the 105 year return period from the historical time series.

An additional criterion for the selection of a distribution is its robustness to missing or potentially erroneous data. To estimate the sensitivity of the distributions to changes in the surges of large storms, the parameters of the distributions were recomputed for 15 alternate cases and compared to the original results. To create realistic alternate cases maximum water levels were replaced for one or more of the records for years 1909, 1915,

1919 and 1943. These four years were selected because their annual maxima were either based on building marks rather than water level measurements (1909 and 1919) or measurements during a hurricane were missing (1915 and 1943). For 1909 the second largest water level of 0.85 m was selected as an alternate value to 0.97 m. For year 1919 the alternate value of 1.13 m was computed based on the historical hourly records instead of using the more realistic NOS monthly records and replaces 0.67m. For years 1915 and 1943 the timing of the missing data coincides with the passage of major hurricanes, the category 4 Hurricane #2 of August 1915 and the category 1 Hurricane #1 of July 1943. For these years imputed data was used in the base line data set as described in section 2.1. Alternate values for these two years were selected by computing the means of the surges for category 1 Hurricanes, 1.12 m, and for category 4 hurricanes, 1.78 m. These two water levels were used as alternate values for 2.35 m and 0.59 m in the baseline dataset.

Thus, the 15 alternate time series correspond to the 15 different ways of selecting one or more of the four alternate surges. For each distribution fitted to these alternate time series, exceedance probabilities were computed. The standard deviations of the 15 exceedance probabilities are compared graphically in Figure 1.6. A lower standard deviation indicates a lower sensitivity to changes in single event values and is viewed as a positive characteristic of the distribution. For all distributions maximum sensitivity to changes in the data set is reached for surges just below 1 m. For maximum annual storm surges below 1.1 m the three-parameter Burr distribution shows the lowest standard deviation while for surges larger than 1 m the GEV shows the lowest standard deviation.

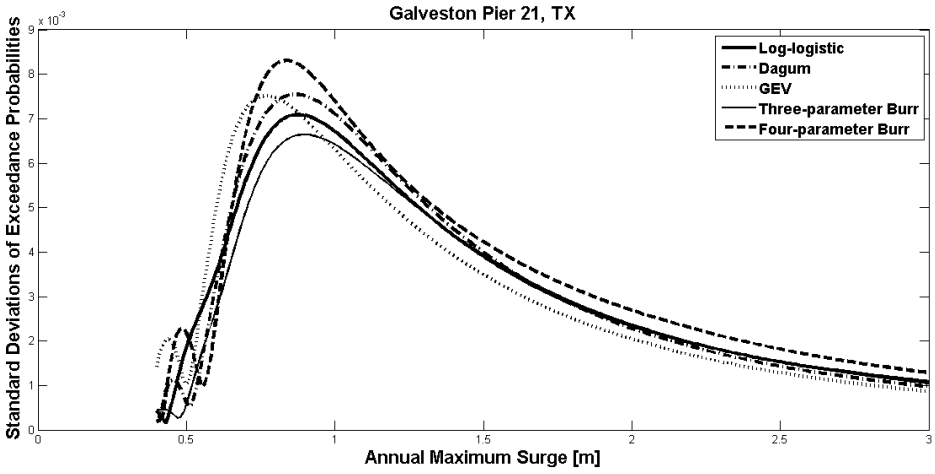

Figure 1.6. ***Standard deviations of the exceedance probabilities of increasing surge levels when considering 16 cases to estimate the parameters of each model.***

In Table 1.3 the performance of the respective distributions is evaluated by comparing modeled and observed surge exceedance probabilities for a wide range of significant events with surges above 0.9 m that impacted Galveston. All the distributions show a good agreement for surges up to one meter. For the larger surges representing 10% or less of the record, a detailed comparison becomes more difficult due to the small number of large storms on record. In particular no events producing annual maximum surges between 1.69 m (1932 Hurricane #2) and 2.35 m (1919 Hurricane #2) have been recorded resulting in a step in the historical surge distribution. The five selected distributions have CDFs below the historical distribution for 1.2 m to 1.4 m surges, then above the empirical distribution for surges between 1.6 m and 2.2 m. Agreement is good for the largest surges but the empirical distribution is based on only three storms for surges above 2 m: 2.35 m for 1919 Hurricane #2, 2.38 m for 1961 Hurricane Carla and

2.85 m for 2008 Hurricane Ike. Overall the performance of the selected distributions for estimating return periods is quite similar with the largest discrepancies driven by the characteristics of the data set rather than by the features of the distributions.

Hurricane or Tropical Storm	Year	Corresponding Water Level [m]	Annual Max Surge [m]	CDF of Historical Data	Three-parameter Burr Model	Log-logistic Model	GEV Model	Four-parameter Burr Model	Dagum Model
Hurricane Allen	1980	0.65	0.91	0.78	0.78	0.78	0.78	0.78	0.78
Hurricane #5, 1933	1933	0.09	0.95	0.81	0.81	0.81	0.81	0.81	0.81
Hurricane #6, 1909	1909	0.39	0.97	0.82	0.82	0.82	0.82	0.81	0.82
Hurricane #3, 1947	1947	0.42	0.98	0.83	0.83	0.83	0.83	0.82	0.83
Hurricane #6, 1916	1916	0.24	0.99	0.84	0.83	0.83	0.83	0.83	0.83
Hurricane Rita	2005	0.86	1.01	0.85	0.84	0.84	0.84	0.84	0.84
TS Delia	1973	0.87	1.18	0.87	0.90	0.90	0.90	0.90	0.90
Hurricane Claudette	2003	0.91	1.21	0.88	0.90	0.90	0.91	0.91	0.91
TS Frances	1998	1.11	1.25	0.89	0.91	0.91	0.92	0.91	0.92
Hurricane Alicia	1983	1.36	1.28	0.90	0.92	0.92	0.92	0.92	0.92
Hurricane #10, 1949	1949	1.13	1.36	0.90	0.93	0.93	0.93	0.93	0.94
Hurricane #2, 1941	1941	1.19	1.41	0.91	0.94	0.94	0.94	0.94	0.94
Hurricane Audrey	1957	1.37	1.44	0.92	0.94	0.94	0.94	0.94	0.95
Hurricane #2, 1942	1942	1.25	1.59	0.95	0.96	0.96	0.96	0.96	0.96
Hurricane #2, 1932	1932	0.88	1.69	0.96	0.96	0.96	0.97	0.96	0.97
Hurricane #2, 1919	1919	2.07	2.35	0.97	0.98	0.98	0.99	0.99	0.99
Hurricane Carla	1961	2.07	2.38	0.98	0.99	0.98	0.99	0.99	0.99
Hurricane Ike	2008	2.76	2.85	0.99	0.99	0.99	0.99	0.99	0.99

Table 1.3. ***Comparison of modeled and observed surge exceedance probabilities listed in order of increasing maximum surge.***

Overall the small differences in performance between the five selected distributions do not lead to the outright exclusion of one or more of the distributions as a realistic description of the surge maxima. For the larger surges the performance of the log-logistic distribution is better than the other three distributions based on the AD test focused on the upper end of the distribution and the best for surges above 1.6 m based on the differences in CDF. While the three-parameter Burr had the best performance by some measures, we

chose not to use it, because its performance was better for the lower surge events. Also, it is missing a location parameter that could make it more difficult to apply to other locations. When considering the robustness of the distributions the GEV distribution has the best performance for the larger surges although the differences are small. Because of the above results, the comparison of the KS and AD statistics, and for its ability to better model the return period of the large events, including the largest event in the data set, Hurricane Ike, the log-logistic distribution was selected for the rest of this study. The equation and parameters of the log-logistic CDF for this study are listed below following the convention by Kleiber and Kotz (2003):

$$F(x) = (1 + (\frac{x-\gamma}{\beta})^{-\alpha})^{-1}, \ \ where\ x > \gamma, \alpha > 0, \beta > 0,$$
$$\alpha = 2.1893, \beta = 0.30158, \gamma = 0.36905 \qquad (5)$$

Impact of sea level rise by 2100 for Galveston Pier 21, Texas

We use the fitted log-logistic maximum annual surge distribution to project inundation exceedance probabilities for future years while considering the two sea level rise scenarios described in section 2.3. Exceedance probabilities are computed for both scenarios and compared in Figure 1.7 for years 2025, 2050, 2075 and 2100. While all exceedance probabilities are rising, as expected, the changes are considerably more pronounced for small surge events. As an example, the sea level rise impact on the frequency of 1 meter water level maximum, the local impact of 2005 Hurricane Rita, is considered. For the second sea level rise scenario the annual frequency of this event will increase from presently about 16% to 26% in 2025 and 62% in 2050. After year 2070 this

type of event is predicted to take place every year. Even for the more conservative scenario, 1 meter water level maximum surges are expected annually by year 2100.

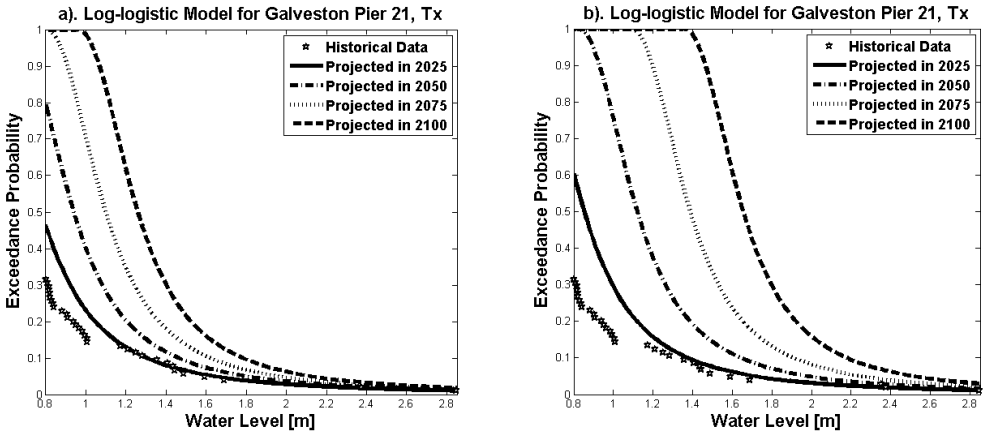

Figure 1.7. ***Comparison of the projected water level exceedance probabilities for present water levels and including impact of two sea level rise scenarios (a) local sea level rise of 6.39 mm/year (b) a quadratic increase of the rate of sea level rise rate based on IPCC AR4 scenario A1FI.***

The change of water level exceedance probability is further compared in Figure 1.8 for the local impact of four storms: 2005 Rita (1.01 m surge), 1983 Alicia (1.28 m surge), 1957 Audrey (1.44 m surge) and 1942 Hurricane #2 (1.59 m surge). The frequency of the maximum annual water levels generated by Rita (1.01 m surge) increases much faster than that of the larger storms from 16% in 2008 to annually by 2100, more than a six fold increase, while for the 1.59 m surge case the frequency rises from about 4.5% to about 16%, more than a threefold increase. The faster rate of sea level rise of scenario 2 leads to substantially larger increases in water level exceedance frequency (Figure 1.8b). For example, while for the 6.39 mm/year sea level rise case the exceedance probability of a

surge of the size generated by1983 Alicia is predicted to be 45% in 2100, such an event is projected to take place annually for the faster rate of sea level rise case.

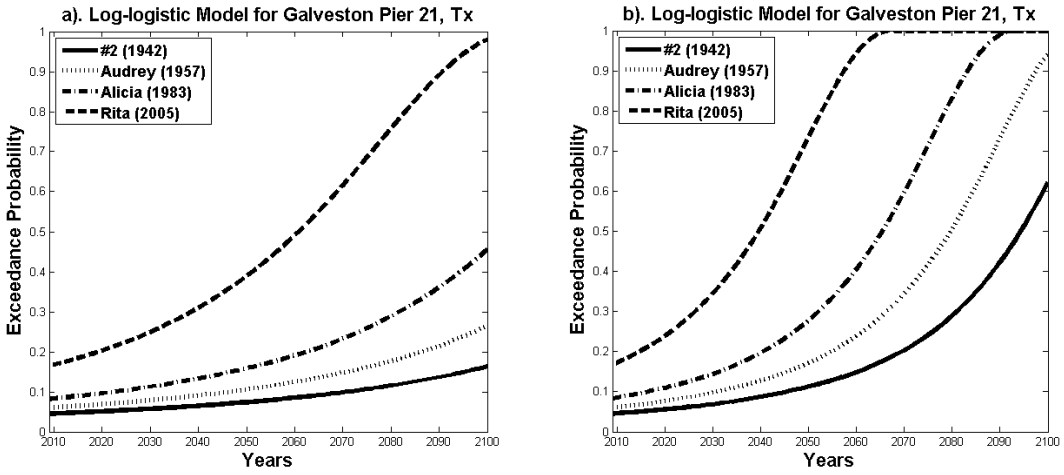

Figure 1.8. ***Comparison of the increase in water level exceedance probabilities over the coming years for two sea level rise scenarios (a) local sea level rise of 6.39 mm/year (b) a quadratic increase of the rate based on IPCC AR4 scenario A1FI.***

Figure 1.9 displays the ratio of the water level exceedance probability in 2100 versus the present exceedance probability in 2009 for the conservative scenario. For relatively small events around 1 m, the ratio increases very rapidly due to the shape of the surge probability distribution. For events leading to smaller maximum water levels the increase is limited by a rapid rise to a 100% probability, i.e. the events are predicted to take place every year. The largest proportional increase is computed for a 1.1 m water level, which is predicted to occur 6.5 times as often in 2100. For events leading to larger surges, the relative exceedance probability ratio decreases progressively to about a factor 1.85 for the maximum water levels generated by 2008 Hurricane Ike. While a 1.85 times increase for such a large event is important given the damage caused by Ike (Report,

2008), this relative increase is considerably smaller than the 6.5 time increase for events generating a 1.1 m water level. This much larger projected increase in the frequency of the small to medium inundation events must be accounted for when projecting damage costs and insurance rates.

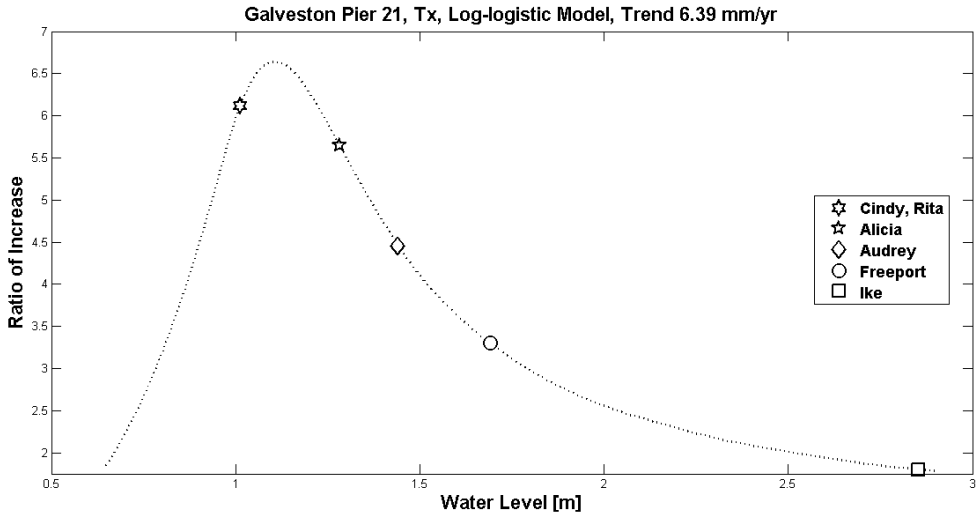

Figure 1.9. ***Ratios of increase of projected exceedance probabilities in 2100 and 2008 for all water levels.***

Finally, projected changes in return periods are computed up to year 2100 for a variety of storms that have impacted Galveston and for both scenarios. The results are presented in Table 4. Return periods directly based on observations are listed under year 2008 while results for 2025, 2050 and 2100 are model based estimates. Differences in methodologies (more variability from the observational method) lead to the smaller estimated return periods for 2008 than for the 2025 and 2050 model estimates for two of the three largest surge events and for surges around 1.25m. For the faster sea level rise

scenario, the maximum surge expected every year in Galveston is greater than the surge of all but four hurricanes from the historical record, while the return period of an event of the magnitude of Hurricane Ike is predicted to decrease to 29 years from presently 105 years.

Hurricane or Tropical Storm	Year	Month	Corresponding Water Level [m]	Annual Max Surge [m]		Return Period (in years), Log-logistic Model							
						Trend 6.39 mm/yr				Quadratic Increase of Rate of SLR			
					in2008	in 2025	in 2050	in 2075	in 2100	in 2025	in 2050	in 2075	in 2100
Hurricane Allen	1980	8	0.65	0.91	4.6	3.2	1.8	1.1	1.0	2.2	1.1	1.0	1.0
TS Fay	2002	9	0.70	0.91	4.8	3.2	1.8	1.1	1.0	2.2	1.1	1.0	1.0
	1906	10	0.50	0.94	5.0	3.5	2.0	1.2	1.0	2.5	1.1	1.0	1.0
Hurricane #5, 1933	1933	8	0.09	0.95	5.3	3.7	2.1	1.2	1.0	2.6	1.2	1.0	1.0
Hurricane #6, 1909	1909	8	0.39	0.97	5.5	3.9	2.2	1.3	1.0	2.7	1.2	1.0	1.0
Hurricane #3, 1947	1947	8	0.42	0.98	5.8	4.1	2.4	1.4	1.0	2.9	1.3	1.0	1.0
Hurricane #6, 1916	1916	8	0.24	0.99	6.2	4.3	2.4	1.4	1.0	3.0	1.3	1.0	1.0
Hurricane Rita	2005	9	0.86	1.01	6.6	4.5	2.6	1.5	1.0	3.1	1.3	1.0	1.0
Hurricane Cindy	1963	9	1.00	1.01	7.0	4.5	2.6	1.5	1.0	3.2	1.4	1.0	1.0
TS Delia	1973	9	0.87	1.18	7.5	7.3	4.6	2.6	1.5	5.4	2.4	1.0	1.0
Hurricane Claudette	2003	7	0.91	1.21	8.1	8.0	5.1	3.0	1.7	6.0	2.8	1.1	1.0
TS Frances	1998	9	1.11	1.25	8.8	8.9	5.7	3.5	1.9	6.7	3.2	1.2	1.0
Hurricane Alicia	1983	8	1.36	1.28	9.5	9.6	6.3	3.9	2.2	7.4	3.6	1.3	1.0
Hurricane #10, 1949	1949	10	1.13	1.36	10.5	11.4	7.7	4.9	2.9	8.9	4.5	1.6	1.0
Hurricane #2, 1941	1941	9	1.19	1.41	11.7	12.8	8.8	5.7	3.4	10.1	5.3	2.0	1.0
Hurricane Audrey	1957	6	1.37	1.44	13.1	13.6	9.5	6.2	3.8	10.8	5.8	2.2	1.0
Hurricane #3, 1934	1934	7	1.25	1.44	15.0	13.8	9.6	6.3	3.9	11.0	5.9	2.3	1.0
	1969	2	0.76	1.49	17.5	15.2	10.7	7.2	4.5	12.2	6.7	2.7	1.0
Hurricane #2, 1942	1942	8	1.25	1.59	21.0	18.5	13.5	9.4	6.2	15.2	8.8	3.8	1.2
Hurricane #2, 1932	1932	8	0.88	1.69	26.3	22.1	16.5	11.8	8.0	18.3	11.2	5.2	1.6
Hurricane #2, 1919	1919	9	2.07	2.35	35.0	55.8	46.1	37.3	29.6	49.5	36.1	23.3	11.9
Hurricane Carla	1961	9	2.07	2.38	52.5	57.3	47.4	38.5	30.6	50.9	37.2	24.1	12.5
Hurricane Ike	2008	9	2.76	2.85	105.0	93.1	79.9	67.8	57.0	84.3	66.2	47.6	29.5

Table 1.4. ***Projected return periods for inundation levels that have been generated by a range of historical storms for the study's two sea level rise scenarios.***

CONCLUSION

This study focused on quantifying the changing risks of flooding as the century progresses. The study started by comparing several extreme value distributions for estimating the probability of annual surge maxima for the station of Galveston Pier 21 in Galveston Bay, Texas. The comparison focused on five frequently used distributions: GEV, log-logistic, three-parameter and four-parameter Burr, and Dagum. A comparative analysis of the distributions does not reveal significant differences in performance. The log-logistic distribution was selected to evaluate the probability of future flooding because of its good performance for the largest surges.

The study then uses the fitted log-logistic model to examine the effects of two forecasts of future sea level rises, a conservative scenario that continues the linear increase of the 20th century, and a scenario based on the upper end of the IPCC AR4 A1FI. Both scenarios show continuously increasing risks of flooding as the century progresses. By the end of the century, for the conservative scenario, inundations caused by the recent impact of Hurricane Rita are expected to take place annually, as compared to the current return period of 6.6 years. For the IPCC A1FI based scenario a Rita like flooding is expected to take place annually shortly after year 2050. The research shows differences in the relative increase in frequency of inundation caused by events of different sizes, and in particular a much larger proportional increase of flooding caused by smaller size storms. By year 2100 water level exceedance probabilities are expected to about double for the impact of the largest storms such as Hurricane Ike, but increase by a factor over six times for the impact of smaller storm surges associated locally with the impact of storms such as Hurricanes Cindy, Alicia, and Rita for the conservative

scenario. These results should be taken into account while estimating future insurance rates to cover the growing flooding damages as the century progresses.

\

CHAPTER 2

Estimated Increase in Inundation Probability with Confidence Intervals for Galveston Bay, Texas

ABSTRACT

This study uses bootstrap methods to estimate confidence intervals for increases in inundation probability at the Pier 21 tide gauge in Galveston, Texas. The local surge is modeled using the generalized extreme value (GEV) distribution. Resamples of the historical record are created, and a GEV model is fit to each resample. This ensemble of models is then used to estimate future water level exceedance probabilities under two possible sea level rise scenarios, a conservative linear continuation of the past century's trend and a scenario based on the upper limit of the sea level range in the IPCC AR4 report, i.e. the A1FI scenario. The distribution of future exceedance probabilities is trimmed to estimate 90% and 95% confidence intervals around the estimated proportional change in annual water level exceedance probabilities by 2100. The study shows that even under the conservative scenario and using the wider 95% intervals, the frequency of surges of height 1.1 m (current return period of 16 years) becomes at least 4 times as common by the end of the century.

INTRODUCTION

One of the most frequent and costly natural disasters that affect societies around the world is flooding. According to the United States Federal Emergency Management Agency (FEMA), 2.03 million properties were affected by floods from January 1978 to November 2012 in the United States with total monetary loss approximately 42 billion dollars (NFIP, 2013). The confluence of sea level rise and population growth in coastal regions makes it essential to continue improving flood management strategies. Relative sea level rise occurs where there is a local increase in the level of the ocean relative to the land, which may be due to rising ocean levels and/or subsiding land levels (Bates et al., 2008) The required investments to protect such areas will be very large, and as sea levels rise, available resources will likely not be sufficient to protect all areas. For efficient planning of coastal investments, it is therefore essential to develop accurate flooding estimates that take into account both local effects such as land subsidence and global effects such as estimated rates of sea level rise linked to climate change (IPCC, 2007).

Effective flood management strategies significantly reduce the vulnerability of people to the risks of property damage. Research for the UK by Purvis (2008) focused on the methodology to estimate the probability of future coastal flooding given uncertainty over possible sea level rise. The authors conclude that undertaking a risk assessment using the most plausible sea level rise value may significantly underestimate monetary loss as it fails to account for the impact of low probability, high consequence events. This paper focuses on evaluating the impact of sea-level rise on the historical range of surge

events in Galveston Bay, Texas and estimates the 90% and 95% confidence intervals for the relative increases in the probability of inundation in the study area.

Because the prediction of large floods requires knowledge of the underlying distribution, this study starts with the statistical modeling of extreme surges at the study site. A number of studies have been conducted to model the extreme value distributions of flood data. The generalized extreme value distribution (GEV) is recommended by (FEMA, 2007) for modeling floods, and has been used by previous researchers (Kotz and Nadarajah, 2000; Nadarajah and Shiau, 2005; ÖnÖz and Bayazit, 1995). Warner and Tissot (2012) determined that the GEV was one of the best distributions for modeling surges at Galveston Pier 21, the station with the longest record in the Gulf of Mexico. In Chapter 1, we noted that GEV had some advantages over log-logistic, although we indicated a slight preference for log-logistic at that point. However, for computational efficiency when dealing with 10,000 bootstrap fits, we chose to switch from log-logistic to GEV distribution. The main focus of this study is to use the GEV model along with bootstrap methods (Efron, 1979) to estimate confidence intervals for increases in inundation probability at this station. Accurate estimation of confidence intervals for the probability of flooding is an important requirement for the development of appropriate flood control structures in the future.

The estimation of a model for a stochastic process from a historical sample is a classical problem in statistics. Since a historical sample is necessarily an incomplete record of the entire distribution of the process, there is inevitably some uncertainty in estimates of model parameters, and hence in the predictions made from them. General methods of model fitting, such as Maximum Likelihood Estimation (MLE), provide a

convenient method of estimating model parameters, but not for estimating their uncertainty. For some models (e.g., normal distributions) there is a well-understood theory to guide the applied modeler; however, for other models such as the GEV, no such specific theory exists. For these situations, the bootstrap method (Efron, 1979) is widely used by statisticians to estimate uncertainty in model parameters. In this paper, we apply bootstrap techniques to MLE model fitting to estimate uncertainty in both the parameters of the GEV model as applied to Galveston Pier 21 data, and more importantly, to estimate uncertainty in predictions of the likelihood of future inundations of different sizes. The bootstrap method has been used for many statistical applications, but to our knowledge has not been used to estimate confidence intervals for surge distributions. There are several different techniques that are described by the umbrella rubric of "bootstrap"; we employ two of them. The first method ("nonparametric") uses resampling with replacement of the historical record to construct alternative "historical records". Then each such "historical record" is refit using MLE to generate a new estimate of model parameters and of future inundations. The second method ("parametric") begins with the MLE model of the single historical record, and then generates new "historical records" randomly from this model. Again, each new "historical record" is refit using MLE. Repeated use of each technique generates a large set of estimates for parameters and inundations, which serves as an estimate of the true distribution of each, and can be used to generate confidence intervals for the unknown quantities. Kyselý (2008) compares performance of nonparametric and parametric bootstraps to fit GEV models for time series of lengths 20, 40, 60 and 100 extreme values, and concludes that $n = 60$ is enough information for either technique to achieve

their nominal level of significance. In our research there are 105 years of records available for Galveston Pier 21. Annual maximum surges are computed and exceedance probabilities are estimated for surges ranging from 0.4 m. to 3.0 m. Two different sea level rise scenarios are employed to estimate the ratio between exceedance probability by the end of the century and present values of the probability of inundation. 90% and 95% confidence intervals for the ratios are estimated using the bootstrap techniques. The results of this study show the relative importance of the surge events of different sizes and predict substantial differences in the increase of the probability of inundation depending on the size of the surges.

DATA AND METHODS

Study site and data

The Galveston Pier 21, Texas station was selected for this research (Figure 2.1). The station is part of the US National Water Level Observation Network and is located on the north-east side of Galveston Island, Texas (Latitude 29° 18.6' N, Longitude 94° 47.6' W).

Hourly water level records are available at this station from January 1904 until December 2008 from NOAA's Tides and Currents data repository (NOAA, 2011a) with only a few very short gaps. Previous studies (Huang et al., 2008; Turner, 1991) used the same data to examine statistical distributions of the water levels in the Gulf of Mexico and along the coast of the United States. Verified hourly water levels were used to calculate monthly maximum water levels, and the resulting time series were compared with NOAA's monthly extremes time series (NOAA, 2011a) for quality control. The station's Mean Range of Tide is 0.31 m (NOAA, 2011b) and most of the differences in records were within this range with two exceptions: Hurricane #6 in August 1909 and Hurricane #2 in September 1919. The monthly maximum water levels were retained for this study, 0.39 m for the 1909 storm and 2.07 m for the 1919 storm. Next the mean sea level trend of 6.39 mm/year (NOAA, 2011c) was removed from the hourly time series with the zero mean sea levels set for the year 1999 to match tidal predictions (NOAA, 2011d). The harmonically predicted water levels were also obtained from (NOAA, 2011a) and were subtracted from water level records to remove tidal variability and to

calculate surge time series. It was not possible to remove the tidal component for the two cases described above (August 1909 and September 1919) as the timings of the maximum water levels are not available. Overall missing data accounted for 2.35% of the time series. Missing records were imputed by the means of the maximum surges for the corresponding months. Then the maximum annual surges were computed and used for this study. The timing of the missing data did not coincide with hurricanes impacting the Texas coast with two exceptions, Hurricane #2 in August 1915 and Hurricane #1 in July 1943. Reliable data was not found for these two events. The resulting surge time series is compared to the water level time series in Figure 2.2. The sea level rise is clearly discernable in Figure 2.2a.

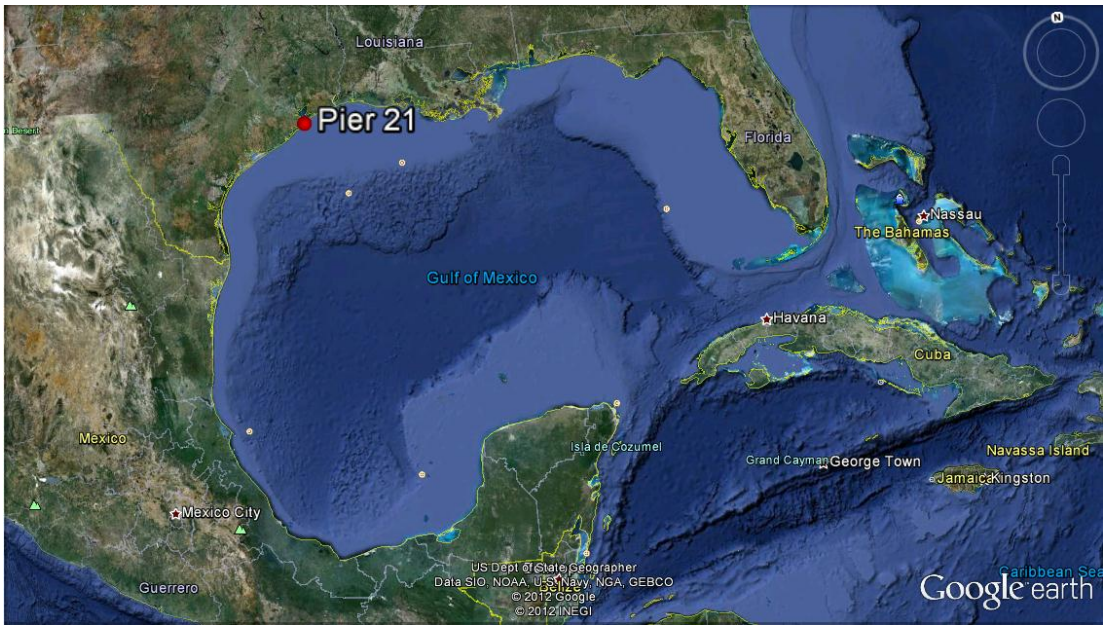

Figure 2.1. ***Map of the study area. The study station is indicated by the red dot.***

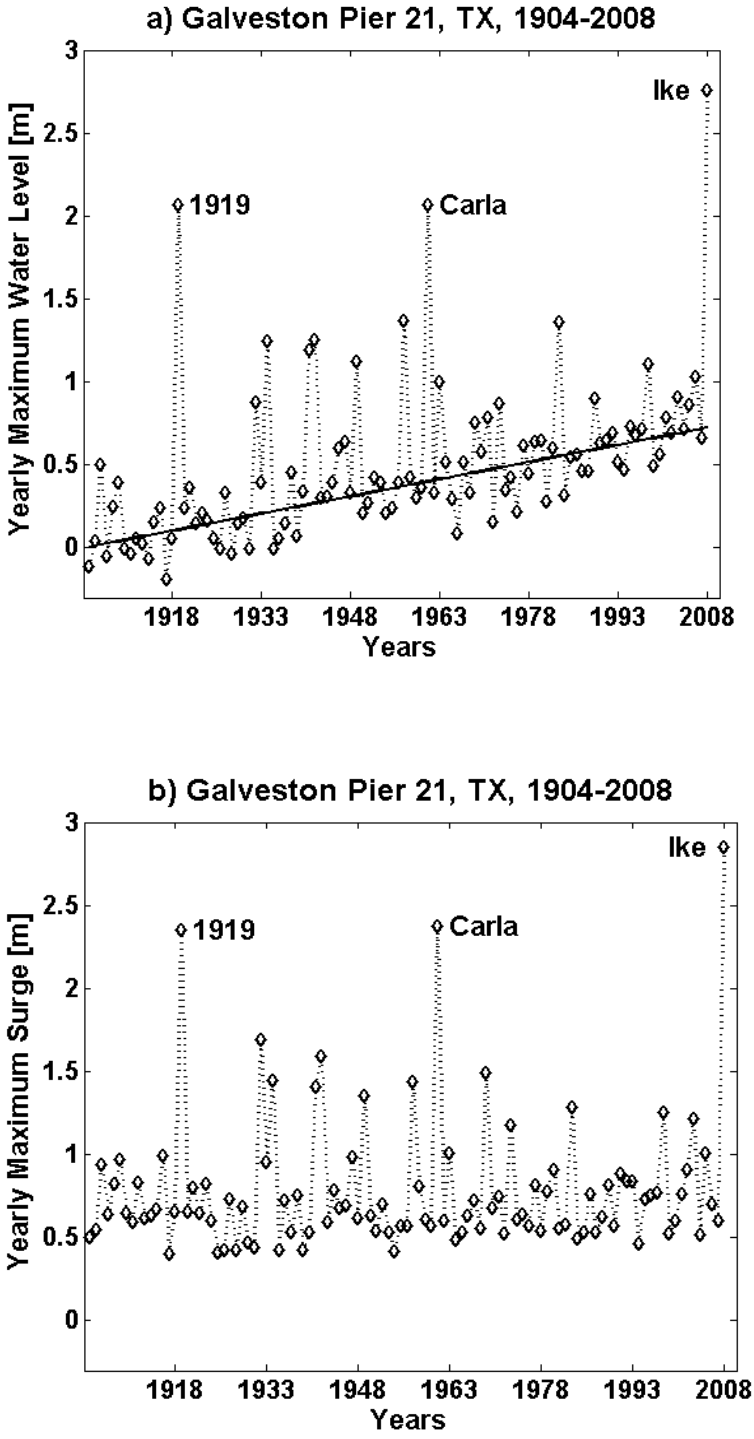

Figure 2.2 (*a) Annual maximum water level time series (b) Annual maximum surge time series. The black line represents the 6.39 mm/year sea level rise for the Galveston Pier 21, Tx station.*

Generalized Extreme Value Distribution

The generalized extreme value distribution (GEV) is selected for this study as discussed in the introduction. The equation and parameters of the cumulative distribution function (CDF) of the GEV for this study are listed below with parameters following the convention of Kotz and Nadaraiah (2000):

$$F(x) = e^{-(1+\xi((x-\mu)/\sigma))^{-1/\xi}}, \quad \mu - \sigma/\xi \le x < \infty \text{ for } \xi > 0,$$

where ξ is a shape parameter, σ is a scale parameter, and μ is a location parameter.

For our data time series, the GEV model was fit using Matlab's gevfit function (MatLab®, 2009a), which uses MLE to estimate the model parameters.

Bootstrap methods to estimate confidence intervals

The bootstrap technique was introduced by Efron (1979) and is further described in Efron and Tibshirani (1993) and Davison and Hinkley (1997). To investigate the uncertainty of the surge distribution, both nonparametric and parametric methods were used. For the nonparametric method, the bootstrap samples are replicated from the empirical distribution. For the parametric method, the bootstrap samples are drawn from the estimated parametric model. The nonparametric bootstrap is used to approximate parameters of a population or probability distribution when we do not know the

distribution. The parametric bootstrap is used to approximate parameters of a population or probability distribution when we think we know the distribution.

For the parametric bootstrap we perform the following steps:

- Determine parameters of the GEV distribution for the historical data using Matlab's (MatLab®, 2009a) gevfit function.
- Generate 10,000 bootstrap samples by randomly sampling from this GEV fitted distribution. Firstly, 3,000 samples were found to be sufficient to obtain stable parameter distributions, the larger number of 10,000 samples was selected as computational efficiency was not a major issue. The generated samples have the same sample size as the original data, 105 annual surge values.
- For each bootstrap sample re-estimate the parameters of the GEV distribution.
- Calculate the CDF and exceedance probability function for each re-estimate of the parameters using the gevcdf function in Matlab (MatLab®, 2009a).

For the nonparametric bootstrap we use the following procedure:

- Generate 10,000 bootstrap samples by assuming all Annual maximum surges as equally likely and randomly picking with replacement any of the values from the historical dataset. The stationarity of the extreme value distribution parameters was analyzed and confirmed by Warner and Tissot (2012) for a succession of 15 periods of monthly maximum water levels each 7 years long. Furthermore the present study is interested in surge distributions over long periods, longer then decadal variability in hurricane activity. The drawn samples have the same sample size as the original data, 105 Annual surge values.

- For each bootstrap sample re-estimate the parameters of the GEV distribution.
- Calculate the CDF and exceedance probability function for each re-estimate of the parameters using the gevcdf function in Matlab (MatLab®, 2009a).

Rates of sea level rise

Various studies (Bindoff et al., 2007; Domingues et al., 2008; Edwards, 2007; Gregory, 2008; Vermeer and Rahmstorf, 2009) indicate a large uncertainty in projections of the sea level rise by the end of the century. The difficulties in accurate estimation of sea level rise are due to uncertainty related to future changes in global atmospheric temperatures, as well as ongoing research on possible contributions of melting ice sheets from Greenland and Antarctica (Gregory, 2008; Hansen, 2007; Meehl et al., 2007; Shum et al., 2008). The IPCC Fourth Assessment Report (AR4) (Meehl et al., 2007) projections do not include the likelihood of future acceleration of glacial contributions (Shum et al., 2008). Also substantially higher sea level rise predictions can be found in recent work, e.g. in (Vermeer and Rahmstorf, 2009).

For the purpose of this study, two scenarios of sea level rise were selected:

- A very conservative continued linear sea level rise of 6.39 mm/year, based on the 20^{th} century trend for Galveston Pier 21 station (NOAA, 2011c), resulting in a 0.65 m increase in sea level by year 2100 as compared to the 1999 mean sea level;
- A quadratic model of sea level rise, resulting in a total 1.08 m increase in sea level by year 2100 as compared to the 1999 mean sea level. For this second scenario the local vertical land motion of 4.69 mm/year was estimated by comparing last century's rate of local sea level rise (6.39 mm/year) with the global rate of sea

level rise of 1.7 mm/year (Bindoff et al., 2007). A quadratic model of sea level rise was then added to the vertical land motion rate to bridge the years between the last water level measurements and the global increase in sea levels as estimated for the A1FI 2090-2099 upper bound level (Meehl et al., 2007).

Computing the ratios of increase in exceedance probability by 2100

We use the previously selected GEV distribution to project water level exceedance probabilities for future years while considering the two possible sea level rise scenarios, described in section 2.3. For this research we assume the surge distribution and meteorological forcings that drive the surge and frequency of the tropical storms in the study area are unchanged for the next century. To evaluate the impact of sea level rise on future indundation frequencies we compute the ratio between exceedance probability in 2100 and exceedance probability in 2008. Then these ratios are trimmed to estimate 90% and 95% confidence intervals.

RESULTS

GEV model of the historical data and its parameters

The parameters of the GEV distribution based on the historical surge record were estimated: shape parameter ξ=0.35, scale parameter σ = 0.17 and location parameter μ=0.60.

GEV models of the bootstrap ensemble members and the ranges of their parameters

Both bootstrap techniques involve the generation of 10,000 alternate time series of annual maximum surges and refitting the surges with the GEV model. Each bootstrap technique results in a range of values for each of the three parameters. The ranges of the GEV parameters are the same for the ensemble members computed using parametric and nonparametric methods. The distributions of all the GEV parameters from both bootstrap methods are nearly symmetrical and centered on the values of the historical GEV parameters. As an example, the range of values for the shape parameter in the nonparametric method is illustrated in Figure 2.3. This graph demonstrates that the distribution of a given parameter from a bootstrap method has a "simple" distribution, somewhat symmetric, with a single mode.

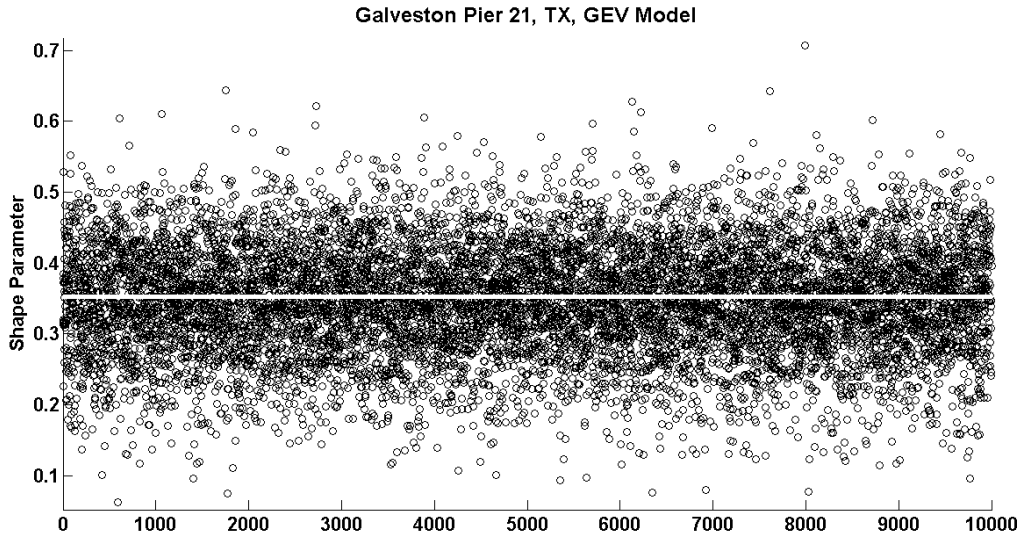

Figure 2.3. ***The values of the shape parameter of the GEV model for the nonparametric bootstrap technique. The white line indicates the value of the shape parameter computed over the historical data set.***

The ratio of exceedence probabilities by 2100

To evaluate the impact of sea level rise on future inundation frequencies, ratios of increase in exceedance probabilities by 2100 are computed based on the two selected sea level rise scenarios: the conservative linear continuation of the past century trend and the A1FI scenario in the IPCC AR4 report. These ratios are presented in Figure 2.4. The risk of flooding significantly increases by the end of the century for both scenarios.

For water levels up to about 1 m, both sea level rise scenarios predict exceedance probabilities of 100% by the end of the century. Thus, the two curves in Figure 2.4 are the same for that range of water levels. At 1 m, both models predict a six-fold increase in exceedance probabilities over the 2008 levels. From this point, the models diverge

sharply. For the conservative scenario, the ratio of exceedance probabilities increases a little, up to 1.1 m, and then gradually declines to a two-fold increase in probabilities of 2.8 m surges (corresponding to Hurricane Ike in 2008). For the A1FI scenario, the ratios of increase in exceedance probabilities continue to increase sharply, peaking at a predicted twenty-fold increase for surges of 1.6 m. From there the ratios decline almost as sharply to a four-fold increase in 2.8 m surges in 2100.

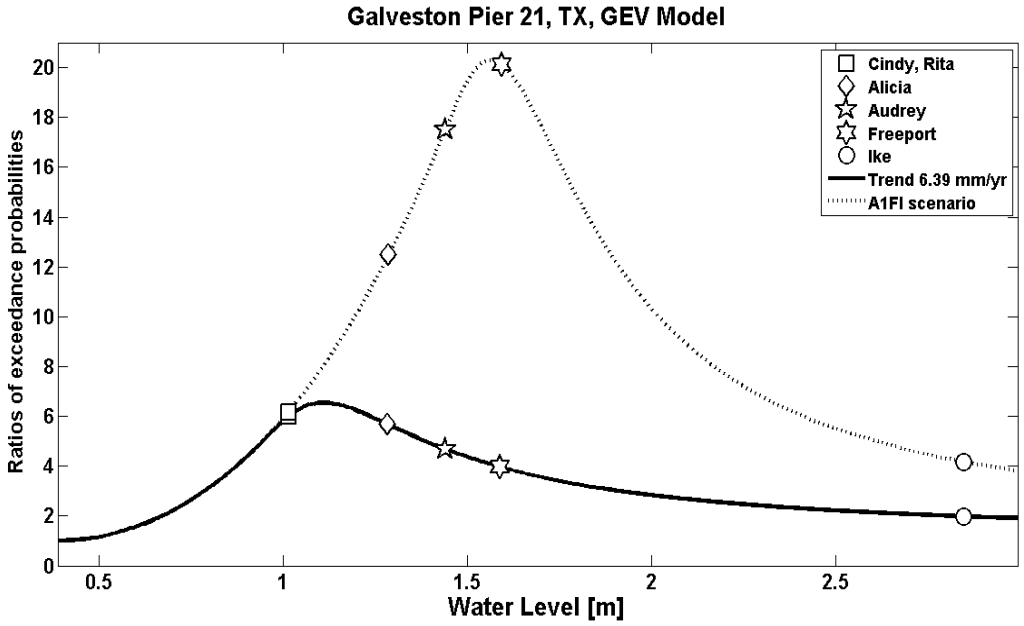

Figure 2.4. ***Ratios of water level exceedance probability in 2100 versus the exceedance probability in 2008 for the conservative and A1FI scenarios of sea level rise (nonparametric bootstrap).***

90% and 95% confidence intervals for the ratios of increase in exceedance probabilities

The results from the two bootstrap techniques were extremely close, and the nonparametric bootstrap was selected to discuss the results of the study. Figure 2.5 presents 90% and 95% confidence intervals around ratios of increase in exceedance probabilities for both sea level rise scenarios. As the century progresses the risk of flooding significantly increases for both scenarios. The greatest uncertainties in the estimates coincide with the greatest increases. Even with these uncertainties, the lower bounds of the confidence intervals imply a four-fold increase in surges of 1 m for the conservative scenario, and at least a ten-fold increase in surges of 1.6 m for A1FI scenario. As a practical example, the conservative scenario takes the current 16% annual chance of a 1.01 m surge (impact of Hurricane Rita in 2005 in the Galveston Bay) to at least a 64% annual chance of the same surge in 2100. Note also that there is almost no difference in the lower bounds of the 90% and 95% confidence intervals.

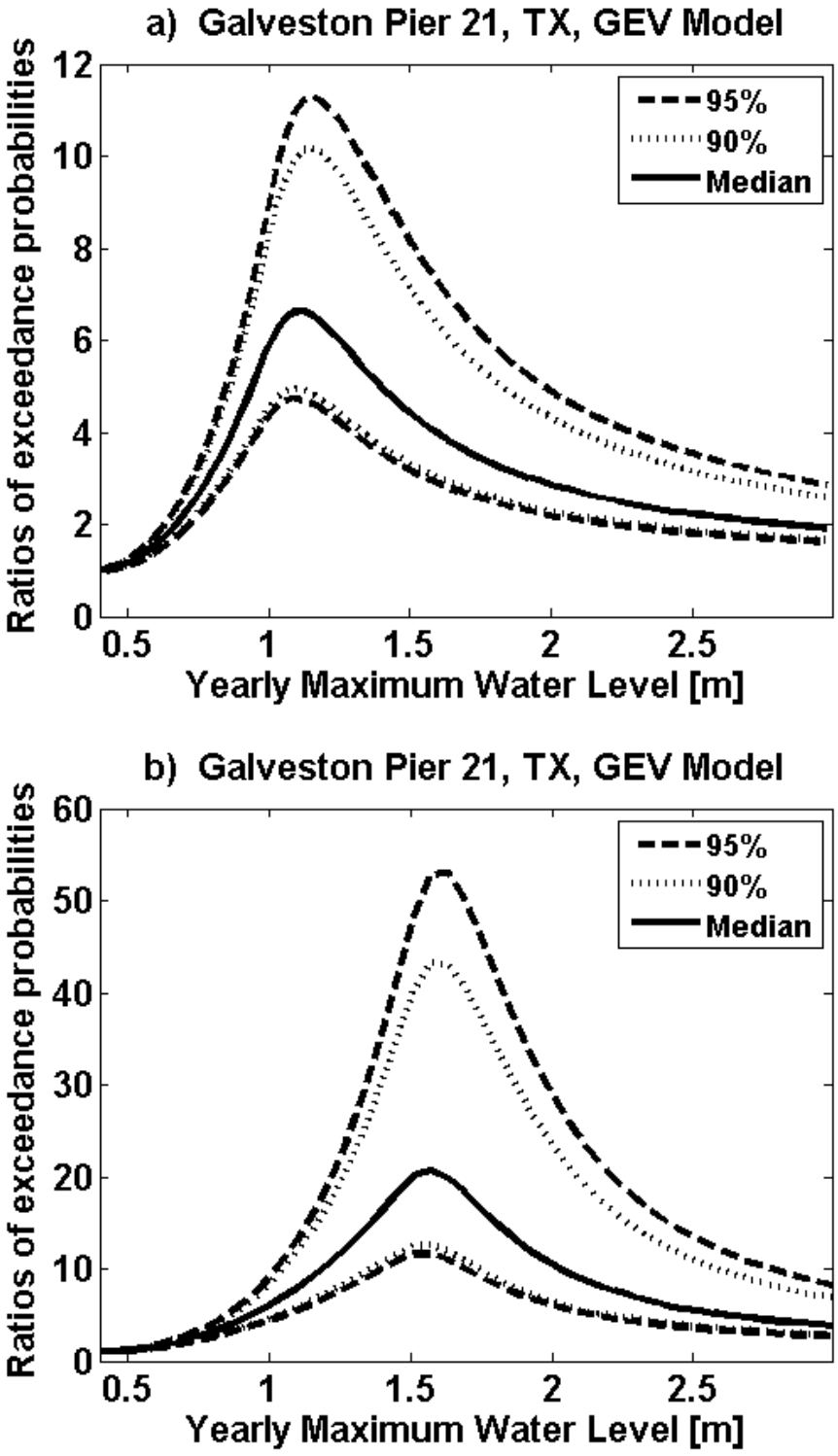

Figure 2.5. ***(a) The 90% and 95% confidence intervals (nonparametric bootstrap) around the ratios of increase of the water level exceedance probability in 2100 versus the present exceedance probability in 2008 for the conservative scenario and (b) A1FI scenario (on the right).***

DISCUSSION

The confidence intervals for the ratio of exceedance probability in 2100 versus the exceedance probability in 2008 were estimated by two different techniques, by a nonparametric bootstrap and by a parametric bootstrap. The fact that the two methods result in the same confidence intervals is an indication that the GEV distribution appropriately models surge height distribution for the data set. While there is still a great deal of uncertainty in the current projections of the rate of sea level rise, results show that even without acceleration of the rate of sea level rise the probability of inundation will increase substantially. As it is unlikely that the rate of sea level rise will remain the same, a higher ratio of exceedance probabilities is more likely, unless the local rates of subsidence decrease.

An important feature of the confidence intervals in Figure 2.5 is their asymmetry with narrower spans between the medians and lower bound estimates than between the medians and upper bound estimates. For an understanding of the cause of this asymmetry consult Figure 2.6. In Figure 2.6a we have plotted 10,000 exceedance probabilities for 1.11 m (the highest ratio for the conservative scenario) in 2008 (on the *x*-axis) and 2100 (on the *y*-axis), as predicted by the GEV fits for our nonparametric bootstrap resamples. The increase in exceedance probabilities is thus the ratio of the *y*-coordinate for each point in Figure 2.6a, divided by its *x*-coordinate. Compare an example point in the lower right hand quadrant—say, (0.16, 0.75)—with the point in the center of the crosshairs, (0.12, 0.81)—with a mirror image point in the upper left hand quadrant—say, (0.08, 0.87). The corresponding ratios are 4.69, 6.75, and 10.875. The change in the numerators (y-coordinate) is only about 20%, but the change in the denominators (x-

coordinate) is about 100%. Thus, the exceedance probabilities for the two years are roughly symmetrically distributed in Figure 2.6a. However, their ratios are not, and the quadrant with small x-coordinates and large y-coordinates will have much greater variation than the quadrant with large x-coordinates and small y-coordinates.

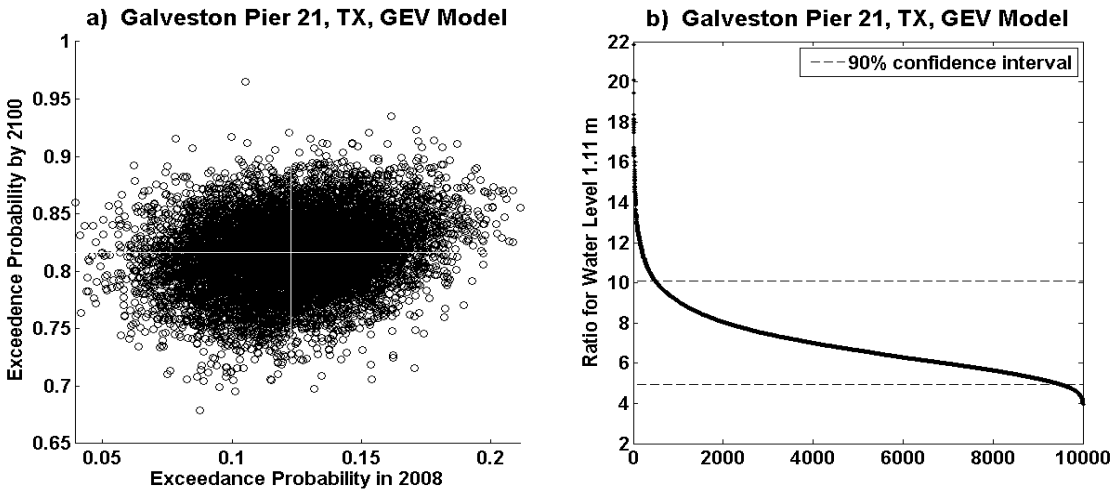

Figure 2.6. (*a) Exceedance probability in 2008 versus exceedance probability by 2100 for the conservative scenario for water level 1.11 m (the highest ratio); the crosshairs represent the corresponding quantities for the GEV fit on the historical data and (b) Ratios of all 10,000 nonparametric bootstraps for water level 1.11 m sorted in descending order.*

As one considers expanding this analysis to other locations the length of the time series available will be a limiting factor. Accordingly to Kyselý (2008) our ability to use the bootstrap and achieve nominal confidence levels for the increase in exceedance probabilities by 2100 for other stations will require at least 60 years of data. There are presently only three other stations along the Gulf of Mexico that satisfy this requirement:

Saint Petersburg, FL (63 years of data), Pensacola, FL (86 years of data), and Key West, FL (97 years of data).

The next step of the research may be analyzing the economic impact of the elevated sea levels and associated storm surges. As sea level increases, flood events will threaten more lives, and damage more public and private properties. This problem may become more severe due to population growth in coastal areas. With this in mind, public demand for seawalls, bulkheads, beaches nourishments and other shoreline maintenance will increase in order to protect coastal communities.

CONCLUSION

This study examines the impact of sea-level rise on storm surge for Galveston Bay, Texas and estimates the 90% and 95% confidence intervals for increases in the probability of inundation in the study area. To estimate uncertainty in predictions of the likelihood of future inundations by 2100 two bootstrap techniques (parametric and nonparametric) were combined with two sea level rise scenarios (a conservative continued linear sea level rise and a scenario based on the upper end of the IPCC AR4 A1FI estimates). The minimum values of the increase in exceedance probabilities are high with very little difference between the 90% and 95% confidence intervals. Both scenarios show continuously increasing risks of flooding as the century progresses.

With advancing sea level rise, there are substantial differences in the relative increase in probability of inundation caused by events of different sizes. In particular, relatively small storms will cause a larger proportional increase in flooding frequency. At a minimum the frequency of reaching an annual maximum water level of 1.1 m will increase by a factor 4 with 95% confidence for the most conservative sea level rise scenario. The insurance industry will use this information when estimating future insurance rates to cover the growing flooding damages as the century progresses. In addition, decision makers can use the results of this research for better preparation of coastal infrastructure and coastal land use. More frequent, smaller storm surges may have a larger impact on coastal communities than the effect s of less frequent, larger storm surges.

CHAPTER 3

Estimated Increase in Inundation Probability with Confidence Intervals for the Gulf of Mexico

ABSTRACT

The primary goal of this research is to compare the relative increase in frequency of inundation caused by storms of different sizes for different sea level rise scenarios and regions of the Gulf of Mexico. The research is based on locations around the Gulf of Mexico that benefit from existing long term sea level records and are located near population centers: Galveston Pier 21, Galveston Pleasure Pier, Port Isabel, Rockport, Texas, Grande Isle, La, and Pensacola, Key West, and St. Petersburg, Florida stations. Differences in oceanographic setting are discussed and affect the quantitative estimate of vulnerability to sea level rise. Increases in inundation frequencies are computed based on two possible sea level rise scenarios, a conservative linear continuation of the past century trend and a scenario based on the upper limit of the sea level range in the IPCC AR4 report, i.e. the A1FI scenario. Results are expressed as the ratios of water level exceedance probabilities between years 2100 and 2011.

Water levels at maximum ratios have a strong correlation with most common moment- and quantile - based statistics except the maximum annual surges. This indicates that the results of this study are not overly sensitive to the most extreme values or largest surge on the record provided that the record includes at least one large surge. Statistical bootstrap methods are used to estimate 90% and 95% confidence intervals for increases in

inundation probability at the study locations. For most cases the confidence intervals show a substantial decrease in interval width for stations with lengths of datasets of 50 years or longer indicating a preferred data length provided that a large surge event is included.

The lower bounds of the confidence intervals imply significant increase in exceedance probabilities for each station for both scenarios. While expected increases in inundation frequencies are substantial for all stations, the results show considerable variation depending on the sizes of the surges, the station locations and the sea level rise scenarios. More frequent, smaller storm surges may have a larger impact on coastal communities than the effects of less frequent, larger storm surges. Ratios of the exceedance probabilities depend mostly on sea level trends and the shape of the curves of the exceedance probabilities with the relative importance of these parameters depending on the sea level rise scenario: the maximum ratios are strongly correlated to the sea level trends for the conservative scenario, but for higher rates of global sea level rise local subsidence becomes less important. Locations with low rates of vertical land motion combined with narrow surge ranges such as the Key West station have the largest ratios of exceedance probabilities and become the most at risk for the A1FI based scenario. Results for both scenarios show that by 2100 the Grande Isle station will experience substantial increases in inundation frequencies due to the large local subsidence. For the faster sea level rise scenario water levels accoiated with majority of the hurricanes are predicted to take place every year by 2100.

INTRODUCTION

One of the most frequent and costly natural disasters that affect societies around the world is flooding. According to the United States Federal Emergency Management Agency (FEMA), 2.03 million properties were affected by floods from January 1978 to November 2012 in the United States with total monetary loss approximately 42 billion dollars (NFIP, 2013). The combination of sea level rise and population growth in coastal regions makes necessary to continue improving flood management strategies. This problem will become even more severe due to population growth in coastal areas. From 1990-2008, population density increased by 32% in Gulf coastal counties, 17% in Atlantic coastal counties, and 16% in Hawaii (U.S. Census Bureau 2010) (NOAA, 2013a). Sea level rise, whether caused by downward vertical land motion or global sea level rise, will cause storm surge floods to progress further inland, thereby increasing flood damage and the recurrence interval of present 30- or 50-year floods. Recent research results indicate that effects of sea level rise on storm surge impact and occurrence rate estimates may not be adequately accounted for. A study by Frazier et al. (2010) concludes that the impact of storm surges in Sarasota County, Florida, caused by small hurricanes will increase due to sea level rise. Park et al. (2011) analyzed long term tidal records from Key West, Pensacola, and Mayport, Florida and concluded that one-in-fifty year surge event can become a one-in-five year event depending on the sea level rise scenario and station. Tebaldi et al. (2012) investigated the influence of sea level rise on expected storm surge-driven water levels and their frequencies along the contiguous United States by analyzing records of 55 stations. They concluded that even at the

locations with relatively slow relative sea level rise the frequency of what is now considered extreme water levels may substantially increase. Frey et al. (2010) investigated the effect of sea level rise and hurricane intensification on storm-surge flooding on the city of Corpus Christi, Texas. Their conclusion is "events that currently cause minor or negligible damage might become significant events, causing much greater damage in the future. Events that currently cause moderate damage might become devastating hurricanes, possibly resulting in significant loss of property and lasting economic and social impacts".

Relative sea level rise occurs where there is a local increase in the level of the ocean relative to the land, which may be due to rising ocean levels and/or subsiding land levels (Bates et al., 2008). The subject of this study is the impact of sea level rise on storm surges of various magnitudes in low-lying coastal zones around the Gulf of Mexico. The research is based on locations that benefit from existing long term sea level records: Galveston Pier 21, Galveston Pleasure Pier, Port Isabel, Rockport, Texas; Grande Isle, Louisiana; and Pensacola, Key West, and St. Petersburg, Florida stations. Different portions of the Gulf of Mexico (Figure 3.1) are experiencing different sea level rise trends and can be divided into five regions, based on the characteristics of the land masses: Florida Gulf Peninsula, Northeastern Gulf Coast, Mississippi Delta Area, Texas Coast, and Mexico Coast (Davis, 2011). Only about 20 million years ago the Florida Peninsula was isolated from the mainland. Geologically the Florida Gulf Peninsula did not have a substantial sediment input and can be characterized as a carbonate platform that can accumulate limestone, but did not receive sediment runoff from the continent.

The local rate of sea level rise in this area is influenced mostly by global sea level rise, and has been about 2-2.2 mm over the past century depending on location (Davis, 2011). The Florida Gulf Peninsula is currently experiencing substantial erosion of its open beaches. Estuarine shorelines are dominated by wetlands. These wetlands areas are stable at the present time because of the stability of the carbonate platform, and provide natural protection from hurricanes. The current sea level rise is slow for Florida Gulf Peninsula and is presently not a significant problem. The Northeastern Gulf Coast is a wave-dominated, barrier coast that has substantial streams running into the Gulf. The Mobile River and the Apalachicola River are contributing a considerable amount of sediment to the Gulf. The sea level rise for this region varies between 2.4-4.0 mm per year at the present time (Davis, 2011). The Mississippi Delta Area experiences the largest rate of sea level rise because of mud compaction and withdrawal of fluids. These factors together with global sea level rise drive regional rates of rise up to 8-10 mm per year and at even larger rates locally (Davis, 2011). Many areas along the Texas Coast area are experiencing fluid withdrawal as well (for example, Houston-Galveston area), oil and gas extraction and/or groundwater pumping. The sea level rise for this area varies from 12 mm per year at the Louisiana-Texas border to 4 mm per year at the Rio Grande area (Davis, 2011). The Mexico Coast is an area with thick accumulation of the sediments in river deltas. There is no substantive data on the rates of the sea level rise for this area. The area close to the Rio Grande can be assumed to experience rates of the sea level rise similar to the south most portions of the Texas coast or about 4 mm per year (Davis, 2011).

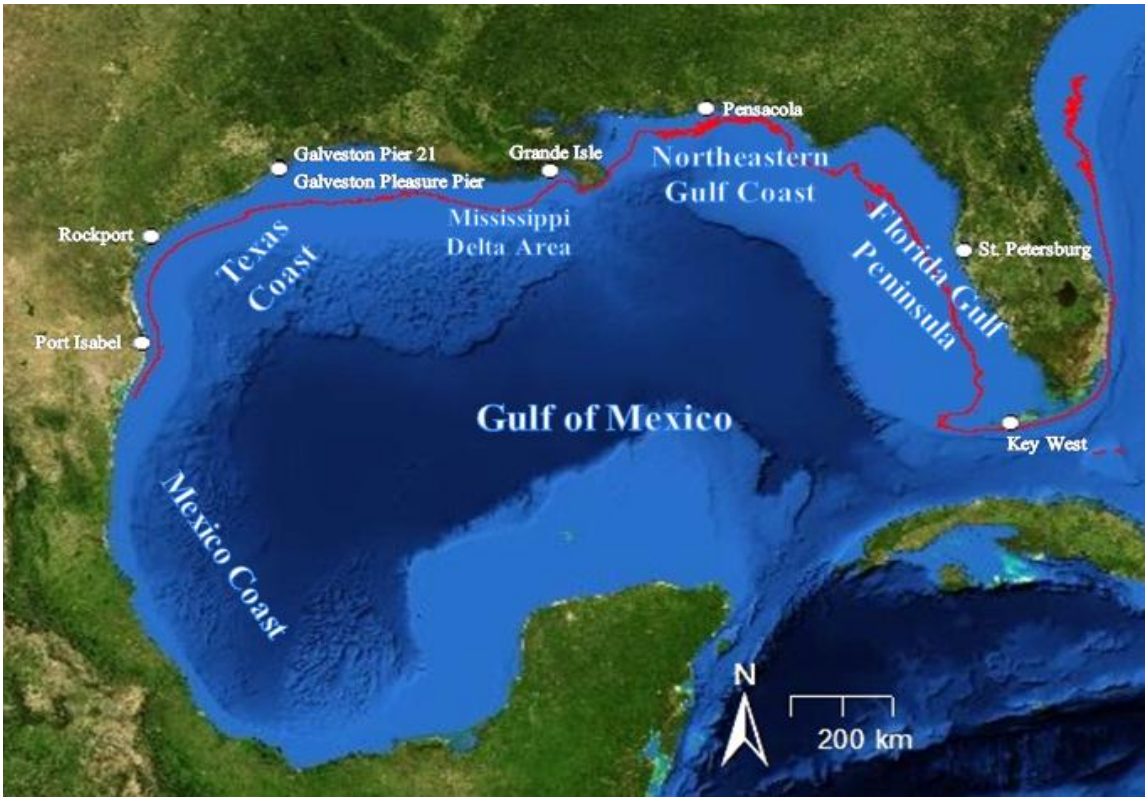

Figure 3.1. ***Map of the study area (red line indicates the 30 m depth contour). White dots indicate the study locations.***

The bathymetry along the coastline of the Gulf of Mexico also varies noticeably (Figure 3.1). Knowledge of the offshore bathymetry is important, as shallow water close to shore tends to increase the magnitude of the storm surge generated by hurricanes. The height of the surge is directly proportional to the width of the shallow water, and inversely proportional to the depth (Hicks, 2006). "The largest surges occur when hurricane winds blow for a long time over large expanses of shallow water" (Pugh, 2004). Because the width and the slope of the continental shelf and the shoreline elevation influence the storm surge, coastal communities on steeper coastlines will

typically not see as much surge inundation as communities on shallow sloping coastlines. Accordingly to Irish and Resio (2010) 75% of surge is generated in waters shallower than 30 m. The range to which variations in near shore bathymetry influence the storm surge was examined by Weaver and Slinn (2010). They concluded that as distance offshore decreases (in waters less than 30 m) the bathymetric fluctuation becomes increasingly important. (Fitzpatrick et al., 2009) proposed a new scale that includes combined factors influencing the storm surge. They propose defining the coastal regions by "bathymetry zones". This scale identifies the regions by the extent of the continental shelf and shallow water proximity. Their research is based on the examination of the bathymetry of the different Atlantic and Gulf of Mexico coastal cities. The locations have a large variation of depth and slope of the shallow waters and different continental shelf locations. For example, their analysis concludes that Gulfport, MS is very vulnerable to storm surge as this location is adjacent to very shallow water, while Fort Lauderdale, FL might experience relatively small storm surge since it is near very deep water. They subjectively define six bathymetry zones to represent these variations: very deep, deep, moderate, average, shallow, and extremely shallow.

To estimate future storm surge impact requires knowledge of the underlying distribution. A number of studies have been conducted to model the extreme value distributions of flood data. The generalized extreme value distribution (GEV) is recommended by (FEMA, 2007) for modeling floods, and has been used by previous researchers (Kotz and Nadarajah, 2000; Nadarajah and Shiau, 2005; ÖnÖz and Bayazit, 1995). Warner and Tissot (2012) determined that the GEV was one of the best distributions for modeling surges at Galveston Pier 21, the station with the longest record

in the Gulf of Mexico. Unfortunately, a historical sample is necessarily an incomplete record of the entire distribution of the process, which leads to some uncertainty in estimates of model parameters, and consequently in the predictions made from them. The bootstrap method (Efron, 1979) is widely used by statisticians to estimate uncertainty in model parameters. The parametric and nonparametric bootstrap methods were used by Warner et al. (2012b) to estimate 90% and 95% confidence intervals for the ratios between exceedance probability by the end of the century and present values of the probability of inundation for the Galveston Pier 21, Texas station. The main focus of this study is to use the GEV model along with the nonparametric bootstrap method to quantify and compare the future impact of sea level rise on inundation frequencies and to estimate confidence intervals for increases in inundation probability for various water levels. Model results are compared and linked to the physical settings of tidal stations along the Northern Gulf of Mexico: Galveston Pier 21, Galveston Pleasure Pier, Port Isabel, and Rockport, Texas; Grande Isle, La; and Pensacola, Key West, and St. Petersburg, Florida stations.

DATA AND METHODS

Study site and data

The eight stations mentioned above are part of the US National Water Level Observation Network (Figure 3.1). These stations along the Gulf of Mexico were selected because they combine the longest water level time series available, at least 30 years, and are also located in the vicinity of large coastal population centers. The necessary length of the data set will be discussed in the results and discussion section. They have significantly different bathymetries, coastal settings and relative sea level rise rates representative of the various regions of the Northern Gulf of Mexico Coastline. The stations' characteristics are presented in Table 3.1. Return periods of hurricanes of category 1 or larger for Galveston, Pensacola, Key West, and St. Petersburg areas are between 8 and 11 years, 19 years for the Rockport area, 13 years for the Port Isabel area, and 7 years for the Grande Isle area (NOAA, 2013b).

Station name	State	Longitude	Latitude	Years data available for	Sea level trend mm/year	Cross-shore distance to 30 m depth contour [km]	Epoch	Missing data [%]
Port Isabel	Tx	97° 12.9' W	26° 3.6' N	69	3.64	25	1983-2001	6.29
Rockport	Tx	97° 2.8' W	28° 1.3' N	49	5.16	40	1983-2001	2.78
Galveston Pier 21	Tx	94° 47.6' W	29° 18.6' N	108	6.39	78	1997-2001	2.16
Galveston	Tx	94° 47.3' W	29° 17.1' N	53	6.84	80	1983-2001	3.22
Grande Isle	La	89° 57.4' W	29° 15.8' N	32	9.24	25	2002-2006	1.79
Pensacola	Fl	87° 12.6' W	30° 24.2' N	88	2.10	41	1983-2001	2.11
St Petersburg	Fl	82° 37.6' W	27° 45.6' N	65	2.36	65	2002-2006	3.11
Key West	Fl	81° 48.4' W	24° 33.3' N	99	2.24	9	1997-2001	2.39

Table 3.1. ***Characteristics of the study stations.***

The Port Isabel station's records are available starting in January 1944 till present and include water levels measured hourly. Unfortunately, the records have large gaps. One of the gaps coincides with the passage of Hurricane Beulah in September, 1967 that caused large damage to an area including the city of Port Isabel. On 23 July 2008, Hurricane Dolly also caused extensive damage to the city; the surge generated by Dolly is part of the available record.

The Rockport station's water level records measured hourly are available starting in January 1963 till present with data missing during hurricane Celia in 1970. Only sparse data is available for years 1937-1939 and 1948-1954; several large gaps prevented this data from being used. The station is located within Aransas Bay with a connection to the Gulf of Mexico through the Corpus Christi ship channel.

The Galveston Pier 21 station is located on the north-east side of Galveston Island, Texas. This barrier island is made up generally of sand-sized particles and smaller amounts of mud sediments and larger gravel-sized sediments on the Texas Gulf coast near the mainland coast. On September 8, 1900 the island was hit by a major hurricane. This hurricane is known as the deadliest natural disaster of the United States. In September 2008 Hurricane Ike made landfall just north of Galveston causing extensive damage to the Houston-Galveston area. Station Galveston Pier 21 is positioned on a ship channel about 4 km away from the main Galveston Ship Channel and the mouth of Galveston Bay and protected from the open waters wave climate. Water level records measured hourly are available starting in January 1904 till present with only a few interruptions.

The Galveston Pleasure Pier station is located on the Gulf of Mexico side of Galveston Island at the end of a pier. Water level records measured hourly are available starting in January 1957 till July 7th, 2011 with only a few interruptions.

The area of the Grande Isle station has been affected by hurricanes or tropical storms very often with the shortest return period, 7 years, for hurricanes of category 1 or larger. Some of the more severe storms are: a 1909 hurricane (4.57 m storm surge) (Needham and Keim, 2011), a 1947 hurricane, hurricane Flossy in 1956, hurricane Betsy in 1965, tropical storm Frances in 1998, hurricane Katrina in 2005, and hurricane Gustav in 2008. Water level records measured hourly are available starting in January 1980 till present with only minor interruptions.

Pensacola is a sea port on Pensacola Bay, which is directly linked to the Gulf of Mexico. This location is often hit by hurricanes. Major hurricanes Eloise in 1975, Frederic in 1979, Juan in 1985, Erin in 1995, Opal in 1995, Georges in 1998, Ivan in 2004, and Dennis in 2005 have made landfall near Pensacola. Pensacola and surrounding areas were especially devastated by 2004 Hurricane Ivan. Water levels records measured hourly are available starting in January 1924 till present. Unfortunately, missing records for this station coincide with the passage of major hurricane Ivan in 2004, probably due to equipment malfunctions.

The city of St. Petersburg is located on a peninsula between Tampa Bay and the Gulf of Mexico. The station's records are available starting in January 1947 till present and include water levels measured hourly with only a few interruptions. Uniquely among the locations used in this study, St. Petersburg has no major hurricane in its time series.

The Key West station's records are available starting in January 1913 till present and include water levels measured hourly with only a few interruptions. Hurricane Wilma on October 24, 2005, was the worst storm in memory of local residents of Key West.

Annual maximum surge time series

Hourly water level records are available from NOAA's Tides and Currents data repository for all the study stations with only a few very short gaps (NOAA, 2013c). The data for Port Isabel station were provided through personal communications from Chris Zervas (NOAA, Silver Spring). Verified hourly water levels were used to identify monthly maximum water levels and compared with NOAA's monthly extremes time series (NOAA, 2013c) for quality control. Next the mean sea level trends (Table 3.1) (NOAA, 2013d) were removed from the hourly time series with the zero mean sea levels set for the middle of the tidal epoch applicable for each station to match tidal predictions (Table 3.1). For the stations with the most rapid sea level trend (Galveston Pier 21, Galveston Pleasure Pier, Rockport, Grande Isle) data from the latest special modified 5-year epoch (NOAA, 2013e) were used. To compute the surge time series harmonically predicted water levels obtained from (NOAA, 2013c) for each station were subtracted from the respective water level records to remove tidal variability.

Overall missing data accounted for is presented in Table 3.1. Missing records were imputed by the means of the maximum surges for the corresponding months. Then maximum annual surge time series were computed for each station. The timing of the missing data did not coincide with hurricanes impacting study locations with a few

exceptions: hurricane #9 in September 1945 for the Key West station, Hurricane Ivan in September 2004 for Pensacola, Hurricane #2 in August 1915 and Hurricane #1 in July 1943 for the Galveston Pier 21 station, Hurricane Beulah in September 1967 for Port Isabel station, Hurricane Celia in August 1970 for Rockport station, and Hurricane #4 in September 1947 for St. Petersburg station. Reliable data was not found for Hurricane #9, 1945 for Key West station, for Hurricane #4 in 1947 for St. Petersburg station, for Hurricane Celia in 1970 for Rockport station, and Hurricane Beulah in 1967 for Port Isabel station. Needham and Keim (2011) was considered as a source to impute the missing data during the passage of hurricanes. The study identified the locations and heights of peak storm surges for 195 events since 1880, including the mentioned above hurricanes. The Needham and Keim (2011) surge heights were compared with this study's tide gauge maximum surges during several hurricanes. For example, the records during Hurricane Ike in 2008 are 5.33 m for Chambers County (Needham and Keim, 2011) and 2.85 m for Galveston Pier 21 station. The locations are approximately 35 km apart. The records during Hurricane Alicia in 1983 are 3.85 m for San Luis Pass (Needham and Keim, 2011), 1.28 m for Galveston Pier 21 station, and 2.13 m for Galveston Pleasure Pier station. San Luis Pass location is approximately 41 km from Galveston Pier 21 station and 40 km from Galveston Pleasure Pier station. Stations Galveston Pier 21 and Galveston Pleasure Pier are approximately 3 km apart. These large differences in surge heights for locations that are geographically relatively close indicate that records for each geographical location are unique and imputing the missing records during mentioned above hurricanes by the records of nearby locations would be incorrect. To address the issue of the extreme event distribution sensitivity to the absence of data

that coincide with the passage of hurricanes Warner and Tissot (2012) computed the variability in the distribution parameters for a range of likely surges for Galveston Pier 21 station. To test the robustness of the respective models they computed the parameters of the distributions for the first 104 years of the time series, omitting the 2008 surge generated by Hurricane Ike in 2008. The results show that the distribution parameters are not overly sensitive to the presence of the largest surges in the dataset for this station. The assumption for this study is that the missing records for the missing hurricane for Key West, Rockport, St. Petersburg, and Port Isabel stations will not substantially affect results as well. This assumption is further discussed in the results and discussion section. Hourly water level records for the stations close to Pensacola were examined and significant correlation between the Pensacola and the Dauphin Island, Alabama water levels was found for September 2004 (Figure 3.2). The monthly maximum water level missing data for September 2004 for Pensacola was imputed with the monthly maximum water level for Dauphin Island station.

Statistics for the station's maximum annual surges are compared in Table 3.2. Boxplots of the maximum annual surges for all stations are presented in Figure 3.3 and the resulting annual maximum water levels and surges time series for all stations are presented in Figure 3.4.a-g. The sea level rises are clearly discernible when comparing the pairs of figures for each station in Figure 3.4.a-g. Substantial differences in surge ranges and distribution parameters can be seen in Figure 3.4.a-g and Table 3.2 including the presence of large surge events for most stations, but absence of such events for the St.Petersburg and Grande Isle stations.

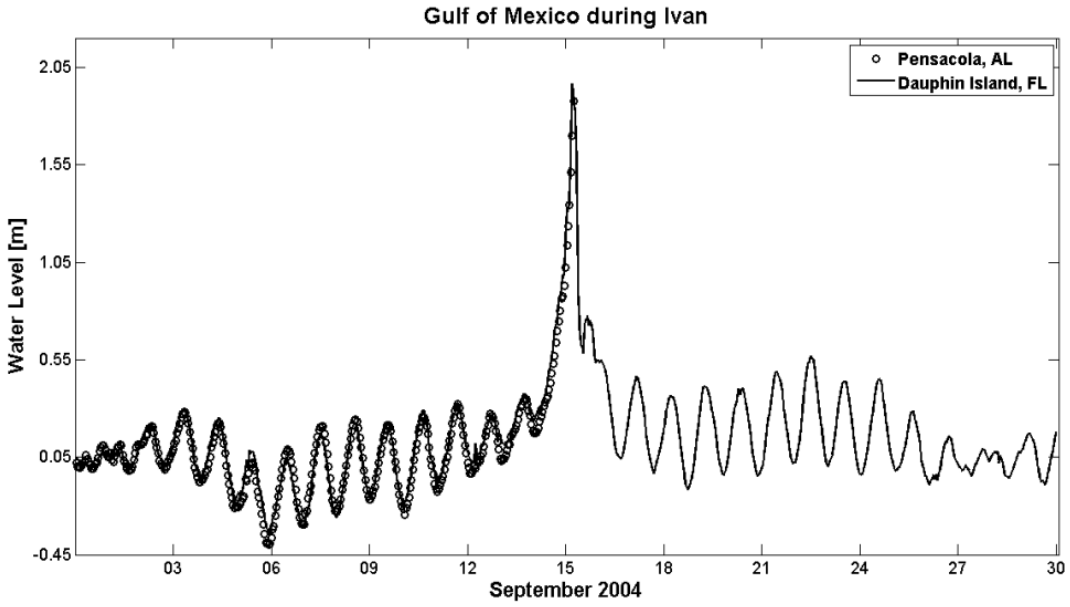

Figure 3.2. ***Hourly water level records during the passage of September 2004 Hurricane Ivan at the Pensacola, FL, and Dauphin Island, AL tide stations (Warner et al., 2012a)***

Station name	State	Mean [m]	Median [m]	Range [m]	Max [m]	Min [m]	Skewness
Port Isabel	Tx	0.52	0.46	1.68	1.98	0.30	3.01
Rockport	Tx	0.46	0.38	1.13	1.37	0.23	2.13
Galveston Pier 21	Tx	0.79	0.68	2.45	2.85	0.40	2.71
Galveston Pleasure	Tx	0.93	0.78	2.39	2.84	0.45	2.43
Grand Isle	La	0.64	0.56	0.96	1.31	0.35	1.22
Pensacola	Fl	0.64	0.54	1.94	2.30	0.35	2.81
St.Petersburg	Fl	0.71	0.67	0.89	1.27	0.37	0.80
Key West	Fl	0.31	0.28	0.75	0.91	0.16	2.48

Table 3.2. ***Statistics of the annual maximum surge time series of the study stations.***

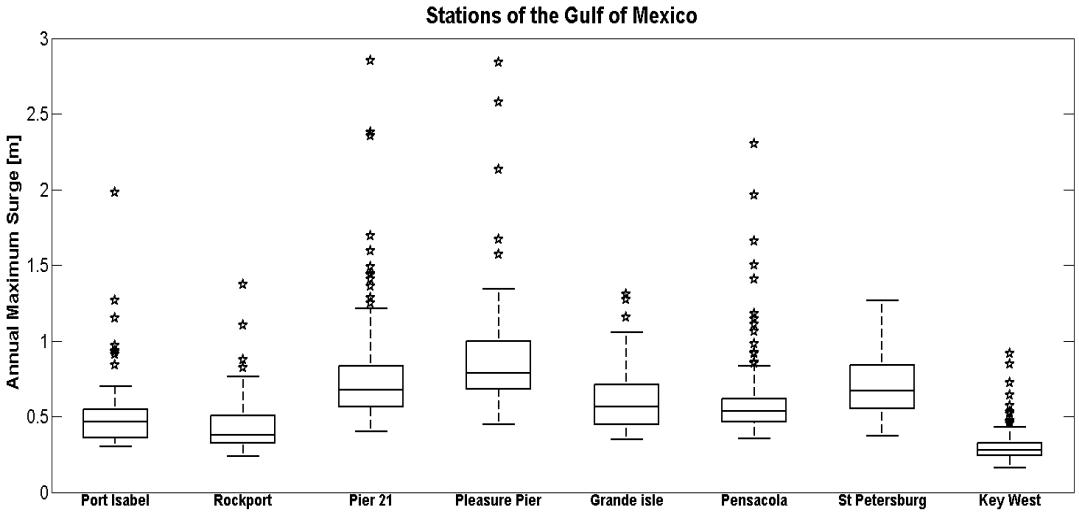

Figure 3.3. ***Boxplots of the annual maximum surge time series of the study stations.***

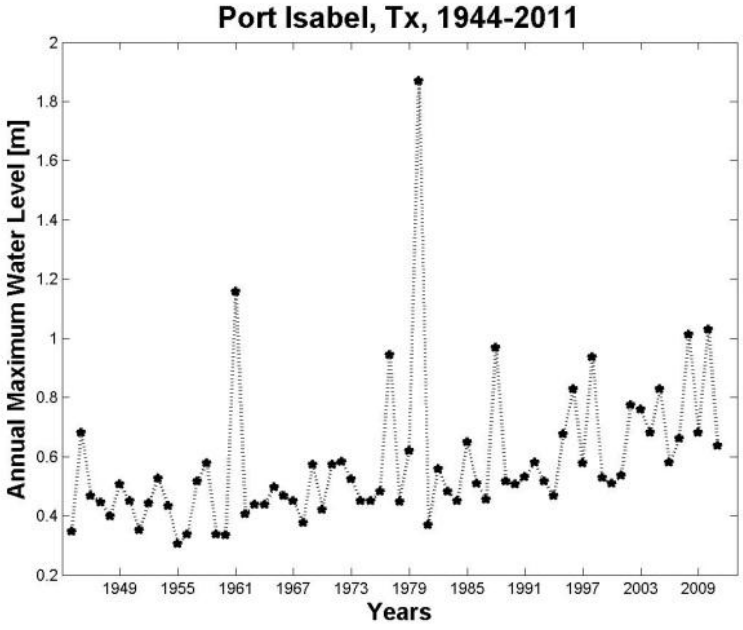

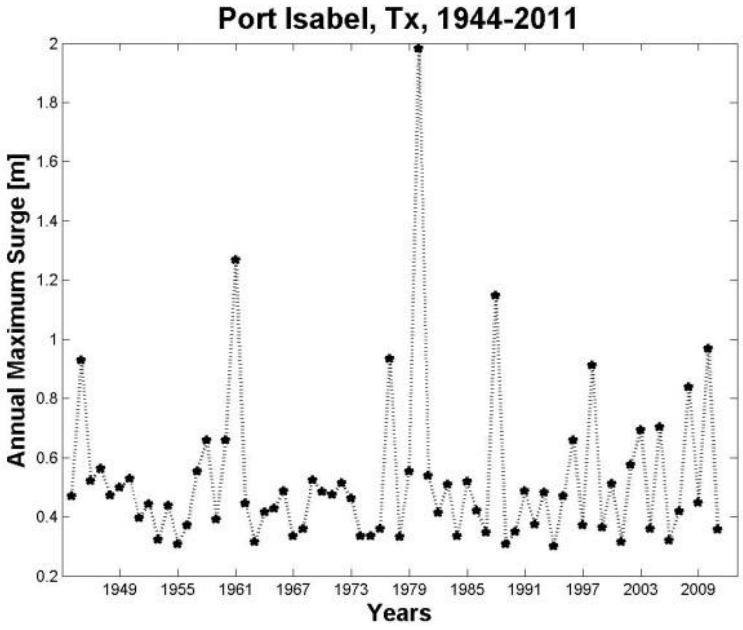

Figure 3.4.a. ***Annual maximum water level time series (on the top) and annual maximum surge time series (on the bottom) forPort Isabell station.***

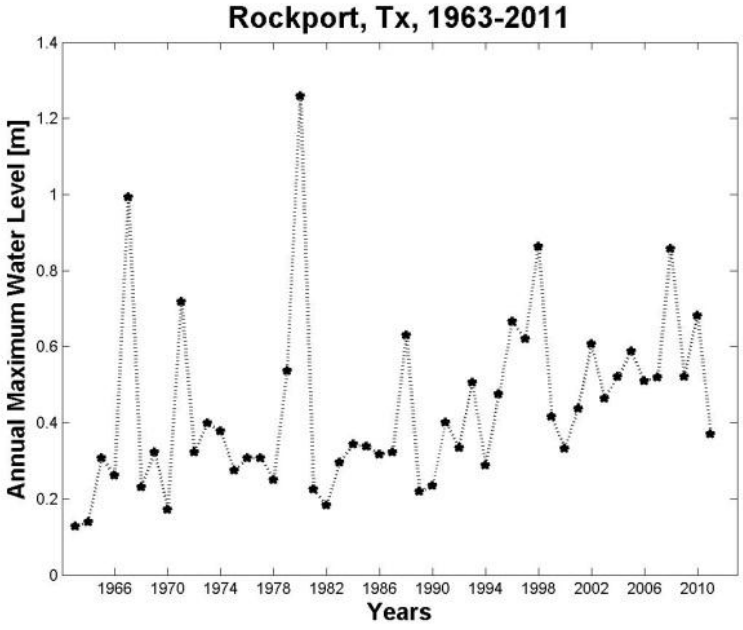

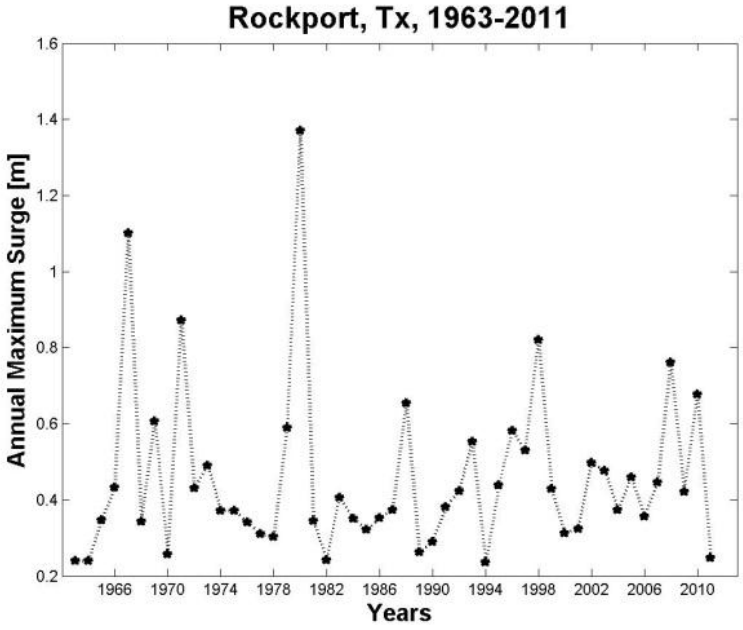

Figure 3.5.b. ***Annual maximum water level time series (on the top) and annual maximum surge time series (on the bottom) for Rockport station.***

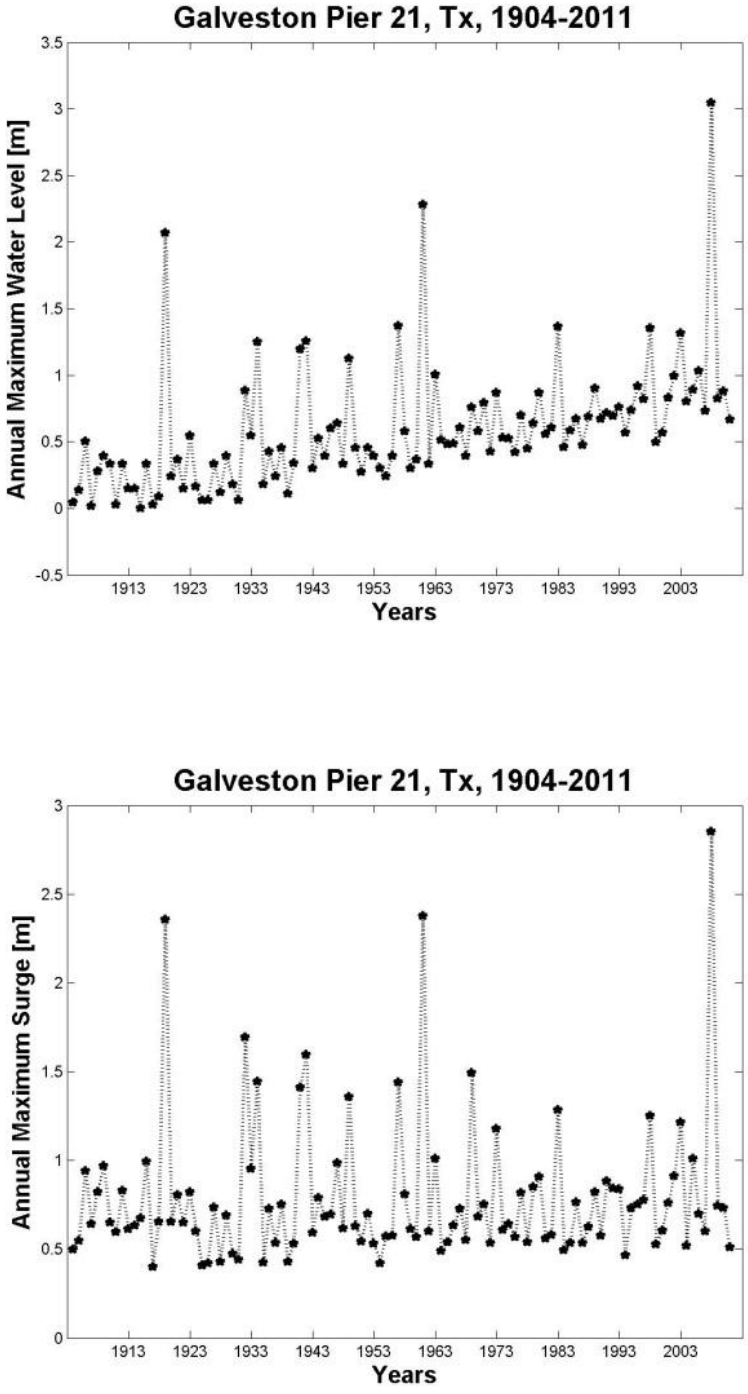

Figure 3.6.c. ***Annual maximum water level time series (on the top) and annual maximum surge time series (on the bottom) for Galveston Pier 21 station.***

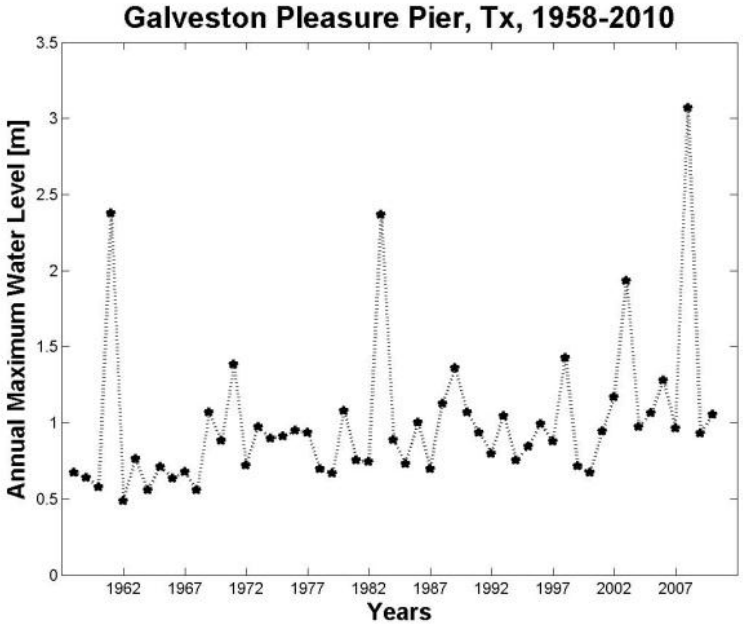

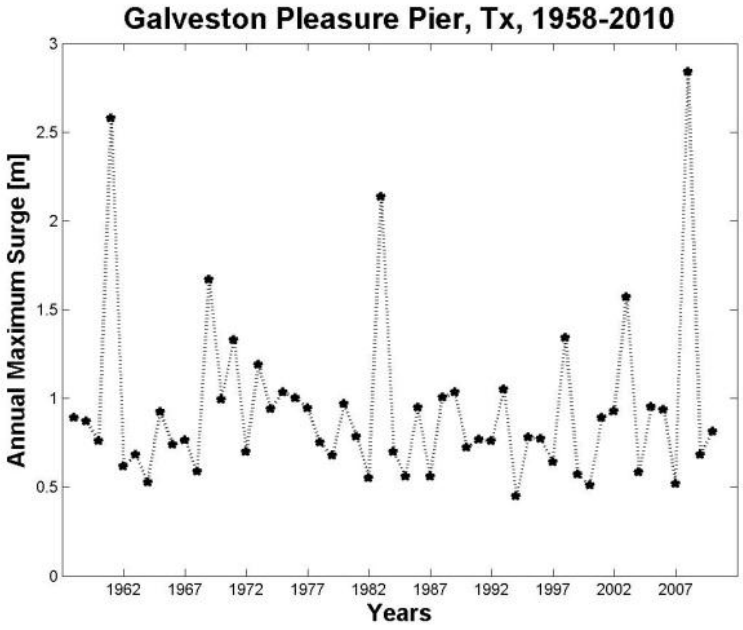

Figure 3.7.d. ***Annual maximum water level time series (on the top) and annual maximum surge time series (on the bottom) for Pleasure Pier station.***

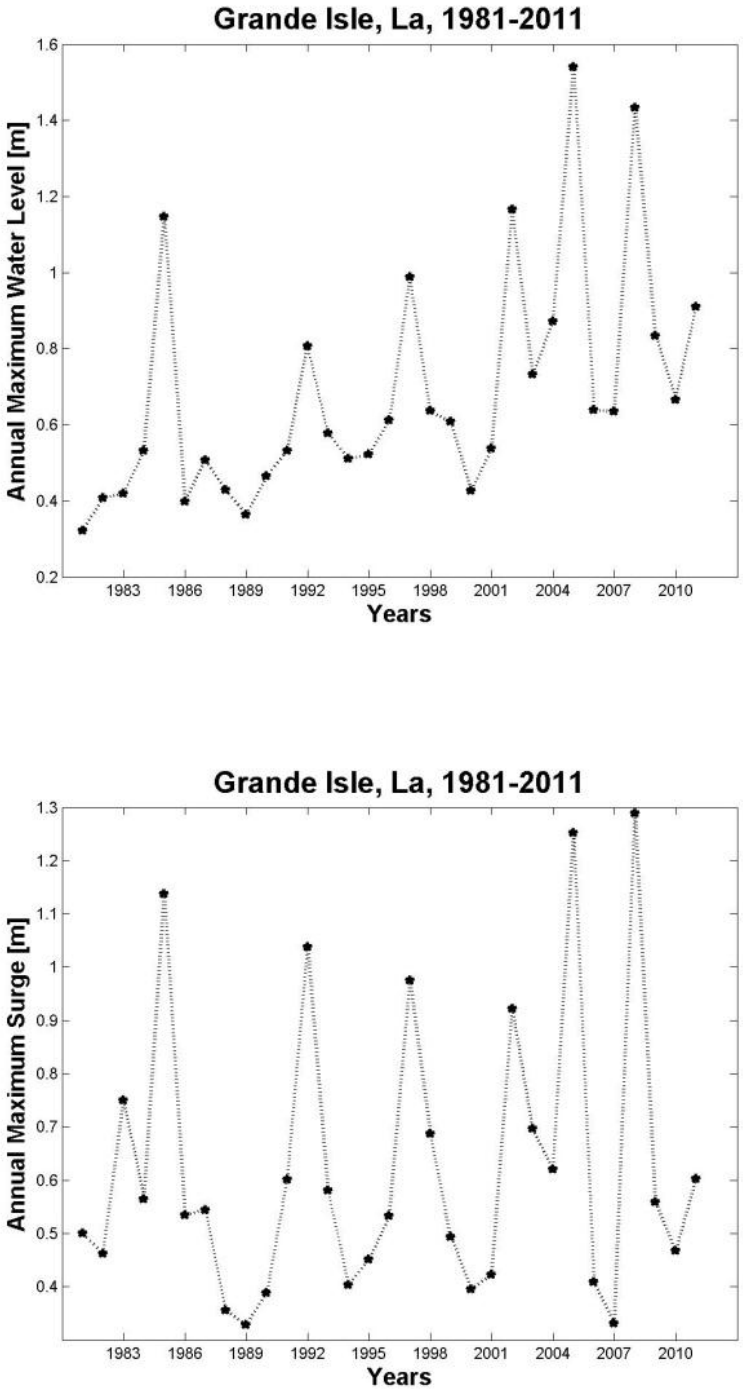

Figure 3.8.e. ***Annual maximum water level time series (on the top) and annual maximum surge time series (on the bottom) for Grand Isle station.***

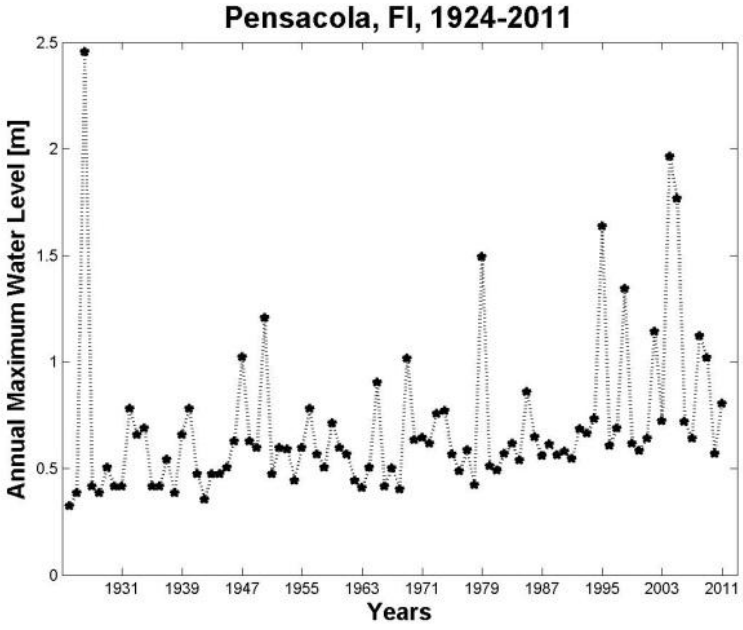

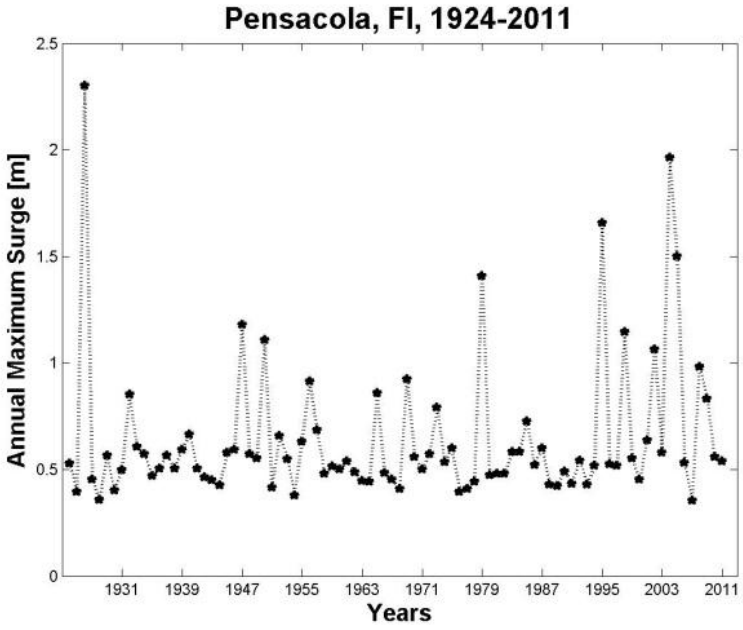

Figure 3.9.f. ***Annual maximum water level time series (on the top) and annual maximum surge time series (on the bottom) for Pensacola station.***

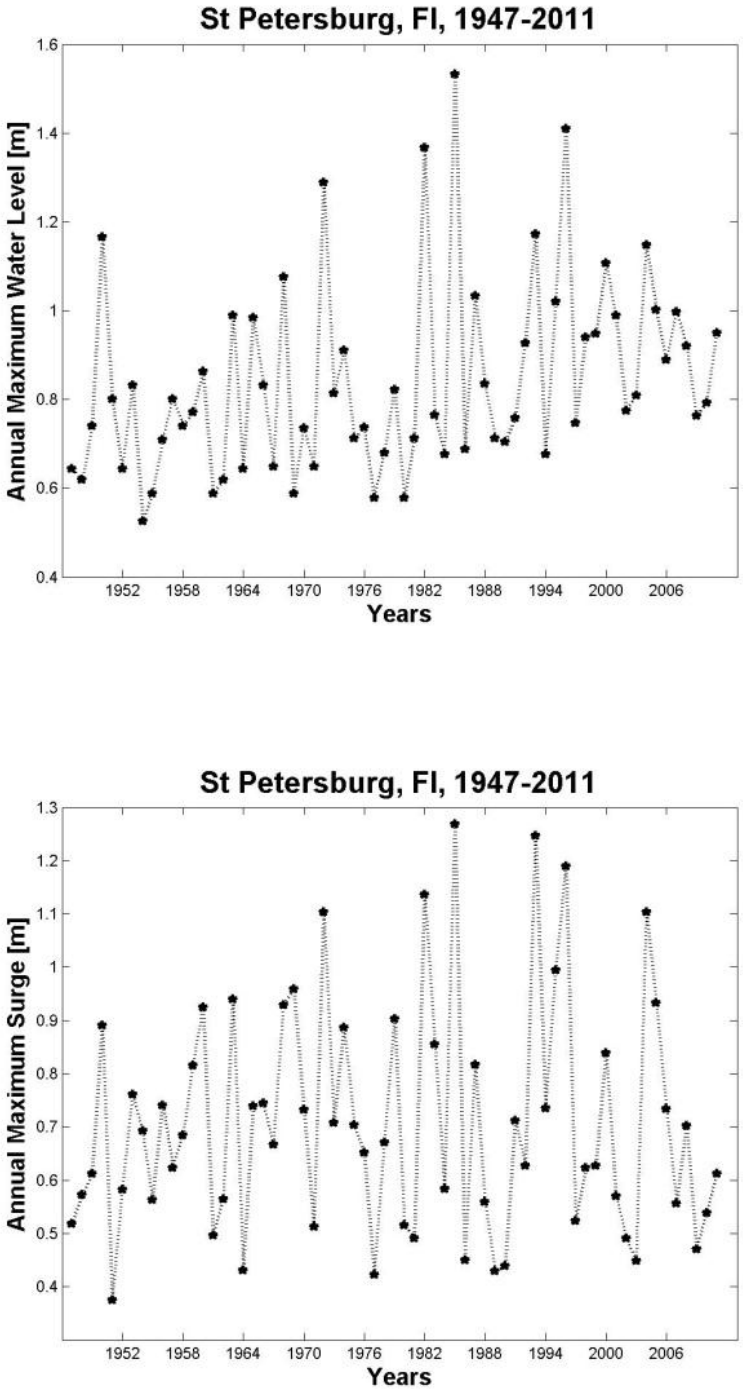

Figure 3.10.h. ***Annual maximum water level time series (on the top) and annual maximum surge time series (on the bottom) for St. Petersburg station.***

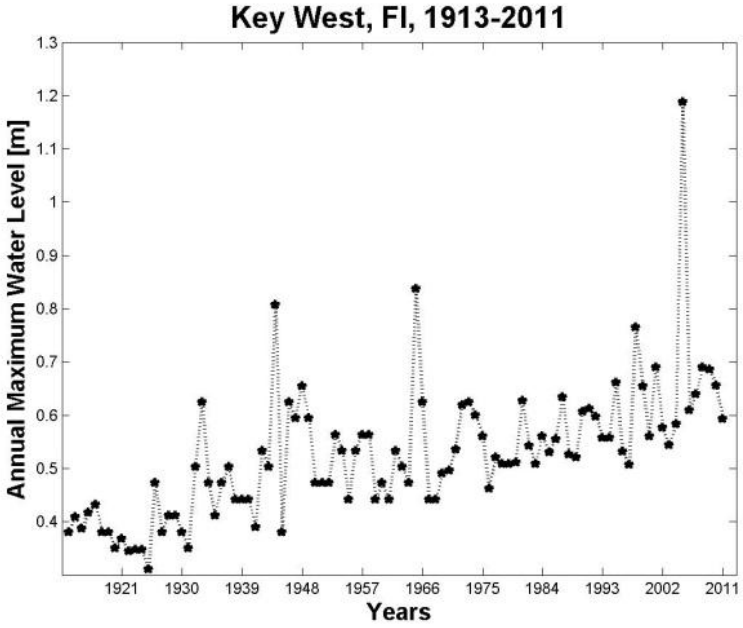

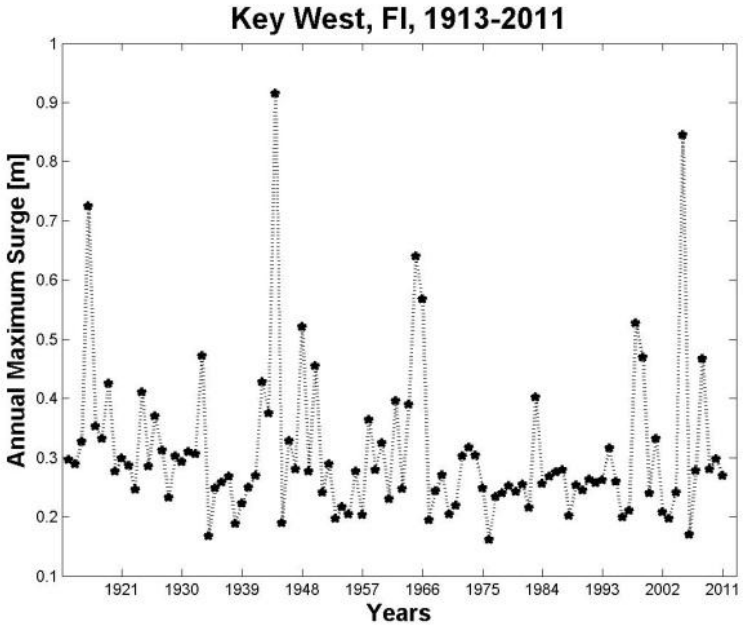

Figure 3.11.g. ***Annual maximum water level time series (on the top) and annual maximum surge time series (on the bottom) for Key West station.***

Generalized Extreme Value Distribution

The generalized extreme value distribution (GEV) is selected for this study as discussed in the introduction. The equation and parameters of the cumulative distribution function (CDF) of the GEV for this study are listed below with parameters following the convention of Kotz and Nadaraiah (2000):

$$F(x) = e^{-(1+\xi((x-\mu)/\sigma))^{-1/\xi}}, \quad \mu - \sigma/\xi \le x < \infty \text{ for } \xi > 0,$$

where ξ is a shape parameter, σ is a scale parameter, and μ is a location parameter.

For our data time series, the GEV model was fit using Matlab's gevfit function (MatLab®, 2009a), which uses maximum likelihood to estimate the model parameters.

Two goodness-of-fit tests were used to evaluate the suitability of GEV probability distribution: the Kolmogorov–Smirnov (KS) and the Anderson–Darling (AD) tests (see Chapter 1 section "Extreme value statistical distributions").

Rates of sea level rise

Various studies (Bindoff et al., 2007; Domingues et al., 2008; Edwards, 2007; Gregory, 2008; Vermeer and Rahmstorf, 2009) indicate a large uncertainty in projections of the sea level rise by the end of the century. The difficulties in accurate estimation of sea level rise are due to uncertainty related to future changes in global atmospheric temperatures, as well as ongoing research on the future contributions of melting ice

sheets from Greenland and Antarctica (Gregory, 2008; Hansen, 2007; Meehl et al., 2007; Shum et al., 2008). For the purpose of this study, two scenarios of sea level rise were selected:

- A very conservative continued linear sea level rise based on the 20th century trends for each station (Table 3.3), resulting in increase in sea level by year 2100 shown in Table 3.3 as compared to the mean sea level referenced to the middle of the respective stations' epochs (Table 3.2);
- A quadratic model of sea level rise, resulting in a total increase in sea level by year 2100 as compared to the mean sea level referenced to the middle of the epoch applicable for each station (Table 3.1) presented in Table 3.3. For this second scenario the local vertical land motions (Table 3.3) for each station were estimated by comparing last century's rate of local sea level rise (Table 3.1) with a global rate of sea level rise of 1.7 mm/year (Bindoff et al., 2007). A quadratic model of sea level rise was then added to the vertical land motion rate to bridge the years between the last water level measurements and the global increase in sea levels as estimated for the A1FI 2090-2099 upper bound level (Meehl et al., 2007).

The first scenario was labeled as "Lowest Scenario" in the recent NOAA report (Parris et al., 2012). While the second scenario is considered here as an upper bound substantially higher sea level rise projections can be found in recent work e.g. in (Vermeer and Rahmstorf, 2009). It is also important to remember that the IPCC Fourth Assessment Report (AR4) (Meehl et al., 2007) projections do not include the likelihood of future acceleration of glacial contributions (Shum et al., 2008). "At this stage, the

greatest uncertainty surrounding estimates of future global SLR is the rate and magnitude of ice sheet loss, primarily from Greenland and West Antarctica" (Parris et al., 2012).

Station name	State	Trend [mm/year]	Sea Level Increase by 2100 for Conservative Scenario [m]	Vertical Land Motion [mm/year]	Sea Level Increase by 2100 for A1FI Scenario [m]
Port Isabel	Tx	3.64	0.32	1.94	0.81
Rockport	Tx	5.16	0.46	3.46	0.96
Galveston Pier 21	Tx	6.39	0.57	4.69	1.09
Galveston Pleasure	Tx	6.84	0.61	5.14	1.13
Grand Isle	La	9.24	0.82	7.54	1.38
Pensacola	Fl	2.10	0.19	0.40	0.68
St. Petersburg	Fl	2.36	0.21	0.66	0.70
Key West	Fl	2.24	0.20	0.54	0.69

Table 3.3. ***Estimated sea level increases by 2100 for all stations for the conservative and A1FI scenarios.***

Computation of increases in exceedance probabilities by 2100

Water levels are driven by high frequency forcing, tidal, and meteorological, and by longer term factors such as local subsidence and global sea level rise (CCSP, 2009). For the study locations these events are driven by meteorological forcing such as tropical and extra tropical storms with possible impact from precipitation and riverine input. Bender et al. (2010) suggest that climate change will modify both the overall frequency of tropical storms and the intensity distribution of storms in the Atlantic basin. On the other hand records of past storm activity including recent events are yet to indicate any significant trend for the Atlantic Basin (Landsea, 2007), and Gulf of Mexico in particular (Levinson

et al., 2010). Also, storm surge is not well correlated with the intensity of tropical storms. Estimates of changes in other storm characteristics such as size (Irish et al., 2008) and forward speed (Rego and Li, 2009) would have to be combined with possible changes in storm frequency to attempt estimates of changes in future storm surges. "Although a consensus has not yet been reached on how the frequency and magnitude of storms may change in coastal regions of the US, it is certain that higher mean sea levels increase the frequency, magnitude, and duration of coastal flooding associated with a given storm" (Parris et al., 2012). The stationarity of the surge distribution for Galveston Pier 21 station was verified by Warner and Tissot (2012). For this research we assume that the surge distributions and meteorological forcings that drive the surge and frequency of the tropical storms in the study area will remain unchanged for the next century. The previously selected GEV distributions was fitted to each location to project water level exceedance probabilities for future years while considering the two possible sea level rise scenarios, described in section "Rates of the sea level rise" of this Chapter. To evaluate the impact of sea level rise on future indundation frequencies the ratios between exceedance probability in 2100 and exceedance probability in 2011 for various water levels for each station were computed.

Nonparametric Bootstrap method to estimate confidence intervals

The bootstrap technique was introduced by Efron (1979) and is further described in Efron and Tibshirani (1993) and Davison and Hinkley (1997). To investigate the uncertainty of the surge distribution, a nonparametric method was used. For this method,

bootstrap samples are replicated from the empirical distribution. The method is used to approximate parameters or derived quantities of a population or probability distribution when the true values of the parameters are unknown. This method was used by Warner et al. (2012b) to estimate 90% and 95% confidence intervals for the ratios between exceedance probability by the end of the century and present values of the probability of inundation for Galveston 21, TX station. The present work follows the same method to estimates the 90% and 95% confidence intervals for the relative increases in the probability of inundation for each of the selected locations. The family of the GEV includes three types of distribution (Weibull, Gumbell, and Frechet) depending on the value of the shape parameter. For this study the Frechet type of GEV distribution with positive shape parameter was selected as the best fit. When bootstraps cases resulted in models with negative shape parameters bootstrap samples were rejected as the resulting data do not lead to an appropriate fit with the GEV distribution and new bootstrap samples redrawn. The number of rejected bootstraps was not significant for all stations except St. Petersburg station. For St. Petersburg station ~30% of the bootstrap samples are removed from both scenarios. The impact of the removal of these bootstrap samples will be will be discussed in the Results and Discussion section.

RESULTS AND DISCUSSION

Cross-shore distance and magnitude of the surges

One of the goals of this research is to assess how differences in coastal setting will affect the vulnerability of the locations to sea level rise. The cross-shore distances seaward from the shoreline to the 30 m depth contours were approximated for each of the stations in ArcGIS and presented in Table 3.1. Other characteristics of the annual maximum surges at each station are presented in Table 3.2. To highlight the differences in the magnitude of the storm surges depending on the local coastal morphology cross-shore distances were plotted against medians of the annual maximum surges for each location and presented in Figure 3.5. The correlation coefficients between cross-shore distances to 30 m depth contours and medians, means, maximums, minimums, and ranges of the annual maximum surges are presented in Table 3.4. The results indicate that the distances of the stations from the continental shelf is directly related to the historical ranges of surges, the further away a station is from the continental shelf, the more time for a storm to build a surge. For example, the Key West station is the closest study location to the continental shelf and has a small range of surges, while the Galveston stations have wide continental shelf and have large surge ranges. The results of this study are consistent with previous work stating that the height of the surge is directly proportional to the width of the shallow water (Hicks, 2006) and that 75% of surge is generated in waters shallower than 30 m (Irish and Resio, 2010).

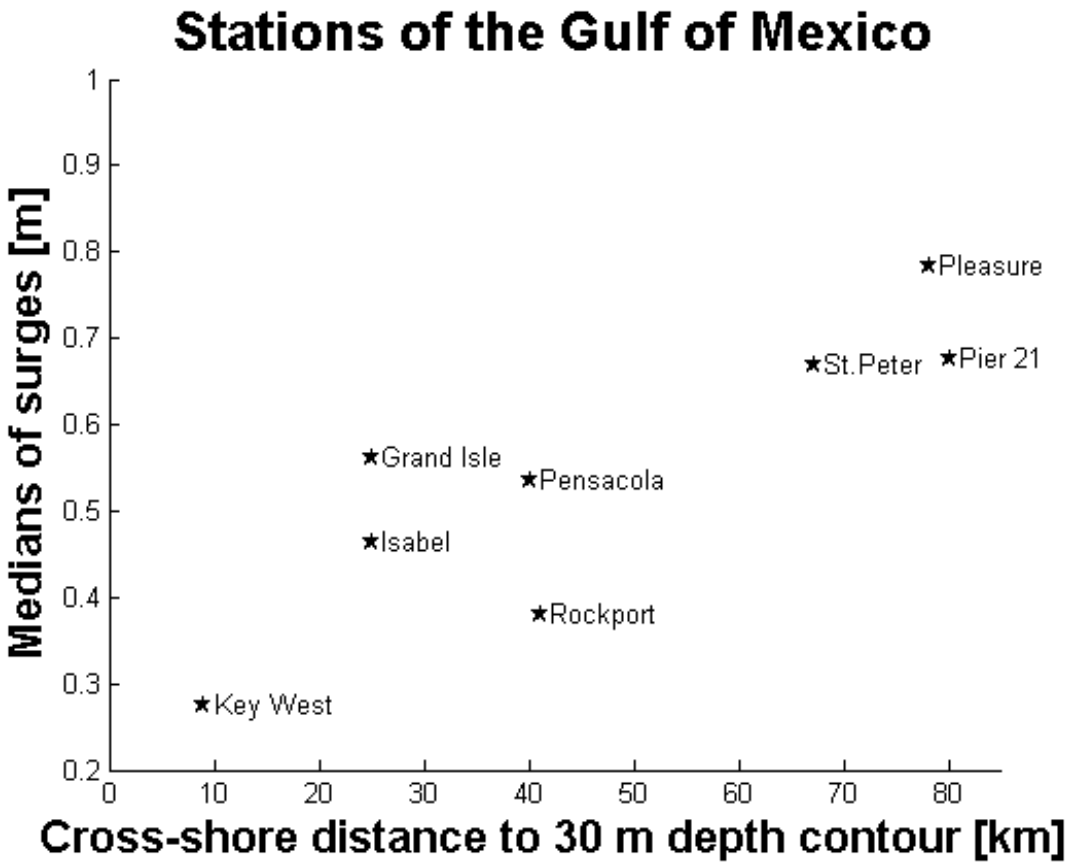

Figure 3.12. ***Cross-shore distances vs. medians of the annual maximum surges.***

	Max	**Min**	**Range**	**Mean**	**Median**
Cross-shore distance to 30 m depth contour	**0.69**	**0.81**	**0.65**	**0.86**	**0.86**

Table 3.4. ***Correlation coefficients between cross-shore distances to 30 m depth contours vs. medians, means, maximums, minimums, and ranges of the annual maximum surges.***

GEV model of the historical data and its parameters

Values of the parameters and graphs of surge exceedance probabilities

The parameters of the GEV distribution based on the historical surge record for each study station were estimated and are presented in Table 3.5. Two goodness-of-fit tests were used to evaluate the suitability of GEV probability distribution: the Kolmogorov–Smirnov (KS) and the Anderson–Darling (AD) tests. The results show that GEV distribution is a good fit for evaluating the probability of inundation for study locations. The exceedance probability is the likelihood that surge will exceed a given level and indicate how often surges of different magnitudes are expected to occur at each location. The exceedance probability curves were calculated by fitting the three parameters of the GEV distribution function and are presented in Figure 3.6 for surges between 0 and 2 m. The exceedance probabilities for the same surges differ significantly among locations. For example, the exceedance probability of a 0.5 m surge for Key West is less than 10% while 0.5 m surges are expected annually for the stations of Galveston Pleasure Pier, Galveston Pier 21, St. Petersburg, Grande Isle, and Pensacola.

Location parameter

The GEV location parameters for the respective stations vary from 0.25 to 0.72. The location parameter describes the shift of a distribution along the horizontal axis i.e. specifies where the distribution is centered. GEV location parameters for our stations are

positively correlated with the mean, median, and maxima of the surge distributions, and the cross-shore distances to the 30 m depth contour.

Station name	State	Shape parameter ξ	Scale parameter σ	Location parameter μ
Port Isabel	Tx	0.50	0.10	0.40
Rockport	Tx	0.32	0.11	0.35
Galveston Pier	Tx	0.34	0.17	0.61
Galveston	Tx	0.30	0.21	0.72
Grand Isle	La	0.33	0.14	0.50
Pensacola	Fl	0.43	0.11	0.49
St.Petersburg	Fl	0.05	0.16	0.60
Key West	Fl	0.24	0.06	0.25

Table 3.5. ***The parameters of the GEV distribution of the historical surge records.***

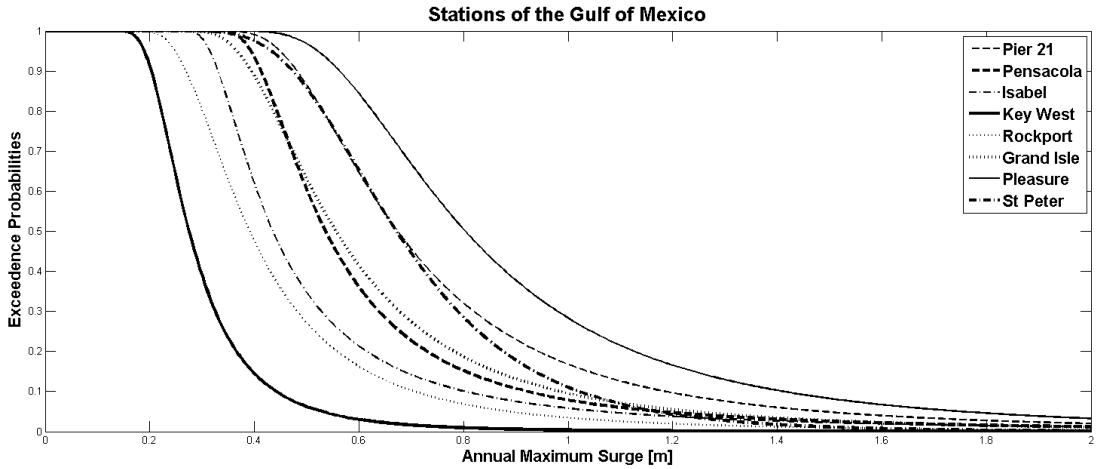

Figure 3.13. ***The exceedance probability curves for surges between 0 and 2 m for all study locations.***

Scale Parameter

The scale parameters for the stations vary from 0.07 to 0.21. The scale parameter describes the spread of the surge distribution and defines where the bulk of the distribution lies. As the scale parameter increases, the distribution will become more spread out. The scale parameter represents the dispersion. The parameter correlates with the cross-shore distances to the 30 m contour, the maximums, means, medians, and ranges of the annual maximum surges. The smallest scale parameter is for the Key West station which experiences the smallest surge range of the study stations.

Shape parameter

The shape parameters vary from 0.05 to 0.50 and are indicative of the respective skewness of the surge distributions and in particular indicative of the distributions' tails. A shape parameter determines the rate of tail decay and the shape of the upper tail of the distribution. The shape parameter for St. Petersburg is substantially smaller at 0.05 as compared to the shape parameters for the other stations ranging from 0.24 to 0.50. The smaller shape parameter for St. Petersburg is indicative of a more rapid decay of the tail of the modeled distribution and is linked to the absence of outliers, i.e. larger surge events as compared to the Annual maximum average surges (see Figure 3.6).

The ratios of water level exceedance probabilities by 2100

We use the respective GEV distributions fitted for each location to project future water level exceedance probabilities while considering the two possible sea level rise scenarios described in section "Rates of the sea level rise" of this Chapter. To evaluate the impact of sea level rise on future indundation frequencies the ratio between exceedance probability in 2100 and exceedance probability in 2012 are computed. The curves of the ratios for different water levels are presented in Figure 3.7 and the values for the maximum exceedance ratios and their corresponding water levels are presented in Table 3.6 for both scenarios.

Station name	State	Water level at max ratio for conservative scenario [m]	Max ratio for conservative scenario	Water level at max ratio for A1FI scenario [m]	Max ratio for A1FI scenario
Port Isabel	Tx	0.65	5.4	1.07	19.7
Rockport	Tx	0.75	10.26	1.15	44.44
Galveston Pier 21	Tx	1.10	6.42	1.50	18.54
Galveston	Tx	1.26	5.36	1.63	13.78
Grand Isle	La	1.23	17.29	1.65	45.16
Pensacola	Fl	0.64	2.60	1.02	12.48
St.Petersburg	Fl	1.02	2.81	1.35	21.15
Key West	Fl	0.44	6.93	0.83	112.52

Table 3.6. ***Water levels at maximum ratios and maximum ratios for both scenarios.***

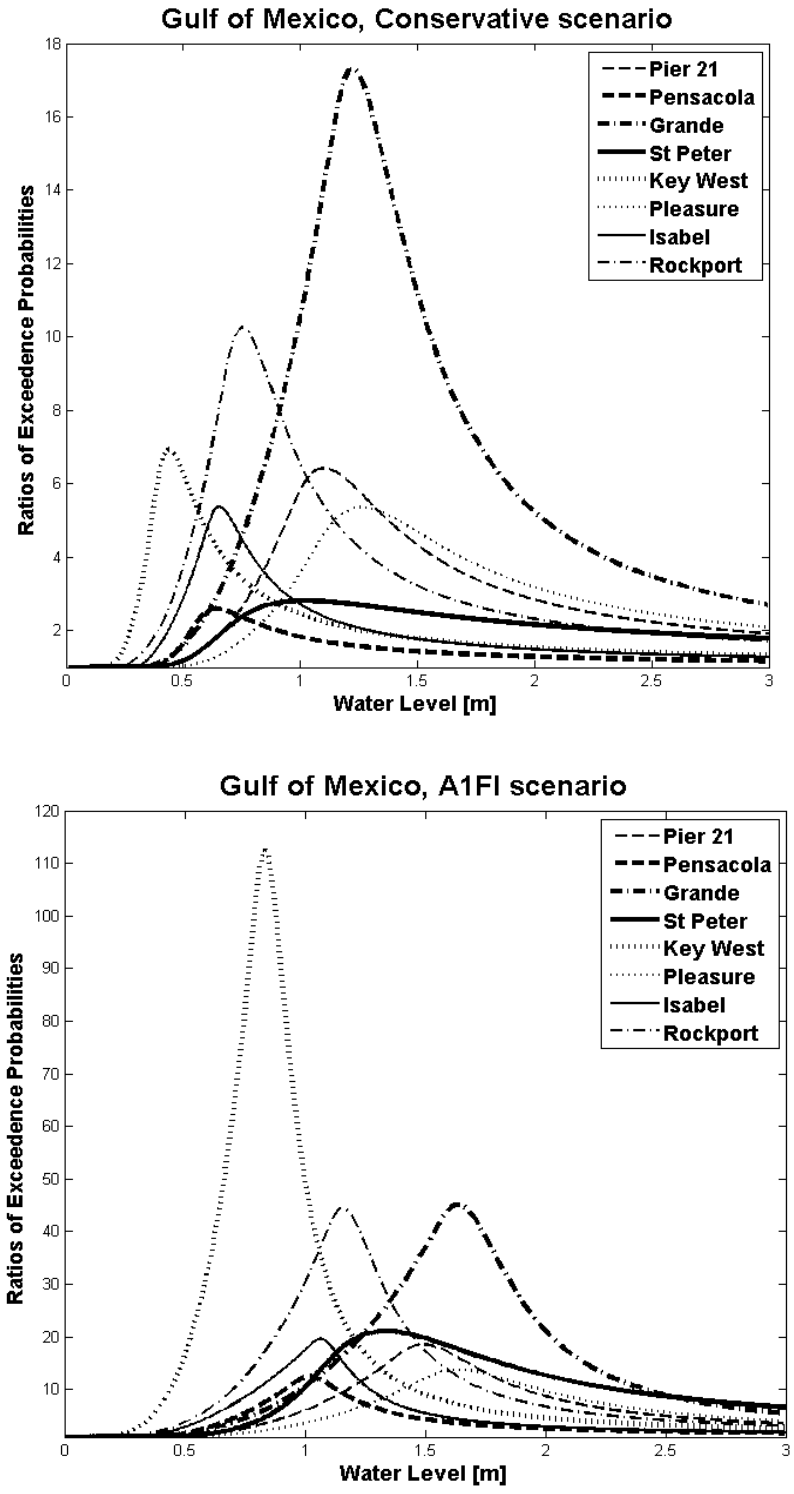

Figure 3.14. ***Ratios of exceedance probabilities for the conservative (on the top) and the A1FI based (on the bottom) scenarios.***

The ratios of exceedance probabilities vary substantially by location and by sea level rise scenario. The smallest maximum ratio is observed for the Pensacola station for both scenarios. It can be explained by the smallest rate of subsidence and a relatively large surge range for this station. The maximum ratio for St. Petersburg is 3, about the same as that for Pensacola for the conservative scenario. The locations have similar rates of sea level rise, 2.10 mm/year and 2.36 mm/year, and similar mean surges of 0.64 m and 0.71 m respectively leading to similar probabilities of inundation by 2100. The difference in maximum ratios for A1FI scenario for these stations can be explained by the diminishing relative importance of subsidence rates with increasing global rates of sea level rises. The difference in maximum ratios between the two stations becomes dominated by the difference in surge ranges leading to the higher ratio of 21 for St. Petersburg versus 12 for Pensacola. As discussed later in this section, the results for St. Petersburg are less robust than those of other stations due to the lack of large surges in the existing record and must therefore be analyzed cautiously.

Key West, Galveston Pier 21, Galveston Pleasure Pier, and Port Isabel stations have similar maximum ratios (between 5.4 and 6.9) for the conservative scenario. These ratios are the combination of either a small rate of sea level rise (Key West station 2.24 mm/year and Port Isabel station 3.64 mm/year) and small surges (mean of surges for Key West station 0.31 m and for Port Isabel station 0.52 m) or a larger rate of sea level rise (Galveston Pier 21 station 6.39 mm/year and for Galveston Pleasure Pier 6.84 mm/year) and larger surges (mean of surges for Galveston Pier 21 station 0.79 m and for Galveston Pleasure Pier 0.93 m). The two groups of stations however differ by the water levels at

the maximum ratios, larger for the Galveston stations (1.10 m and 1.26 m) than for the Port Isabel (0.65 m) and Key West (0.44 m) stations.

Although the Rockport station has small surges (mean 0.46 m), it has a large rate of sea level rise (5.16 mm/year) resulting in a larger increase in inundation probabilities for the conservative scenario (maximum ratio 10.3) as compared to the previously mentioned stations. The largest maximum ratio for the conservative scenario is for the Grande Isle station and is caused by the largest local vertical land motion of 7.54 mm/year among our study locations.

Pensacola, Galveston Pleasure Pier, Galveston Pier 21, and Port Isabel stations have similar maximum ratios for the A1FI scenario (between 13 and 21), which indicates that the future probability of inundation for stations with similar surge ranges will likely be similar. Variation in water levels at maximum ratios for these stations for A1FI scenario (1.02 m -1.63m) can be explained by the differences in medians of the historical surges.

The maximum ratio for A1FI scenario for the St. Petersburg station is similar to the maximum ratios for the Pensacola, Galveston Pleasure Pier, Galveston Pier 21, and Port Isabel stations, but the range of surges is much smaller, which makes the St. Petersburg station an exception. The main reason for this difference is the absence of outliers or large surges for this station (Figure 3.3). While modeled appropriately based on the existing record, its distribution will change substantially when impacted by a major hurricane. Accordingly to Needham and Keim (2011) large surges (3.2 m) were recorded for nearby location in Tampa Bay prior to the available record in 1921 (~25 kilometers from study location). It is reasonable to assume that a big hurricane will eventually land and result in a large surge at St. Petersburg station.

The largest maximum ratio for the A1FI scenario is for the Key West station. A ratio of water level exceedance probabilities of 112 for that station may seem surprising, but it is the result of the relatively narrow range of historical surges (0.8 m) for this station. The small surge range is in large part related to the narrow extent of the continental shelf offshore of the station. This maximum ratio for Key West is reached for a water level of 0.89 m. At the end of 2011 the probability of water level exceeding 0.89 m was less than 1%. With a sea level rise of 0.69 m by year 2100 the probability of reaching the same level increases to 80% leading to a ratio of 112.

Although Grande Isle and Rockport stations differ in the magnitude of their surges (means of 0.64 m and 0.46 m respectively) they both have small surge ranges and as a result will likely experience substantial and similar impact of sea level rise for the A1FI scenario (maximum ratios are 45.2 and 44.4 respectively). The two stations however differ by the water levels at the maximum ratios, larger for the Grande Isle station (1.65 m) than for the Rockport (1.15 m) station.

The large maximum ratios of the exceedance probabilities for Key West, Rockport, and Grande Isle stations indicate that locations with historically narrow surge ranges could be relatively more affected by sea level rise for accelerating sea level rise scenarios.

Maximum ratios of the exceedance probabilities depend mostly on sea level trends and the shape of the curves of the exceedance probabilities. The maximum ratios are strongly correlated to the sea level trends for the conservative scenario (correlation coefficient 0.77), but not for the A1FI. For the conservative scenario the sea level rise trends are 2.10-9.24 mm/year. For the A1FI scenario the relative differences in trends are smaller

(6.36-13.5 mm/year) and the respective shapes of the exceedance probability distributions becomes the dominant factor. This result indicates that for the lower sea level rise scenarios the different rates of subsidence around the Gulf of Mexico, including local anthropogenic impact due to fluid extraction, are the most important for increases in inundation probabilities. For higher rates of global sea level rise local subsidence becomes less important as global sea level rise becomes the dominant factor in local rates of sea level rise. For higher rates of global sea level rise such as this study's A1FI based scenario locations with low rates of vertical land motion combined with narrow surge ranges such as the Key West station have the largest ratios of exceedance probabilities and become the most at risk.

Water levels at maximum ratios

Values of water levels at maximum ratios

Values of water levels at maximum ratios are presented in Table 3.6. Substantial differences in water levels at maximum ratios can be observed for both scenarios. The values vary from 0.44 m to 1.26 m for the conservative scenario and from 0.83 m to 1.65 m for the A1FI scenario. The curves of the probabilities of water levels exceeding these values by 2100 are presented in Figure 3.8 and allow for a comparison of the changes in water level exceedance probabilities by 2100.

The change in inundation frequency for the water levels at maximum ratios increases much more slowly for the St. Petersburg station than for the other stations for both

scenarios. The slower increase is the result of a different surge distribution for this station due to the absence of outliers and the related small skewness of the dataset. Two goodness-of-fit tests were used to evaluate the suitability of GEV probability distribution: the Kolmogorov–Smirnov (KS) and the Anderson–Darling (AD) tests. Although St. Petersburg station's records do not have outliers, the GEV distribution is a good fit for the existing data set and a good model to evaluate the probability of inundation for this area for low to medium surges. As will be discussed later in this section, the absence of outliers or large surges leads to a substantially broader confidence interval for surges around 1.3 m and above. This broader confidence interval for large surges affects the precision of the estimates for the maximum ratios and their associated water levels.

As expected the faster rate of sea level rise of A1FI scenario leads to substantially larger increases in water level exceedance frequency for all stations. For example, for the conservative scenario the exceedance probability of the water levels at maximum ratios increases from 5-30% to 70-90% while for A1FI scenario it increases from 1-7% to 86-97% by 2100. For the A1FI based scenario, exceedance probabilities become similar by 2060-2080 for all stations except St. Petersburg. The stations with the smallest water levels for maximum exceedance probabilities are Key West (0.83m), Pensacola (1.02m), Port Isabel (1.07m) and Rockport (1.15m). These substantial increases in exceedance probabilities for all stations further highlight and quantify the impact of sea level rise as the century progresses.

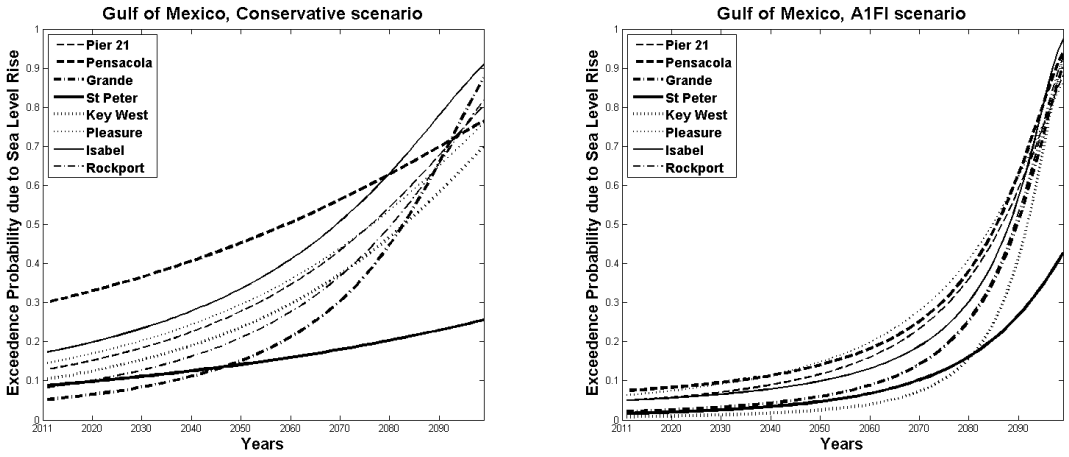

Figure 3.15. ***Exceedance probabilities of water levels at maximum ratios by 2100 for conservative scenario (on the left) and A1FI scenario (on the right).***

Water levels at maximum ratios vs. max, min, mean, median, GEV scale parameter, GEV location parameter, and bathymetry

The correlation coefficients between water levels at maximum ratios and cross-shore distances to 30 m depth contours, medians, means, maximums, minimums, ranges of the annual maximum surges, and parameters of the GEV distribution are presented in Table 3.7. Water levels at maximum ratios have strong correlation with all statistics except the maximum annual surges, which indicates that the results of this study are not overly sensitive to the most extreme value or largest surge on record provided that the record includes at least one large surge.

	Cross-shore distance to 30 m depth contour	Max	Min	Mean	Median	GEV Scale parameter	GEV Location parameter
Water levels at maximum ratios	0.68	0.41	0.80	0.84	0.85	0.92	0.84

Table 3.7. ***The correlation coefficients between water levels at maximum ratios and cross-shore distances to 30 m depth contours, medians, means, maximums, minimums, ranges of the annual maximum surges, and parameters of the GEV distribution.***

The plot of water levels at maximum ratios with respect to the median maximum annual surges is presented in Figure 3.9. The water levels at maximum ratios for the stations with larger median surges are higher for both sea level rise scenarios.

The relation between water levels at maximum ratios and cross-shore distance to 30 m depth contour is shown in Figure 3.10. Locations with shorter distances to the continental shelf will have smaller water levels than locations that are further away from the continental shelf. The result for Grande Isle could be explained by much higher local subsidence for the location influencing the water levels at maximum ratios as discussed in section "Values of water levels at maximum ratios" of this Chapter.

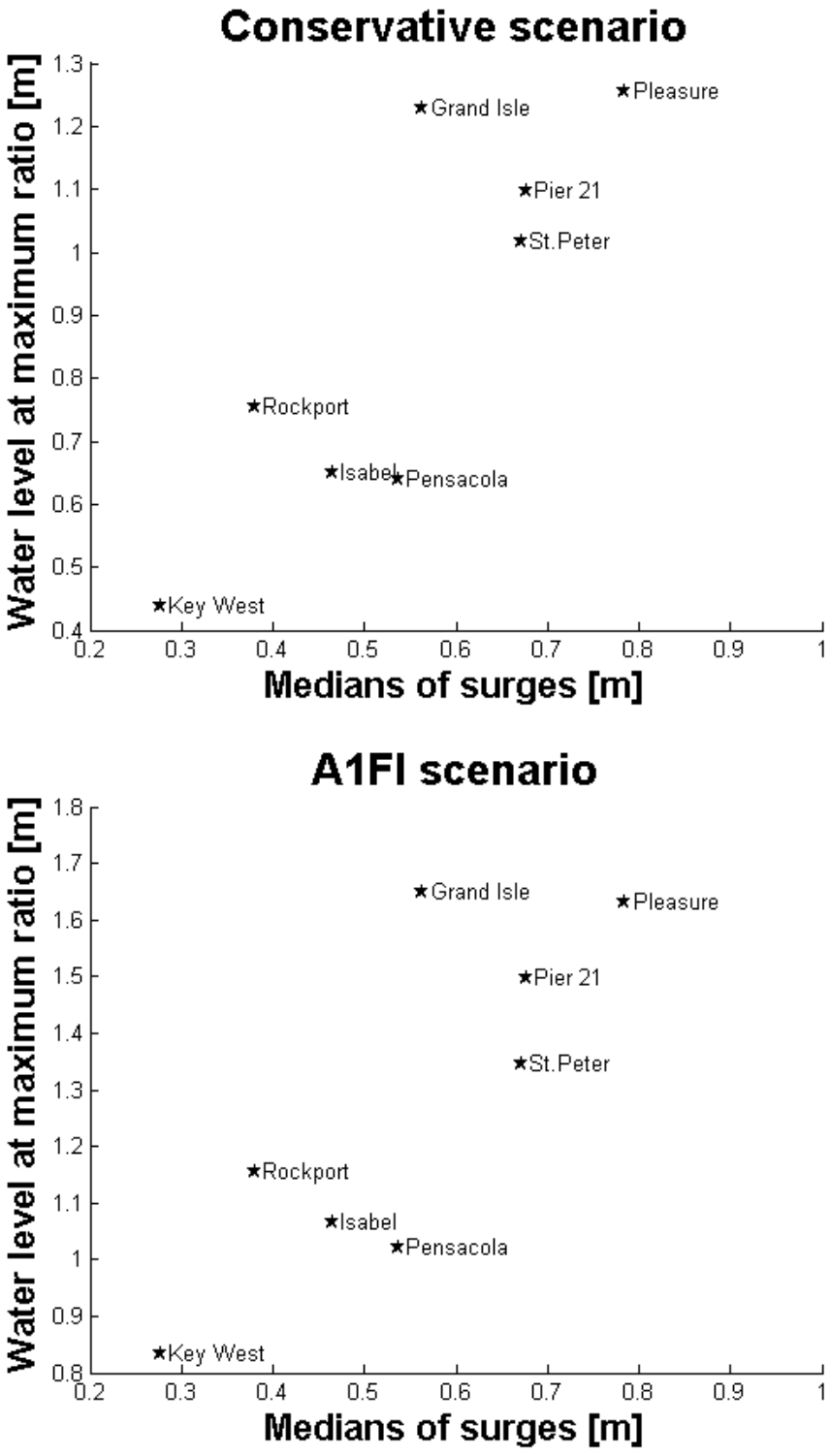

Figure 3.16. ***Water levels at maximum ratios vs. medians of surges for conservative scenario (on the top) and A1FI scenario (on the bottom).***

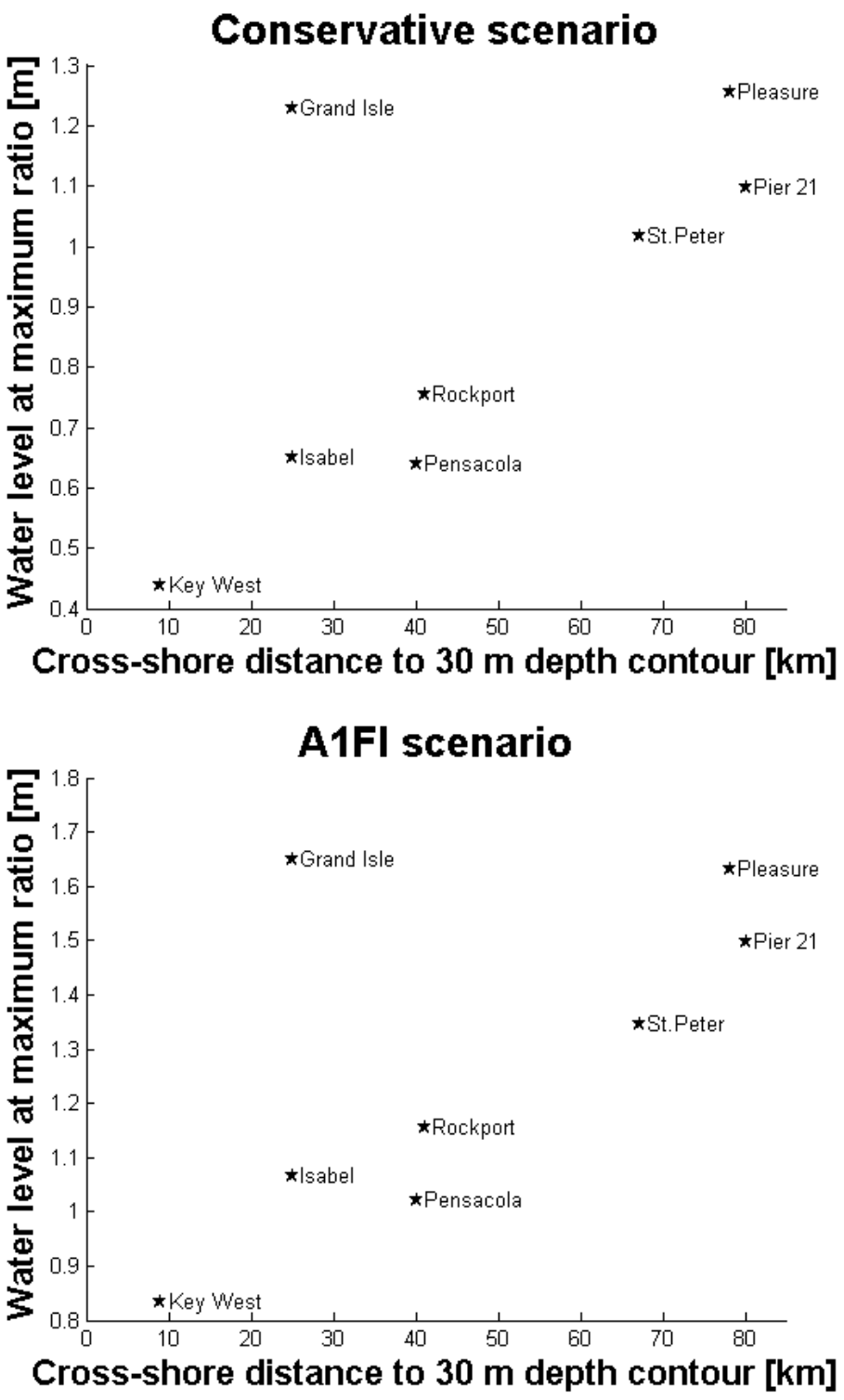

Figure 3.17. ***Water levels at maximum ratios vs. cross-shore distance to 30 m depth contours for conservative scenario (on the top) and A1FI scenario (on the bottom).***

Water levels at maximum ratios and maximums of annual maximum surges

Water levels at maximum ratios for both scenarios and maximums of the historical surges are presented in Table 3.8. It is noticeable that for the Grande Isle station for the conservative scenario the water level at maximum ratio (1.23 m) will be close to the present maximum of annual maximum surges (1.31) m. Based on the historical record through 2011, the probability of water levels exceeding 1.23 m is ~5.3%. With a sea level rise of 9.4 mm/year by year 2100 the probability of reaching the same level increases to ~90% leading to a ratio of ~17 for conservative scenario. For the A1FI scenario the water level at maximum ratio (1.76 m) might be much higher than the present maximum of annual maximum surges. At the end of the dataset in 2011 the probability of water levels exceeding 1.76 m was very small (~1.7%). With a quadratic sea level rise by the year 2100 the probability of reaching the same level increases to ~76% leading to a ratio of ~45 for A1FI scenario.

Key West, St. Petersburg, and Rockport stations have narrower ranges of surges leading to water levels at maximum ratios that exceed the present maximum recorded water level for the A1FI based scenario. For the Grande Isle station the water level at maximum ratio is projected to exceed the maximum of annual maximum surges by 0.45 m.

Results for both scenarios show that by 2100 the Grande Isle station will experience substantial increases in inundation frequencies due to the large local subsidence.

Station name	State	Maximum of the historical surges [m]	Water level at maximum ratio for conservative scenario [m]	Water level at maximum ratio for A1FI scenario [m]
Port Isabel	Tx	1.98	0.65	1.12
Rockport	Tx	1.37	0.75	1.22
Galveston Pier 21	Tx	2.85	1.10	1.57
Galveston Pleasure	Tx	2.84	1.26	1.73
Grand Isle	La	1.31	1.23	1.76
Pensacola	Fl	2.30	0.64	1.08
St.Petersburg	Fl	1.27	1.02	1.35
Key West	Fl	0.91	0.44	0.89

Table 3.8. ***Water levels at maximum ratios for both scenarios and maximums of the historical surges.***

90% and 95% confidence intervals for the ratios of increase in exceedance probabilities

To investigate the uncertainty of the surge distribution, a nonparametric bootstrap method was used. For this method, bootstrap samples are replicated from the empirical distribution. The method is used to approximate parameters or derived quantities of a population or probability distribution when the true values of the parameters are

unknown. When bootstrap cases resulted in models with negative shape parameters such bootstrap samples were rejected as the resulting data did not lead to an appropriate fit with the GEV distribution and new bootstrap samples were redrawn. The number of rejected bootstraps was not significant for all stations except St. Petersburg station. For the station of St. Petersburg ~30% of the bootstrap samples were cut for both scenarios. The impact of the removal of these bootstrap samples was tested by comparing the median of the accepted bootstrap samples with the distribution built from the historic data. For other stations these two distributions are virtually indistinguishable. For the station of St. Petersburg differences are noticeable (See Figure 3.11), but the differences in the ratios of exceedance probabilities remain below 0.33 or about 12% or less for the conservative scenario and about 6 or about 30% for the A1FI scenario. These differences are relatively small as compared to the uncertainty ranges which are about 2 for the conservative scenario and about 40 for the A1FI scenario for most of the water level range at the 90% confidence interval. St. Petersburg was therefore included with the other study locations for the study's overall comparative analysis. The confidence intervals in Figure 3.11 can be further compared with the confidence intervals for the other stations presented in Figure 3.12. Unlike the other stations the St. Petersburg confidence intervals do not decrease substantially for water levels larger after the maximum ratio. These larger uncertainty ranges are due to the lack of large surges in the existing record. These larger uncertainties also affect the estimated values of the maximum ratios and associated water levels and must be taken into account in the related discussions.

Figure 3.12.a-g presents 90% and 95% confidence intervals around the median ratios of increase in exceedance probabilities for both sea level rise scenarios. As the century

progresses the risk of flooding significantly increases for both scenarios. The greatest uncertainties in the estimates coincide with the largest values of the ratios. Even with these uncertainties, the lower bounds of the confidence intervals imply significant increase in exceedance probabilities for each station for both scenarios. The lower and upper bounds of the 90% and 95% confidence intervals for maximum ratios and maximum ratios for both scenarios are presented in Table 3.9. There is almost no difference in the lower bounds of the 90% and 95% confidence intervals for all stations and the ranges between the lower bounds of the confidence intervals and the median ratios are considerably smaller than the differences between the higher bounds of the confidence intervals and the medians. This suggests that coastal planner should make plans for increases in inundation frequencies in at least the range between the 95% confidence interval bound and the median ratio and higher values for larger coastal infrastructure investments.

Station name	State	Maximum ratios for conservative scenario	Lower bound of 90% CI for conservative scenario	Lower bound of 95% CI for conservative scenario	Upper bound of 90% CI for conservative scenario	Upper bound of 95% CI for conservative scenario
Port Isabel	Tx	5.37	4.06	3.87	8.06	9.01
Rockport	Tx	10.26	6.30	5.85	26.39	35.60
Galveston Pier 21	Tx	6.42	4.84	4.61	9.78	10.88
Galveston Pleasure	Tx	5.36	3.78	3.56	9.80	11.86
Grand Isle	La	17.29	9.41	8.59	63.02	96.76
Pensacola	Fl	2.60	2.20	2.14	3.26	3.44
St.Petersburg	Fl	2.81	2.36	2.30	3.40	3.57
Key West	Fl	6.93	4.99	4.74	11.69	13.31

Station name	State	Maximum ratios for A1FI scenario	Lower bound of 90% CI for A1FI scenario	Lower bound of 95% CI for A1FI scenario	Upper bound of 90% CI for A1FI scenario	Upper bound of 95% CI for A1FI scenario
Port Isabel	Tx	19.66	11.51	10.60	49.98	67.74
Rockport	Tx	44.44	18.49	16.41	294.45	593.12
Galveston Pier 21	Tx	18.54	11.48	10.62	37.79	45.73
Galveston Pleasure	Tx	13.78	7.86	7.23	40.94	58.07
Grand Isle	La	45.16	18.28	16.09	289.12	580.95
Pensacola	Fl	12.48	8.11	7.56	23.79	28.39
St.Petersburg	Fl	21.15	11.88	10.96	39.22	46.66
Key West	Fl	112.52	46.39	40.55	596.77	1006.96

Table 3.9. ***The lower and upper bounds of the 90% and 95% confidence intervals for maximum ratios and maximum ratios for both scenarios.***

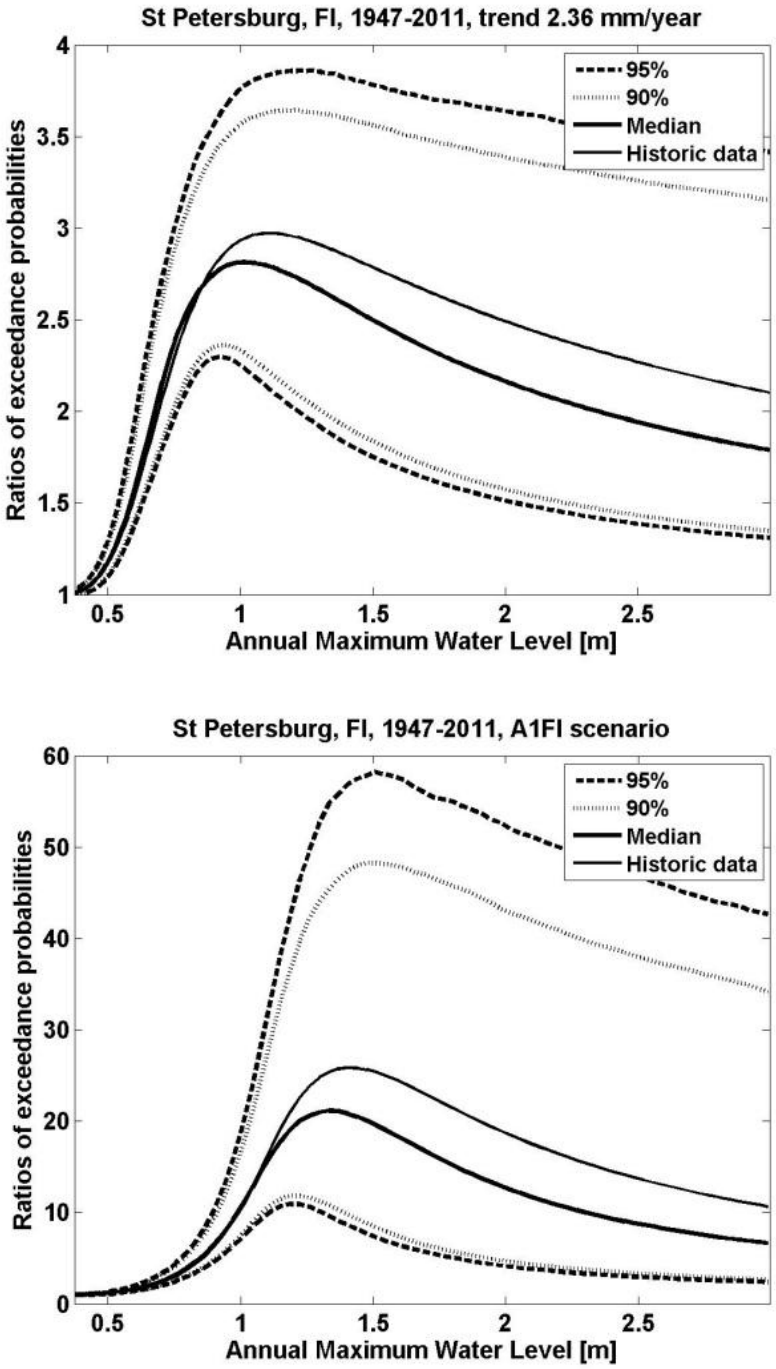

Figure 3.18. ***90% and 95% confidence intervals of the ratios of exceedance probabilities for conservative scenario (on the top) and A1FI scenario (on the bottom) for St. Petersburg station.***

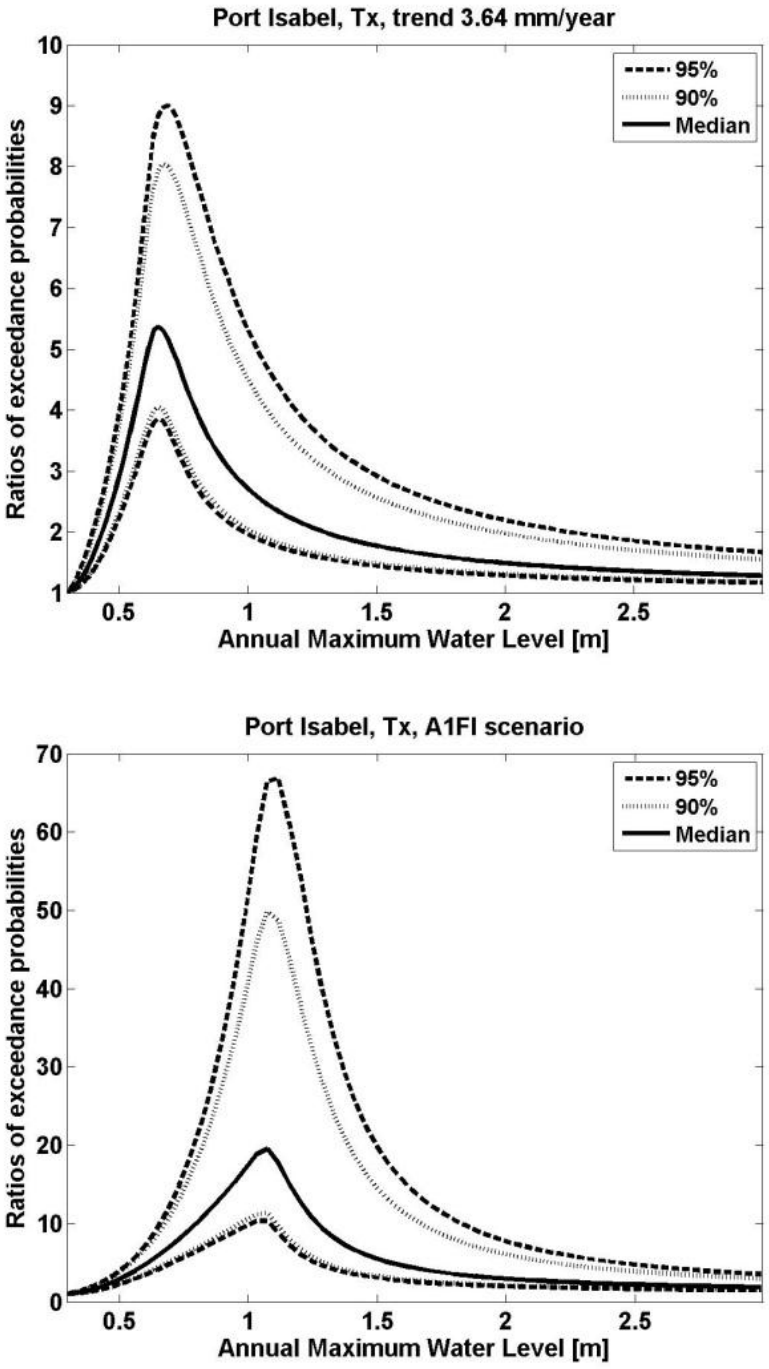

Figure 3.19.a. ***90% and 95% confidence intervals (nonparametric bootstrap) around the ratios of increase of the water level exceedance probability in 2100 versus the present exceedance probability in 2012 for the conservative scenario (on the top) and A1FI scenario (on the bottom) for Port Isabel station.***

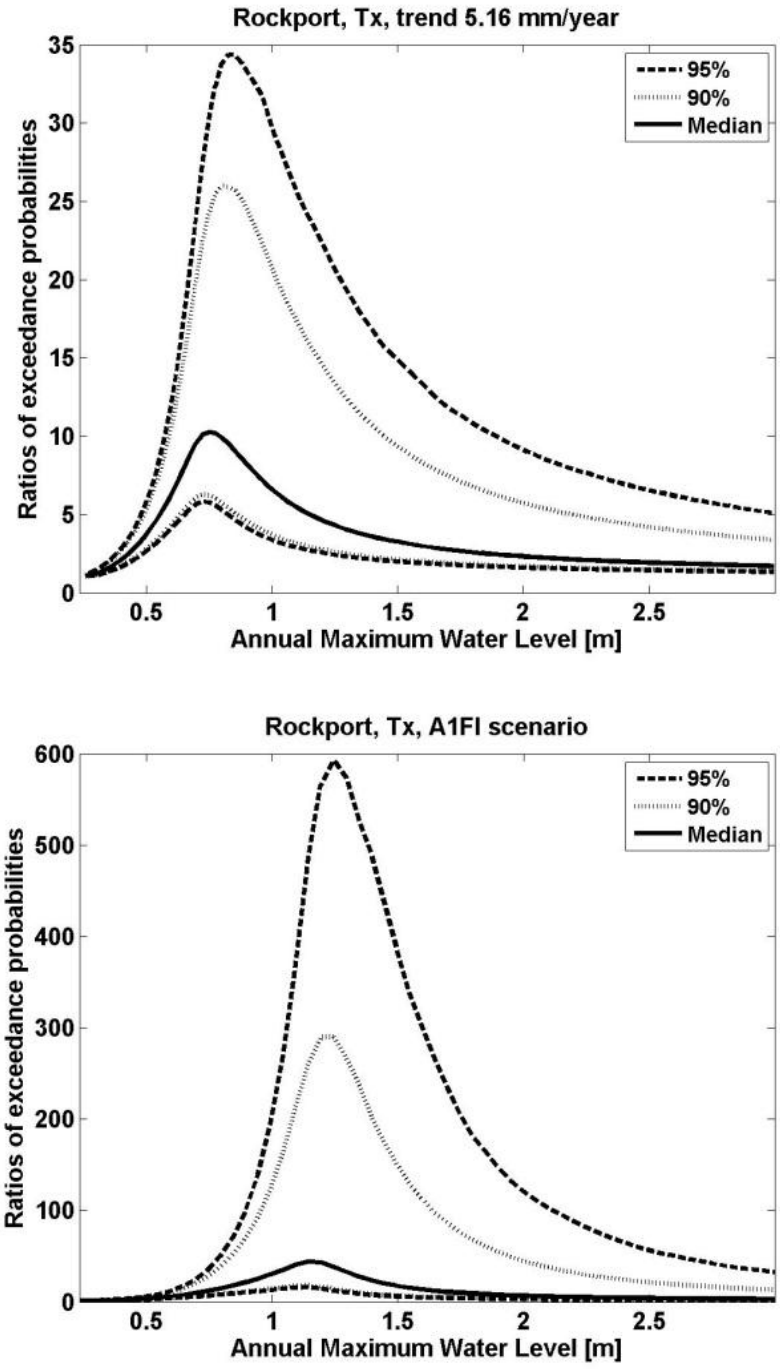

Figure 3.20.b. ***90% and 95% confidence intervals (nonparametric bootstrap) around the ratios of increase of the water level exceedance probability in 2100 versus the present exceedance probability in 2012 for the conservative scenario (on the top) and A1FI scenario (on the bottom) for Rockport station.***

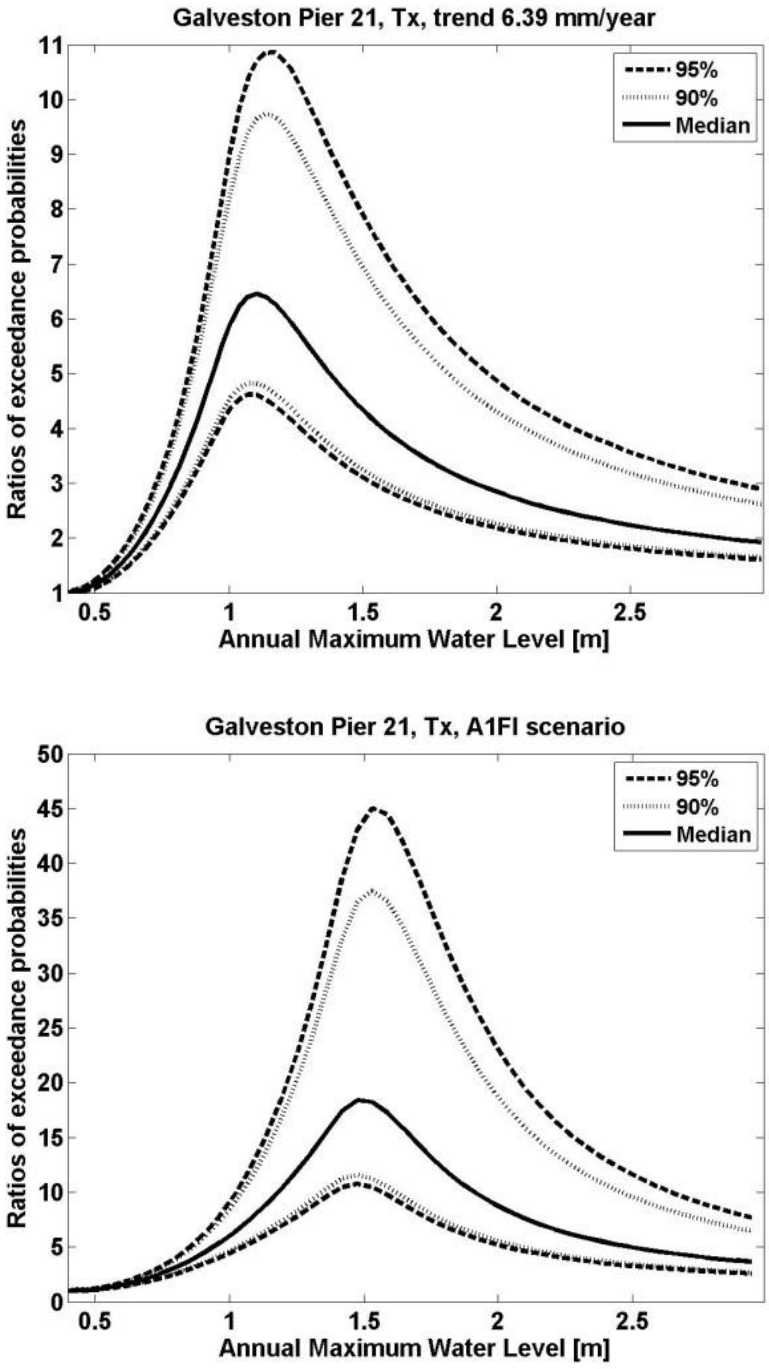

Figure 3.21.c. ***90% and 95% confidence intervals (nonparametric bootstrap) around the ratios of increase of the water level exceedance probability in 2100 versus the present exceedance probability in 2012 for the conservative scenario (on the top) and A1FI scenario (on the bottom) for Galveston Pier 21 station.***

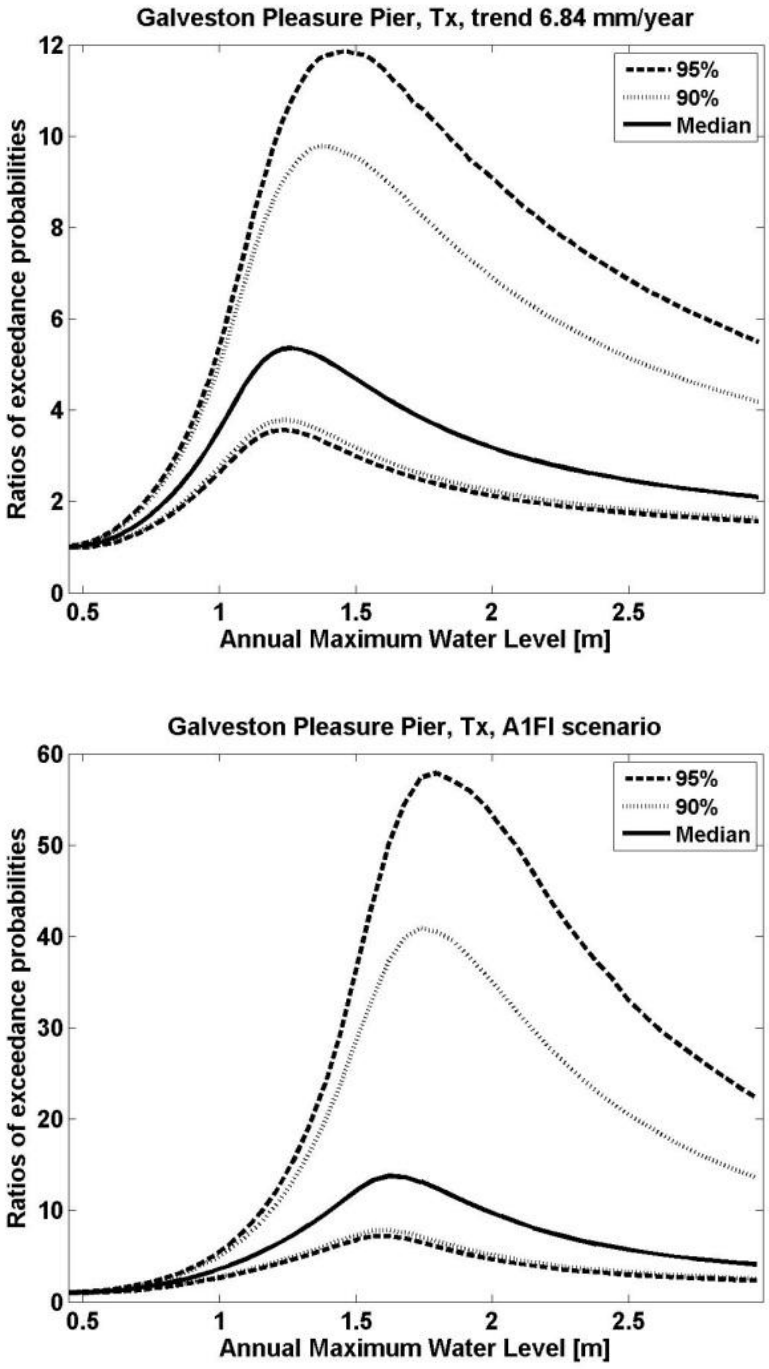

Figure 3.22.d. ***90% and 95% confidence intervals (nonparametric bootstrap) around the ratios of increase of the water level exceedance probability in 2100 versus the present exceedance probability in 2012 for conservative scenario (on the top) and A1FI scenario (on the bottom) for Galveston Pleasure Pier station.***

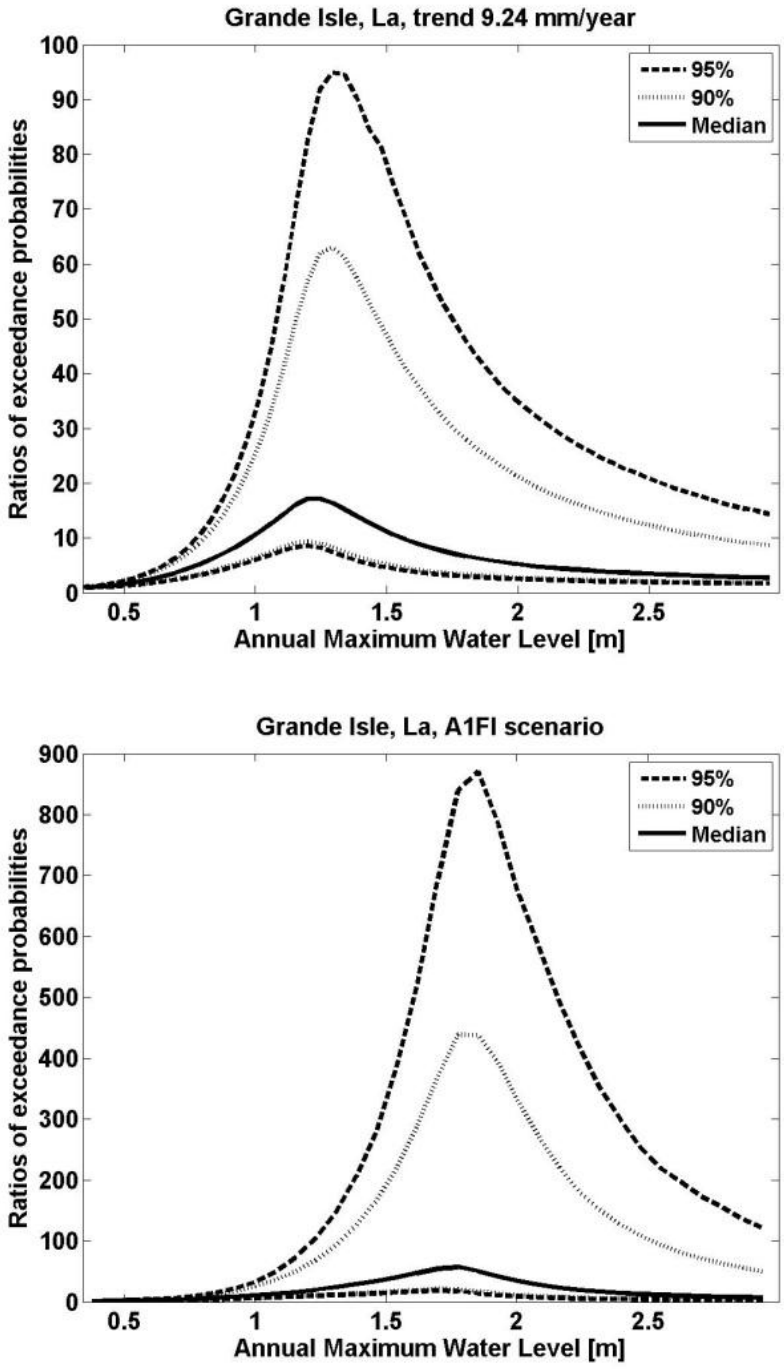

Figure 3.23.e. ***90% and 95% confidence intervals (nonparametric bootstrap) around the ratios of increase of the water level exceedance probability in 2100 versus the present exceedance probability in 2012 for the conservative scenario (on the top) and A1FI scenario (on the bottom) for Grande Isle station.***

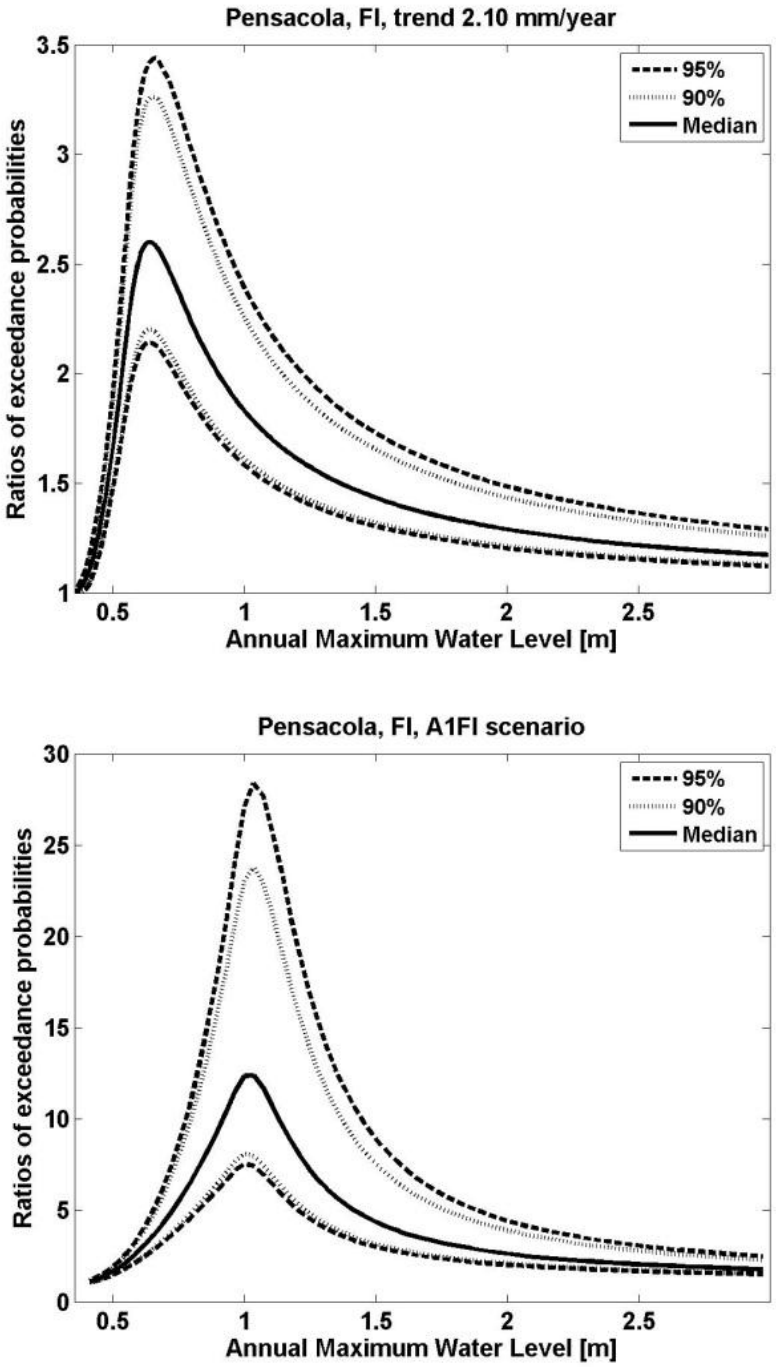

Figure 3.24.f. ***90% and 95% confidence intervals (nonparametric bootstrap) around the ratios of increase of the water level exceedance probability in 2100 versus the present exceedance probability in 2012 for the conservative scenario (on the top) and A1FI scenario (on the bottom) for Pensacola station.***

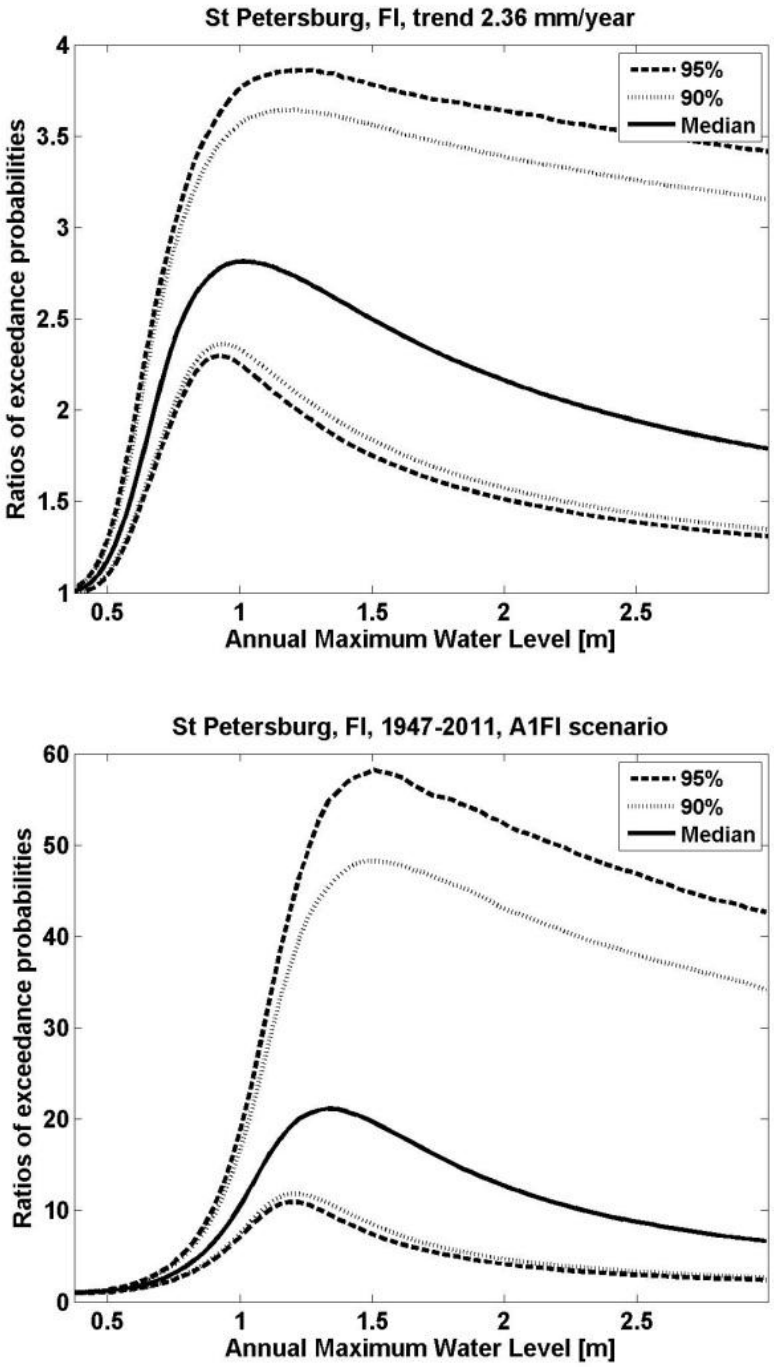

Figure 3.25.h. ***90% and 95% confidence intervals (nonparametric bootstrap) around the ratios of increase of the water level exceedance probability in 2100 versus the present exceedance probability in 2012 for the conservative scenario (on the top) and A1FI scenario (on the bottom) for St. Petersburg station.***

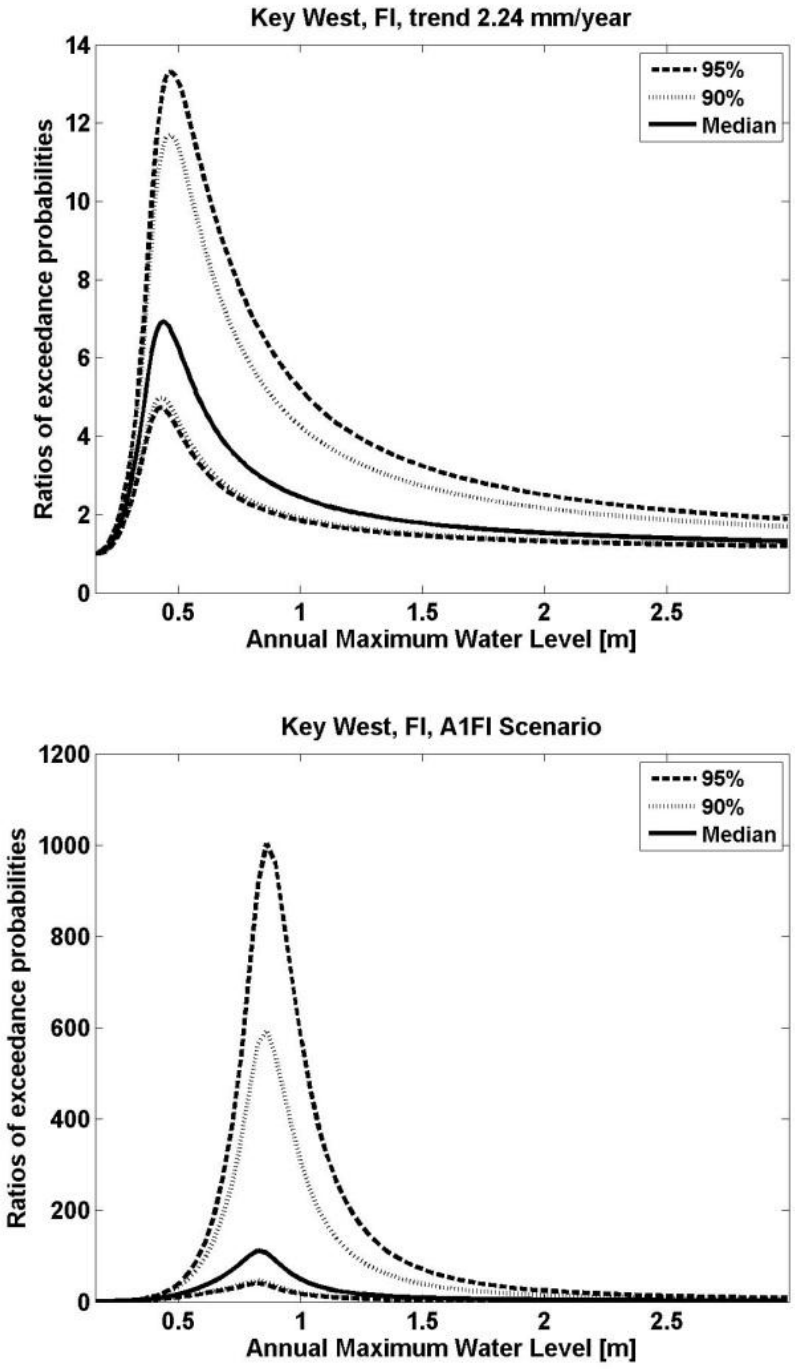

Figure 3.26.g. ***90% and 95% confidence intervals (nonparametric bootstrap) around the ratios of increase of the water level exceedance probability in 2100 versus the present exceedance probability in 2012 for the conservative scenario (on the top) and A1FI scenario (on the bottom) for Key West station.***

To evaluate the robustness of the models the relative difference between maximum ratios of the exceedance probabilities and upper bounds of 95% confidence intervals were computed for both scenarios and plotted against the years of available data. Results are presented in Figure 3.13. The wider confidence intervals for Rockport and Grande Isle stations can be explained by the shorter data sets available for these stations (49 and 32 years respectively). The confidence intervals are narrower for the stations with lengths of the datasets at least 50 years. This observation is consistent with Kyselý's (2008) findings. Kyselý (2008) compares performance of nonparametric bootstraps to fit GEV models for time series of lengths 20, 40, 60 and 100 extreme values, and concludes that $n = 60$ is enough information for the technique to achieve its nominal level of significance. As previously discussed when analyzing confidence intervals for St. Petersburg, the presence of large surges are an additional requirement to provide more precise estimates for larger surges.

The larger result for Key West station for A1FI scenario as compared with stations with similar length of records can be explained by the relatively narrow range of historical surges for this station. The ratios are computed by dividing values of two exceedance probabilities of the datasets obtained from bootstrap replicates. The maximum value of the 95% confidence interval of the ratios for 0.89 m water level for Key West (A1FI scenario) is about 1000. Key West historical surge range (~ 0.8m) is similar to the projected sea level rise of 0.69 m for the A1FI scenario. This leads to a broader confidence interval when moving outside of the historically available range of water level observations.

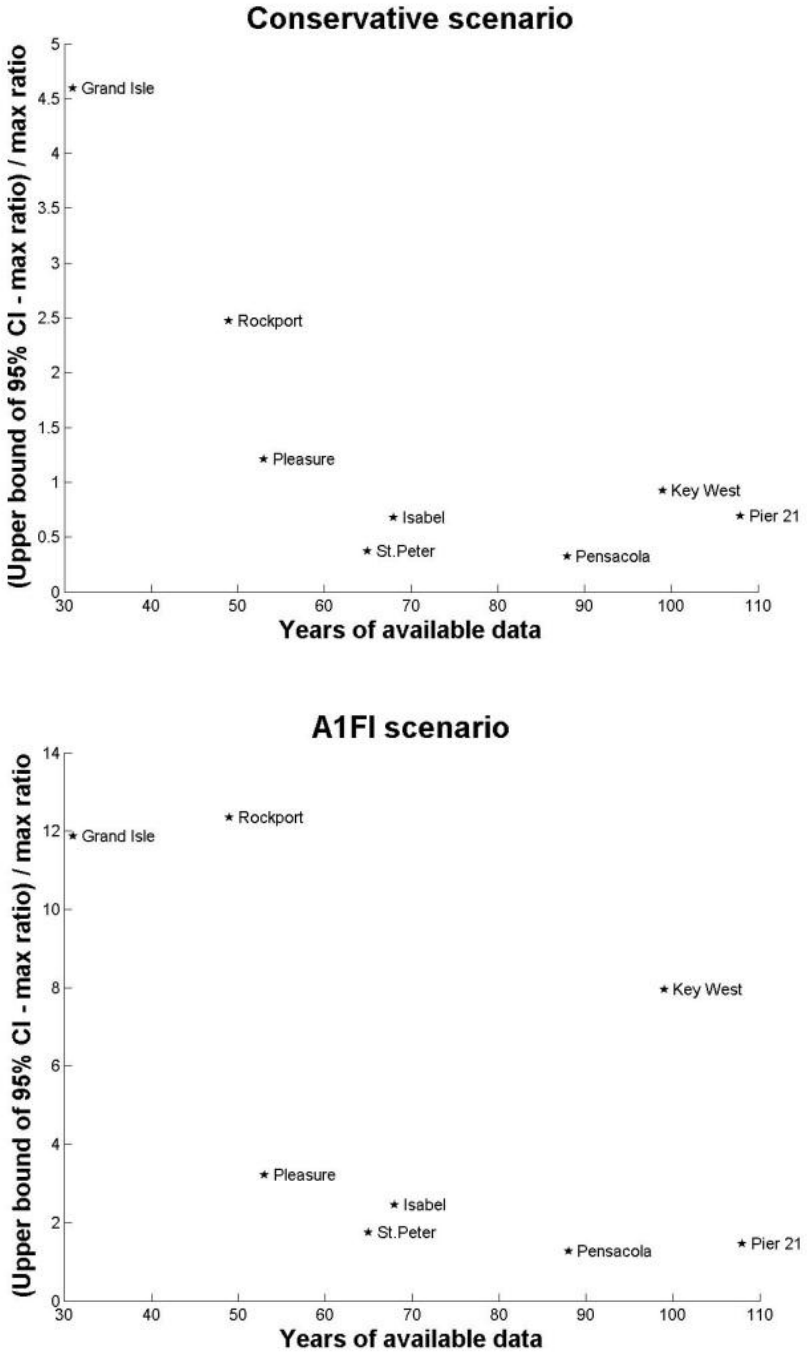

Figure 3.27. ***The relative difference between maximum ratios of the exceedance probabilities and upper bounds of the 90% and 95% confidence intervals vs. years of available data.***

Galveston Pier 21 and Galveston Pleasure Pier

The Galveston Pier 21 station is located on the north-east side of Galveston Island, Texas. Station Galveston Pier 21 is positioned on a ship channel about 4 km away from the main Galveston Ship Channel and the mouth of Galveston Bay and protected from open water waves. The Galveston Pleasure Pier station is located on the other side of Galveston Island and is not protected from Gulf of Mexico wave activity. The distance between the stations is only about 3 km. Although the data record for Galveston Pleasure Pier is only half as long for Galveston Pier 21 the results for quantifying the increase in exceedance probability are relatively similar. Maximum ratios for Galveston Pier 21 and Galveston Pleasure Pier are 6.46 and 5.36 respectively, and water levels at maximum ratios are 1.10 m and 1.26 m for the conservative scenario (Table 3.10). For the A1FI scenario the maximum ratios are 18 and 22, and water levels at maximum ratios are 1.49 m and 1.73 m. These relatively small differences can be explained by the separation of the stations by Galveston Island and their link through the ship channel. The consistency of the results is a further indication of the robustness of the method.

To further confirm that the study results are not overly affected by the lengths of the data sets beyond larger confidence intervals, ratios of exceedance probabilities were estimated based only on annual maximum surges for 1958-2011 years for Galveston Pier 21 station. Results for the conservative scenario are presented in Figure 3.14 and Table 3.10 with comparison with the results obtained for the full data set. The difference between results based on shorter and longer surge series is relatively small. Results for A1FI for 1958-2011 are 16.21 and 1.50 m, and for 1904-2011 results are 18.54 and 1.49

m with no significant difference in lower bounds of 90% and 95% confidence intervals. Furthermore, the results were computed for both stations while omitting the 2008 surge generated by Hurricane Ike. Results for the conservative scenario are presented in Figure 3.15.a, b and Table 3.10. It is noticeable that there is no significant difference between these results for both the maximum ratios and the water levels at maximum ratios.

	Max [m]	Min [m]	Range [m]	Mean [m]	Median [m]	Skewness	Shape parameter	Scale parameter	Location parameter	Maximum ratio	Water level at max ratio
Galveston Pier 21 (1904-2011)	2.85	0.40	2.45	0.79	0.68	2.71	0.34	0.17	0.61	6.46	1.10
Galveston Pier 21 No Ike	2.38	0.40	1.98	0.77	0.68	2.38	0.29	0.17	0.61	7.25	1.12
Galveston Pier 21 (1958-2011)	2.85	0.40	2.45	0.79	0.68	2.71	0.49	0.14	0.62	7.22	1.08
Galveston Pleasure Pier	2.84	0.45	2.39	0.93	0.78	2.43	0.30	0.21	0.72	5.36	1.26
Galveston Pleasure Pier No Ike	2.58	0.45	2.13	0.89	0.78	2.35	0.23	0.20	0.72	6.59	1.30

Table 3.10. ***Results for Galveston stations for conservative scenario based on various surge time series.***

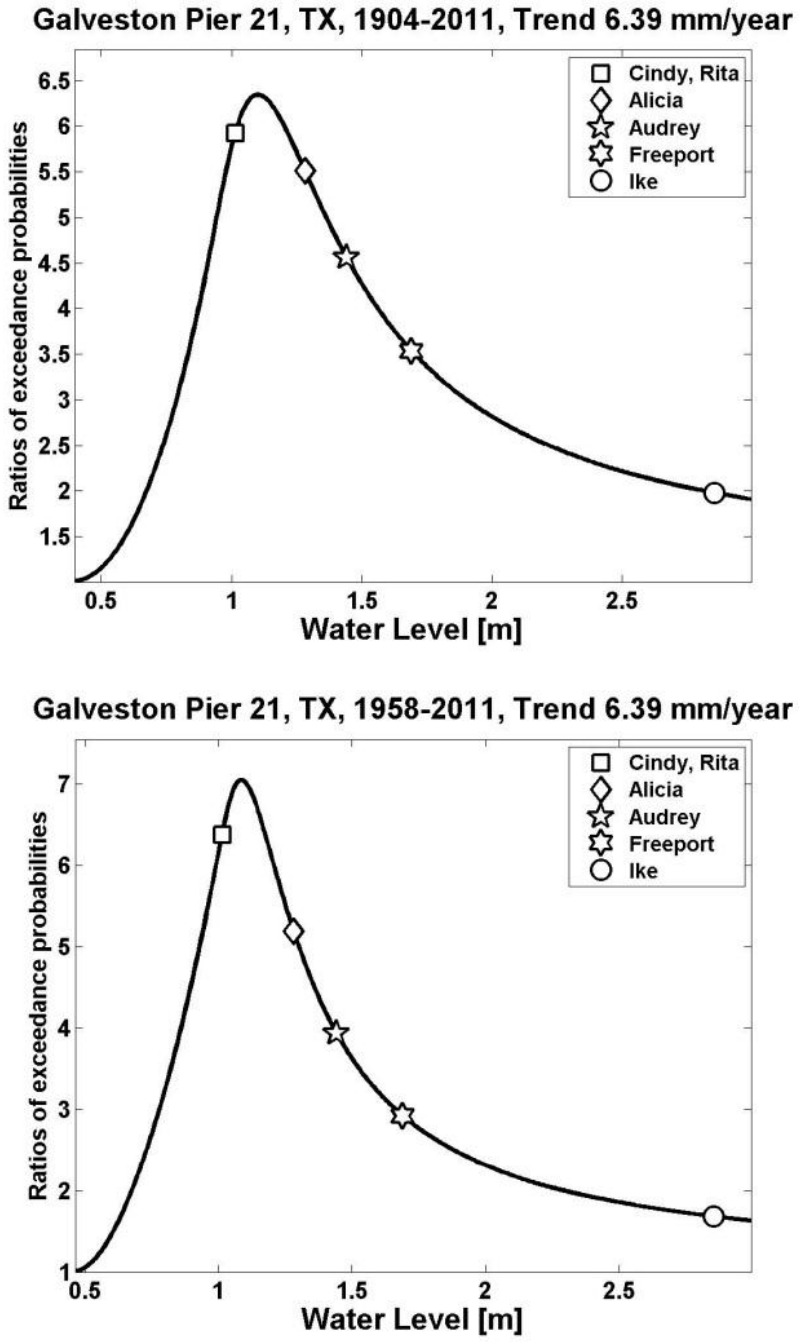

Figure 3.28. ***Ratios of exceedance probabilities for Galveston Pier 21 based on annual maximum surges for 1904-2011 years (on the top) and annual maximum surges for 1958-2011 years (on the bottom) for conservative scenario.***

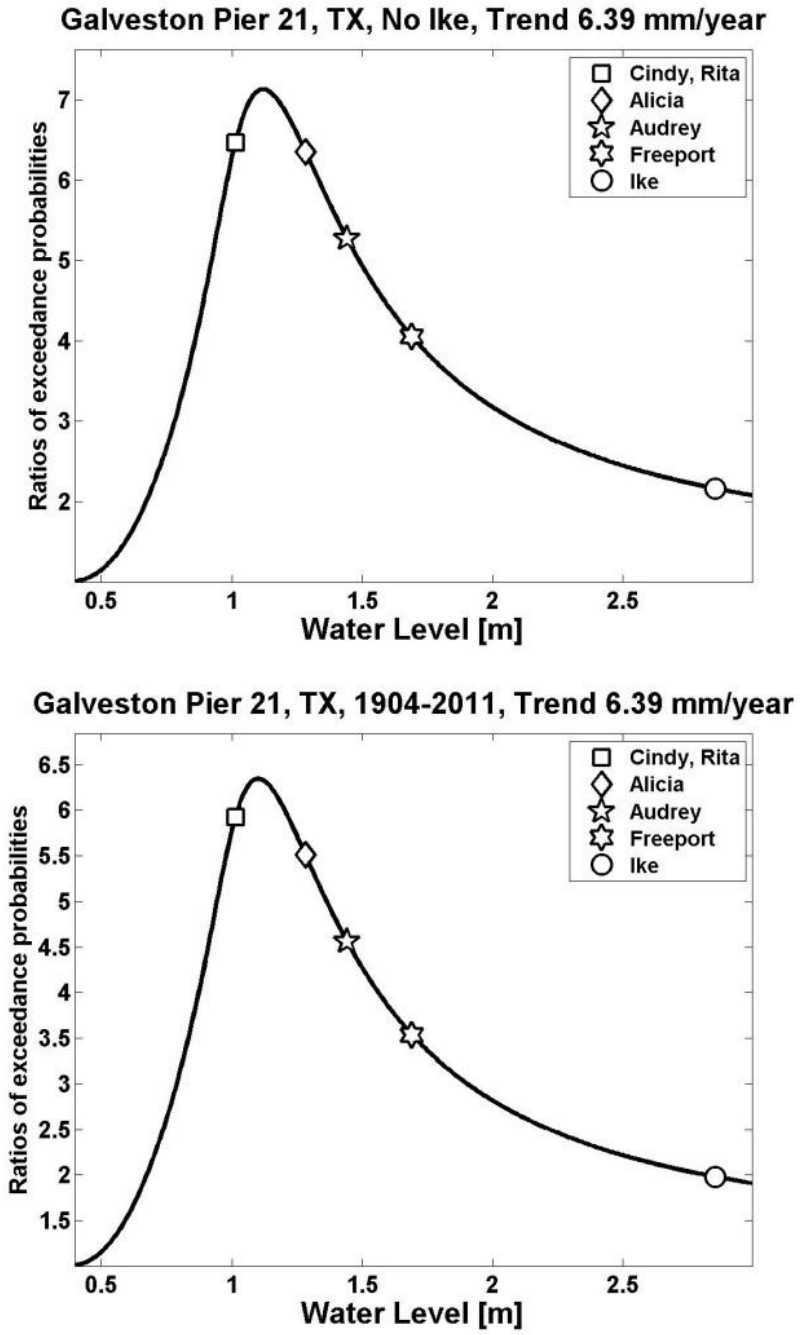

Figure 3.29.a. ***Ratios of exceedance probabilities for Galveston Pier 21 station based on annual maximum surges for all available data (on the top) and annual maximum surges except records during Hurricane Ike in 2008 (on the bottom) for conservative scenario.***

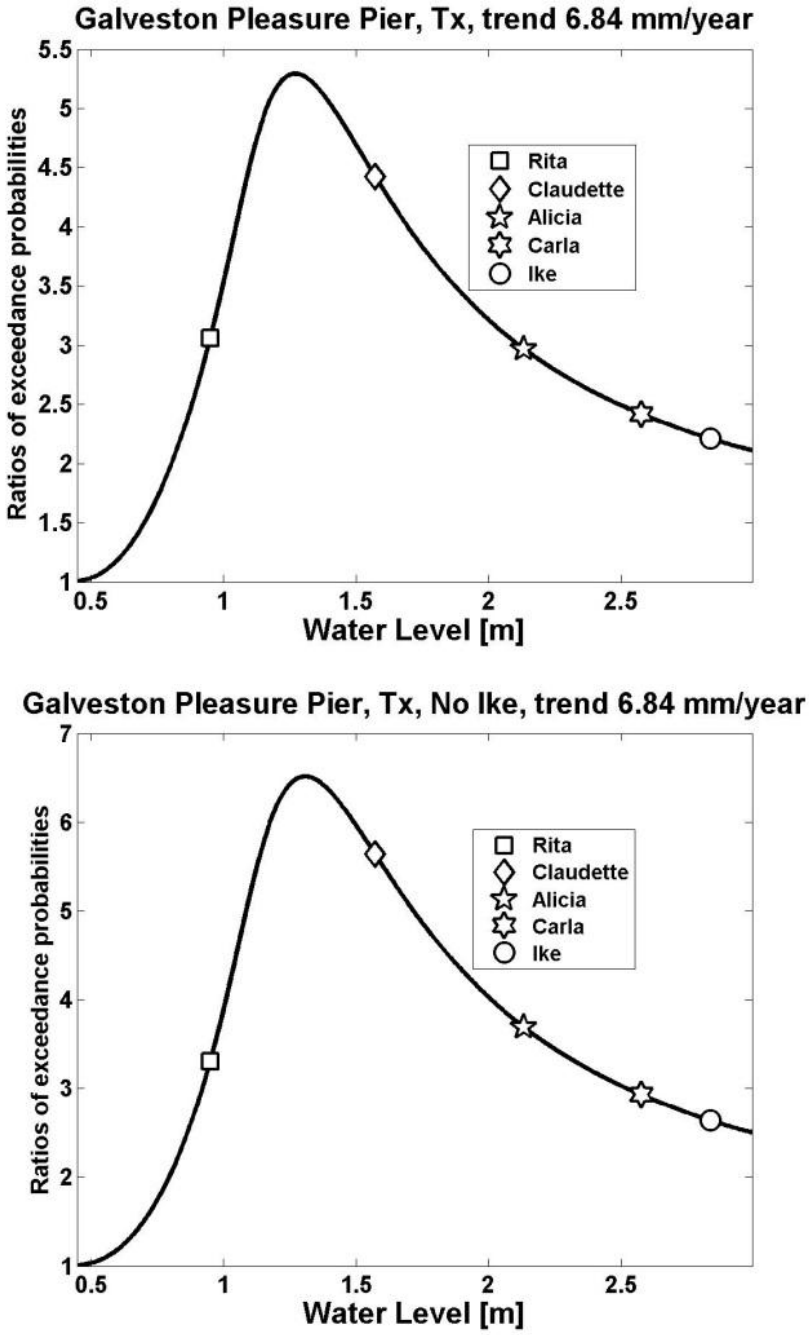

Figure 3.30.b. ***Ratios of exceedance probabilities for Galveston Pleasure Pier station based on annual maximum surges for all available data (on the top) and annual maximum surges except records during Hurricane Ike in 2008 (on the bottom) for conservative scenario.***

Water level at maximum ratio and water levels associated with hurricanes

To further analyze the impact of sea level rise on inundation frequencies it is helpful to consider the future impact of surges generated by historical storms. The projected changes in return periods for both scenarios are computed by year 2100 for a variety of storms that have impacted stations of the Gulf of Mexico. These hurricanes were selected because water levels associated with them have the higher predicted increases in the probability of inundation under both scenarios. The results are presented in Figure 3.16, Figure 3.17.a, b, c, d, and Table 3.11. Return periods directly based on observations are listed under year 2011 while results for 2100 are model based estimates. For the faster sea level rise scenario water levels associated with the majority of the hurricanes are predicted to take place every year by 2100. More frequent, smaller storm surges may have a larger impact on coastal communities than the effects of less frequent, larger storm surges. For example, at this point in time (2011) the probability of water levels associated with Hurricane Alex for Port Isabel station is very small (~6%), with a quadratic sea level rises by the year 2100 the probability of reaching the same level increases to 100%. The return period of an event of the magnitude of Hurricane Elena for St. Petersburg station is predicted to decrease to 1.7 years from presently 65 years for A1FI scenario.

								Return periods in years	
Station	State	Hurricane	Year	Month	Corresponding water level [m]	Corresponding surge [m]	in 2011	Conservative scenario by 2100	A1FI scenario by 2100
Port Isabel	Tx	Gilbert	1988	9	0.97	1.15	23	10.7	1.5
		Alex	2010	6	1.03	0.97	17	5.6	1.0
Rockport	Tx	Beulah	1967	9	0.99	1.10	25	7.5	1.0
		Allen	1980	8	1.26	1.37	49	22.0	3.2
Galveston Pier 21	Tx	Audrey	1957	6	1.37	1.44	15	4.0	1.0
		Alicia	1983	8	1.36	1.28	10	2.3	1.0
Galveston Pleasure Pier	Tx	Alicia	1983	8	2.37	2.13	18	12.7	4.5
		Claudette	2003	7	1.93	1.57	11	3.2	1.1
Grand Isle	La	Andrew	1992	8	0.81	1.06	8	1.0	1.0
		Katrina	2005	9	1.54	1.27	16	1.3	1.0
		Ike	2008	8	1.43	1.31	31	1.5	1.0
Pensacola	Fl	Georges	1998	9	1.26	1.14	13	11.0	1.8
		Ike	2010	9	0.87	0.98	9	6.5	1.0
St.Petersburg	Fl	Elena	1985	8, 9	1.32	1.27	65	14.3	1.7
Key West	Fl	Wilma	2005	10	1.18	0.84	50	44.2	1.1

Table 3.11. ***Projected return periods for inundation levels that have been generated by a range of historical storms for the study stations for both sea level rise scenarios.***

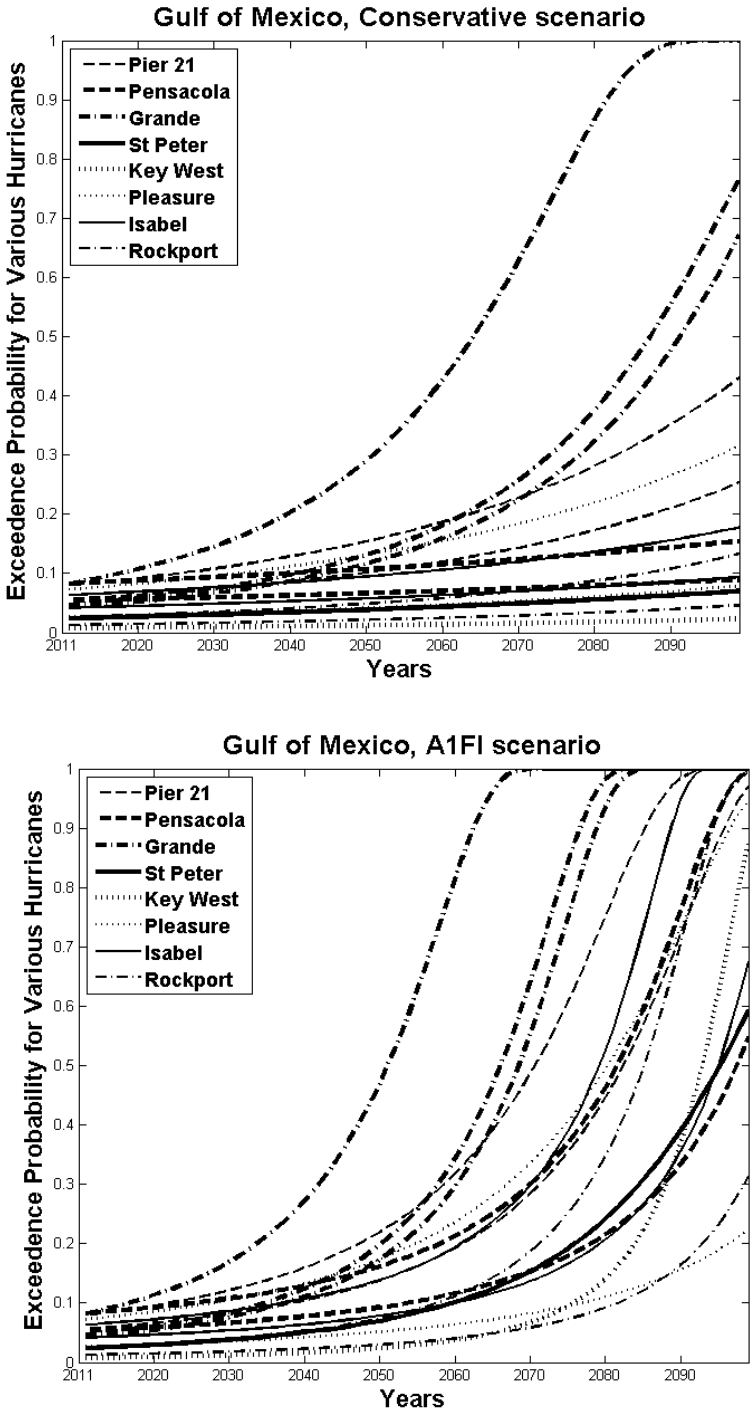

Figure 3.31. ***Exceedance probabilities in 2100 versus the present exceedance probabilities in 2011 for the conservative scenario (on the top) and A1FI scenario (on the bottom) for study stations.***

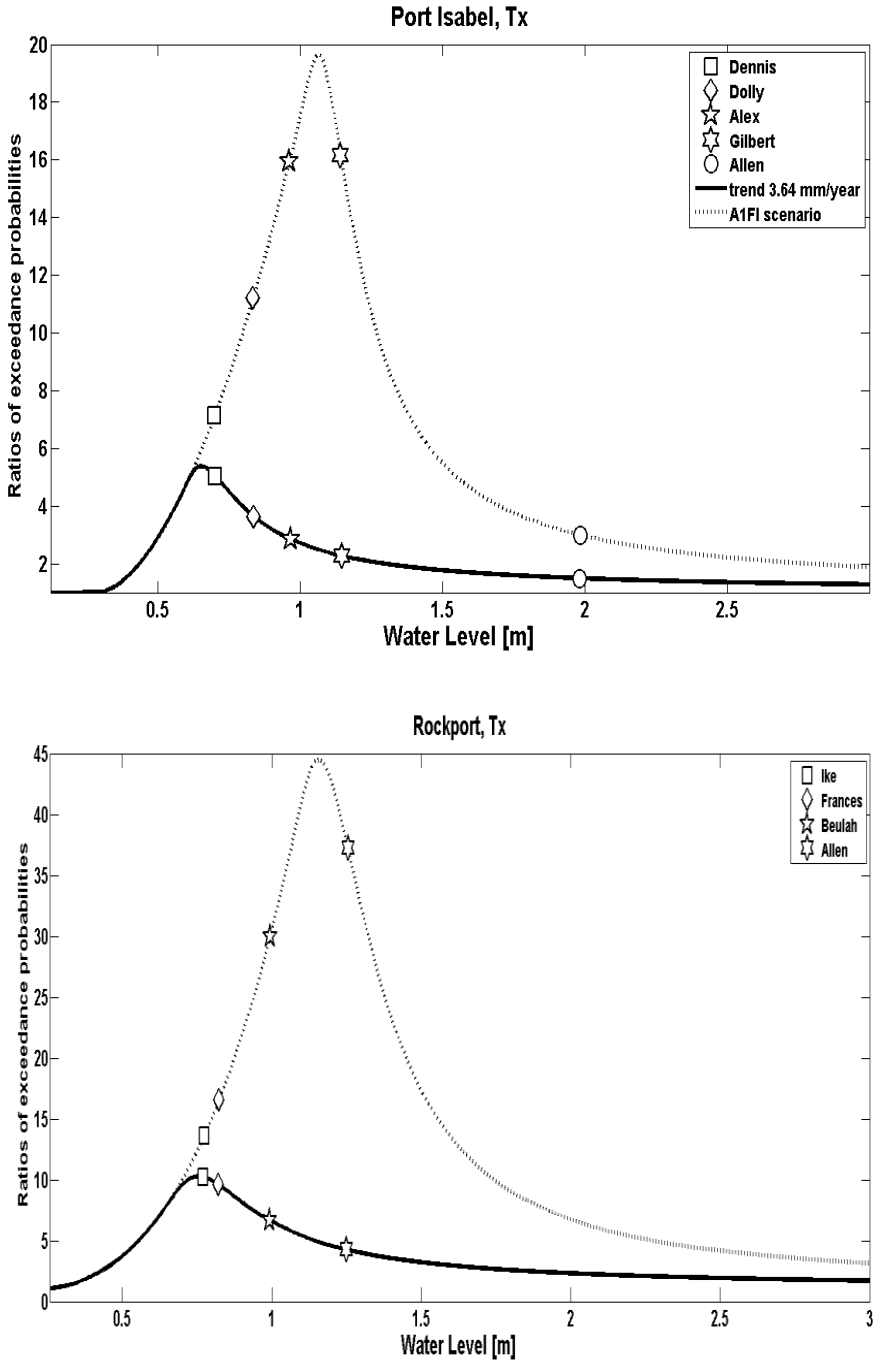

Figure 3.32.a. ***Ratios of water levels exceedance probabilities in 2100 vs. the exceedance probabilities in 2011 for the conservative and A1FI scenarios of sea level rise for Port Isabel and Rockport stations.***

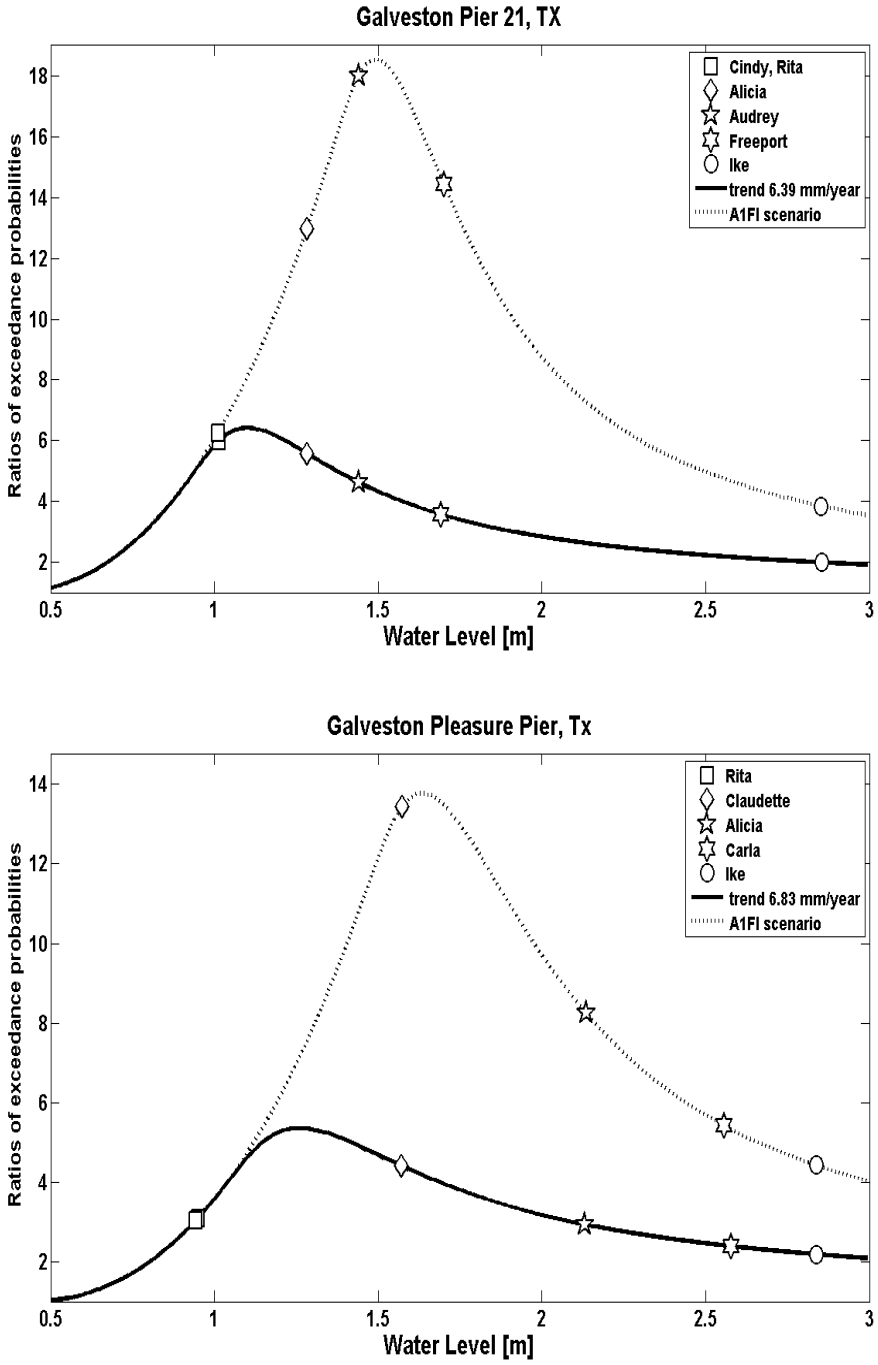

Figure 3.33.b. ***Ratios of water levels exceedance probabilities in 2100 vs. the exceedance probabilities in 2011 for the conservative and A1FI scenarios of sea level rise for Galveston Pier 21 and Galveston Pleasure Pier stations.***

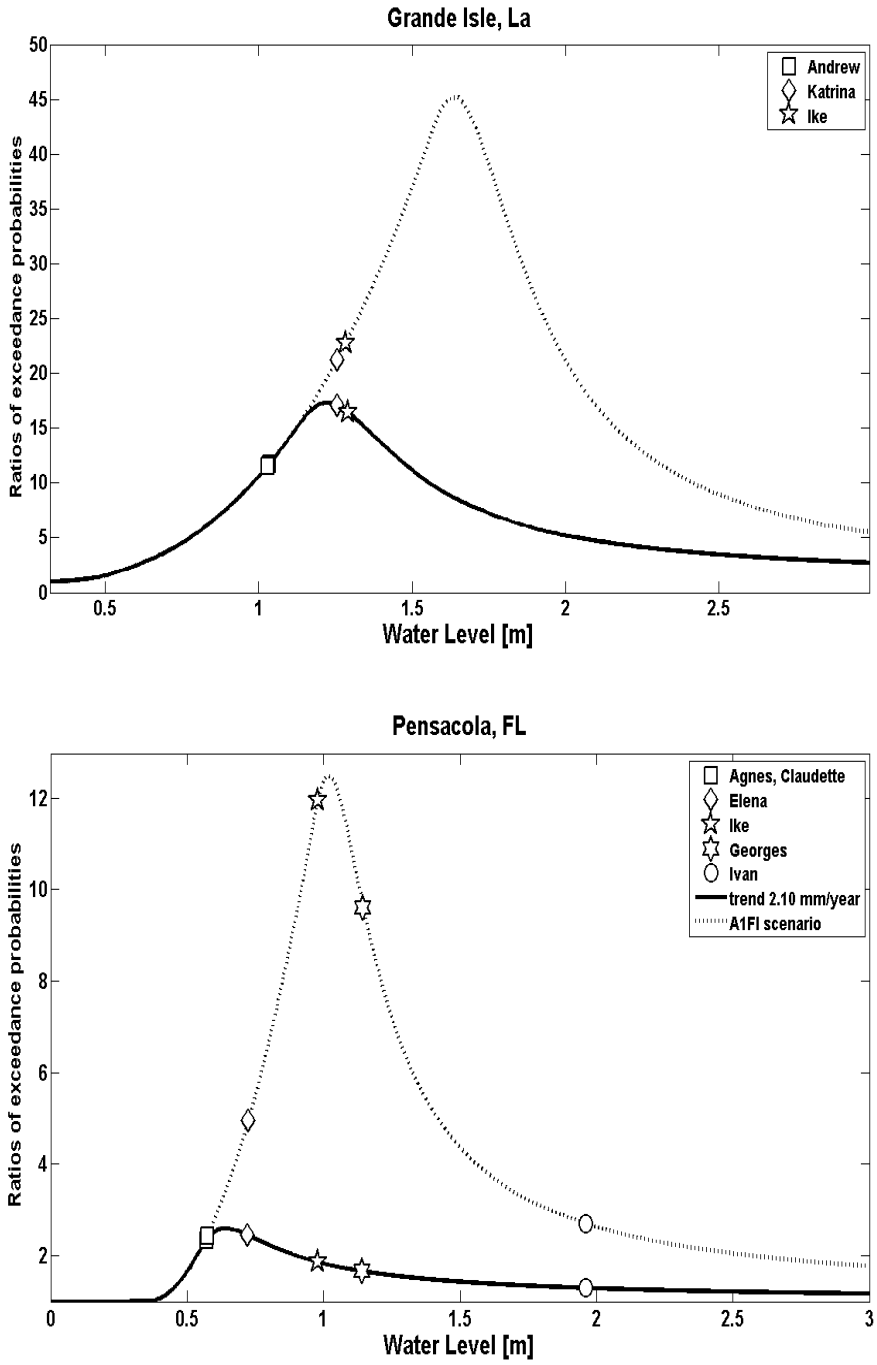

Figure 3.34.c. ***Ratios of water levels exceedance probabilities in 2100 vs. the exceedance probabilities in 2011 for the conservative and A1FI scenarios of sea level rise for Grande Isle and Pensacola stations.***

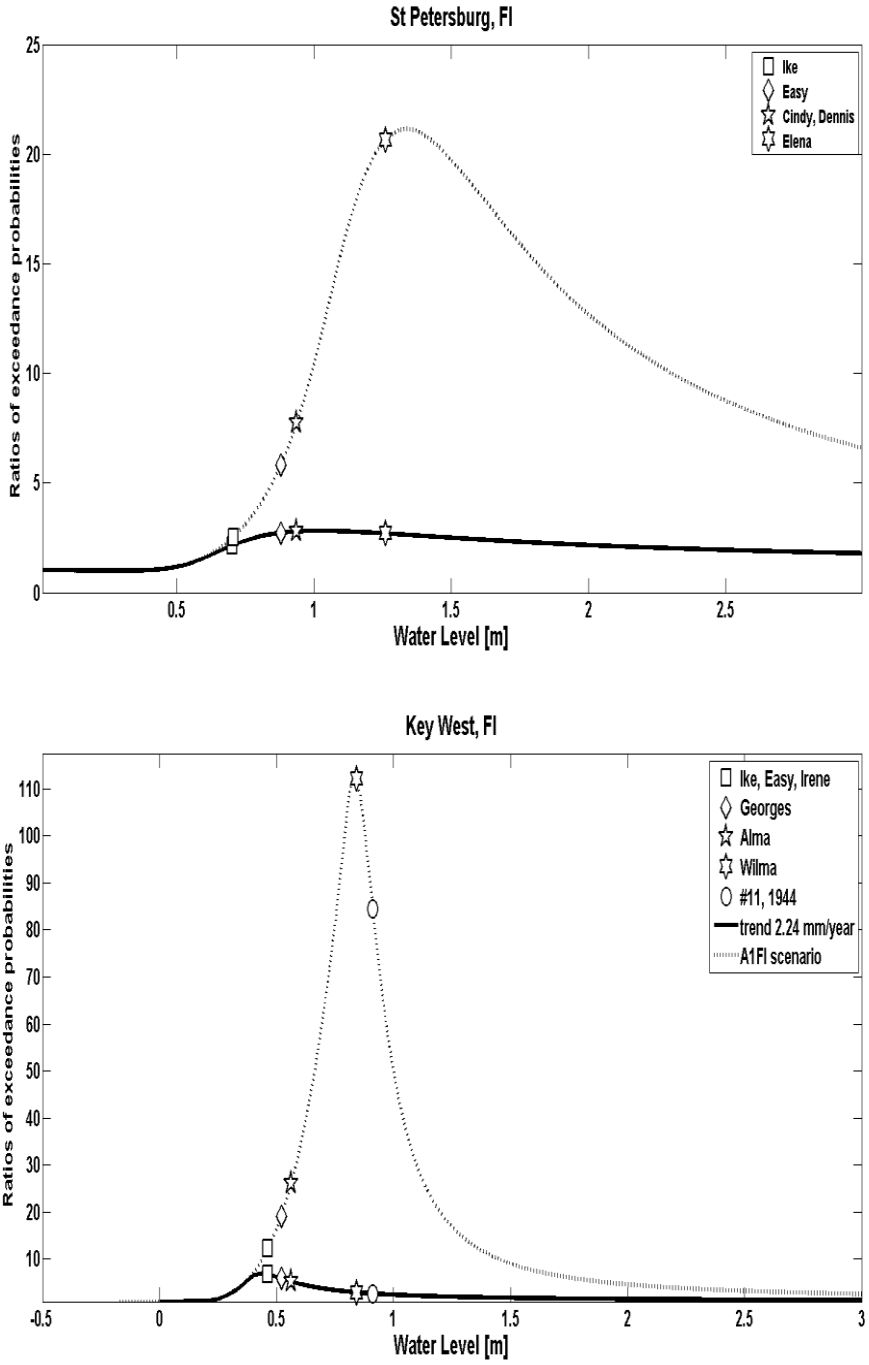

Figure 3.35.d. ***Ratios of water levels exceedance probabilities in 2100 vs. the exceedance probabilities in 2011 for the conservative and A1FI scenarios of sea level rise for St. Petersburg and Key West stations.***

CONCLUSION

This study examined the impact of sea-level rise on future inundation frequencies for eight stations of the Gulf of Mexico and estimated associated 90% and 95% confidence intervals. Results are expressed as the ratio of water level exceedance probability between years 2100 and 2011. To estimate uncertainty in predictions of the likelihood of future inundations by 2100 a nonparametric bootstrap technique was used and combined with two sea level rise scenarios (a conservative continued linear sea level rise and a scenario based on the upper end of the IPCC AR4 A1FI estimates).

While as expected increases in inundation frequencies are substantial for all stations results show considerable differences depending on the sizes of the surges, the station locations and the sea level rise scenarios. The frequency of annual maximum water levels resulting from small storms/surges will increase considerably more, typically by a factor of 3 or more, than the frequency of water levels resulting from large hurricanes. As a result more frequent, smaller storm surges may have a larger impact on coastal communities than the effects of the less frequent, larger storm surges. For the conservative sea level rise scenario the study's highest increase in water level exceedance probability of 17 times is computed for a water level of 1.23m above present mean sea level for Grande Isle, Louisiana. For the study's A1FI based sea level rise scenario, locations with low rates of vertical land motion combined with narrow surge ranges have the largest ratios of exceedance probabilities and become the most vulnerable to sea level rise. For the Key West, Florida, station the predicted increase in water level exceedance probability is over 100 times for a water level of 0.83m above present mean sea level.

For most cases the confidence intervals show a substantial decrease in width for stations with lengths of datasets of 50 years or longer indicating a preferred data length of 50 or more years provided that a large surge event is included. The lower bounds of the confidence intervals of the ratios imply significant increases of the risk of flooding by the end of the century for all stations and both scenarios.

Ratios of exceedance probabilities depend mainly on sea level trends and the shape of the curves of the exceedance probabilities. The relative importance of these parameters depends on the sea level rise scenario: the maximum ratios are strongly correlated to sea level trends for the conservative scenario (correlation coefficient 0.77), but for higher rates of global sea level rise local subsidence becomes less important and the range of maximum annual surges becomes the main factor (correlation coefficient between maximum ratios and ranges of surges -0.66). Water levels at maximum ratios have strong correlation with all statistics except the maximum annual surges, which indicates that the results of this study are not overly sensitive to the most extreme values or largest surge on the record provided that the record includes at least one large surge. The sensitivity of the results to the lengths of the data sets and the presence or absence of the largest storm was further investigated for the stations of Galveston Pleasure Pier and Galveston Pier 21 and the passage of 2008 Hurricane Ike. The results show that the predicted increases in exceedance probabilities for the different alternate scenarios are relatively small and do not affect guidance based on the study results.

This research identifies an important subject: the impact of sea level rise on storm surges in low-lying coastal zones. The approach of this study brings together studies that have focused on distributions of storm surges with sea level rise and studies that

evaluated the exceedance probabilities of flood at a single point over time, and takes into account differences in oceanographic setting at the study sites. The combination of sea level rise and population growth in coastal regions makes it essential to continue improving flood management strategies. Flooding estimates must take into account both local vertical land motion and estimated rates of sea level rise linked to global climate change. As sea level increase flood events will threaten more lives, damage higher number of public and private properties. Public demand for seawalls, bulkheads, beaches nourishments and other shoreline maintenance will increase in order to protect coastal communities. A rising sea level in combination with increasing population will not only increase losses, but also increase the number of policies and thus premium income available to pay losses. The required investments to protect such areas will be very large, and as sea levels rise, available resources will likely not be sufficient to protect all areas. The results of this research provide coastal decision makers quantitative estimates of future inundation risks for two sea level rise scenarios and a calibrated method to compute such risks for more sea level rise scenarios. This research is relevant for engineers, planners, insurance executives, and others to take into account the increasing impacts of storm surges of various sizes as sea level rises. The results will help develop better insurance rates, plan structures, land-use zoning, and others as the century progresses. The models, methodology and estimates developed as part of this research may be used to estimate the time before specific locations may become economically uninhabitable due to surge inflicted damages as sea level rises. Particularly, it is expected that this work will allow better to quantify coastal vulnerability to sea level rise along the Gulf of Mexico.

ACKNOWLEDGMENTS:

The authors would like to thank Chris Zervas (NOAA National Ocean Service, Silver Spring, MD) for his help with the data set and other discussions.

REFERENCES

Ahmad, M.I., Sinclair, C.D., Werritty, A., 1988. Log-logistic flood frequency analysis. Journal of Hydrology 98 (3-4), 205-224.

Bates, B.C., Kundzewicz, Z.W., Wu, S., Palutikof, J.P., 2008. Climate Change and Water.Technical Paper of the Intergovernmental Panel on Climate Change, IPCC Secretariat,Geneva.

Beirlant, J., Goegebeur, Y., Teugels, J., Segers, J., 2005. Statistics of Extremes: Theory and Applications. John Wiley & Sons, Ltd.

Bender, M.A., Knutson, T.R., Tuleya, R.E., Sirutis, J.J., Vecchi, G.A., Garner, S.T., Held, I.M., 2010. Modeled Impact of Anthropogenic Warming on the Frequency of Intense Atlantic Hurricanes. Science 327 (5964), 454-458.

Bindoff, N.L., Willebrand, J., Artale, V., A, C., Gregory, J., Gulev, S., Hanawa, K., Quéré, C.L., Levitus, S., Nojiri, Y., Shum, C.K., Talley, L.D., Unnikrishnan, A., 2007. Observations: Oceanic Climate Change and Sea Level. In: Climate Change 2007: The Physical Science Basis. Contribution of Working Group I to the Fourth Assessment Report of the Intergovernmental Panel on Climate Change [Solomon, S., D. Qin, M. Manning, Z. Chen, M. Marquis, K.B. Averyt, M. Tignor and H.L. Miller (eds.)].Cambridge University Press, Cambridge, United Kingdom and New York, NY, USA.

CCSP, 2009. Coastal Sensitivity to Sea-Level Rise: A Focus on the Mid-Atlantic Region., A report by the U.S. Climate Change Science Program and the Subcommittee on Global Change Research. [James G. Titus (Coordinating Lead Author), K. Eric Anderson, Donald R. Cahoon, Dean B. Gesch, Stephen K. Gill, Benjamin T. Gutierrez, E. Robert Thieler, and S. Jeffress Williams (Lead Authors)]. Washington D.C., USA.

Davis, R.A., 2011. Sea-level change in the Gulf of Mexico. Texas A & M University Press, College Station.

Davison, A.C., Hinkley, D.V., 1997. Bootstrap Methods and Their Application. Cambridge: Cambridge University Press.

Domingues, C.M., Church, J.A., White, N.J., Gleckler, P.J., Wijffels, S.E., Barker, P.M., Dunn, J.R., 2008. Improved estimates of upper-ocean warming and multi-decadal sea-level rise. Nature 453 (7198), 1090-1093.

EasyFit, 2004-2010. Professional Software, 5.3 ed. MathWave Technologies.

Edwards, R., 2007. Sea levels: resolution and uncertainty. Progress in Physical Geography 31 (6), 621-632.

Efron, B., 1979. Bootstrap Methods: Another Look at the Jackknife. The Annals of Statistics 7 (1), 1-26.

Efron, B., Tibshirani, R.J., 1993. An introduction to the bootstrap. Chapman and Hall.

FEMA, 2007. Federal Emergency Management Agency of the United States, Atlantic Ocean and Gulf of Mexico Coastal Guidelines Update. http://www.fema.gov/library/viewRecord.do?id=2458 (cited February, 2013).

Fitzpatrick, P.J., Tran, N., Li, Y., Lau, Y., Hill, C.M., 2009. A Proposed New Storm Surge Scale. NOAA, Northern Gulf Institute.

Frazier, T.G., Wood, N., Yarnal, B., Bauer, D.H., 2010. Influence of potential sea level rise on societal vulnerability to hurricane storm-surge hazards, Sarasota County, Florida. Applied Geography 30 (4), 490-505.

Frey, A.E., Olivera, F., Irish, J.L., Dunkin, L.M., Kaihatu, J.M., Ferreira, C.M., Edge, B.L., 2010. Potential Impact of Climate Change on Hurricane Flooding Inundation, Population Affected and Property Damages in Corpus Christi1. JAWRA Journal of the American Water Resources Association 46 (5), 1049-1059.

Gregory, J.M., 2008. Sea level rise: what makes prediction so difficult? . Planet Earth, Spring 2008, pp.24-27.

Hansen, J.E., 2007. Scientific reticence and sea level rise. Environ. Res. Lett. 2 (024002), 6 pp.

Hicks, S., 2006. Understanding Tides. U.S. DEPARTMENT OF COMMERCE, NOAA, National Ocean Service.

Huang, W., Xu, S., Nnaji, S., 2008. Evaluation of GEV model for frequency analysis of annual maximum water levels in the coast of United States. Ocean Engineering 35 (11-12), 1132-1147.

IPCC, 2007. Summary for Policymakers. In: Climate Change 2007: The Physical Science Basis. Contribution of Working Group I to the Fourth Assessment Report of the Intergovernmental Panel on Climate Change [Solomon, S., D. Qin, M. Manning, Z. Chen, M. Marquis, K.B. Averyt, M.Tignor and H.L. Miller (eds.)]. Cambridge University Press, Cambridge, United Kingdom and New York, NY, USA.

Irish, J.L., Resio, D.T., 2010. A hydrodynamics-based surge scale for hurricanes. Ocean Engineering 37 (1), 69-81.

Irish, J.L., Resio, D.T., Ratcliff, J.J., 2008. The Influence of Storm Size on Hurricane Surge. Journal of Physical Oceanography 38 (9), 2003-2013.

Kleiber, C., Kotz, S., 2003. Statistical Size Distributions in Economics and Actuarial Sciences. Wiley and Sons.

Kotz, S., Nadarajah, S., 2000. Extreme Value Distributions: Theory and Applications. Imperial College Press, London.

Kyselý, J., 2008. A Cautionary Note on the Use of Nonparametric Bootstrap for Estimating Uncertainties in Extreme-Value Models. Journal of Applied Meteorology and Climatology 47 (12), 3236-3251.

Landsea, C., 2007. Counting Atlantic tropical cyclones back to 1900. Eos Trans. AGU 88 (18).

Letetrel, C., Marcos, M., Martín Míguez, B., Woppelmann, G., 2010. Sea level extremes in Marseille (NW Mediterranean) during 1885–2008. Continental Shelf Research 30 (12), 1267-1274.

Levinson, D.H., Vickery, P.J., Resio, D.T., 2010. A review of the climatological characteristics of landfalling Gulf hurricanes for wind, wave, and surge hazard estimation. Ocean Engineering 37 (1), 13-25.

MatLab®, 2009a. The MathWorks, Natick, MA.

Meehl, G.A., Stocker, T.F., Collins, W.D., Friedlingstein, P., Gaye, A.T., Gregory, J.M., Kitoh, A., Knutti, R., Murphy, J.M., Noda, A., Raper, S.C.B., Watterson, I.G., Weaver, A.J., Zhao, Z.-C., 2007. Global climate projections. In Climate change 2007: The physical science basis. Contribution of Working Group I to the Fourth Assessment Report of the Intergovernmental Panel on Climate Change.[Solomon, S., D. Qin, M. Manning, Z. Chen, M. Marquis, K.B. Averyt, M. Tignor and H.L. Miller (eds.)]. Cambridge University Press, Cambridge, United Kingdom and New York, NY, USA.

Nadarajah, S., Shiau, J., 2005. Analysis of Extreme Flood Events for the Pachang River, Taiwan. Water Resources Management 19 (4), 363-374.

Needham, H.F., Keim, B.D., 2011. A storm surge database for the US Gulf Coast. International Journal of Climatology, n/a-n/a.

NFIP, 2013. National Flood Insurance Program, Loss Statistics from Jan 1, 1978 through report as of 11/30/2012. http://bsa.nfipstat.fema.gov/reports/1040.htm (cited February, 2013).

NOAA, 2011a. National Oceanic and Atmospheric Administration, Tides and Currents, Galveston Pier 21, TX. http://www.co-ops.nos.noaa.gov/geo.shtml?location=8771450 (cited October 2011).

NOAA, 2011b. National Oceanic and Atmospheric Administration, Galveston Pier 21, Datums. http://tidesandcurrents.noaa.gov/data_menu.shtml?unit=0&format=Apply+Change&stn=8771450+Galveston+Pier+21%2C+TX&type=Datums (cited October 2011).

NOAA, 2011c. National Oceanic and Atmospheric Administration, Mean Sea Level Trend. http://tidesandcurrents.noaa.gov/sltrends/sltrends_station.shtml?stnid=8771450+Galveston+Pier+21,+TX (cited October 2011).

NOAA, 2011d. National Oceanic and Atmospheric Administration, Tidal Bench Marks. http://www.co-ops.nos.noaa.gov/station_retrieve.shtml?type=Bench+Mark+Data+Sheets (cited October 2011).

NOAA, 2013a. National Oceanic and Atmospheric Administration, Storm Surge. http://www.nhc.noaa.gov/ssurge/ssurge_overview.shtml (cited February, 2013).

NOAA, 2013b. National Oceanic and Atmospheric Administration, Storm Surge. http://www.nhc.noaa.gov/climo/#hrhm (cited February, 2013).

NOAA, 2013c. National Oceanic and Atmospheric Administration, Tides and Currents. http://tidesandcurrents.noaa.gov/station_retrieve.shtml?type=Historic (cited February 2013).

NOAA, 2013d. National Oceanic and Atmospheric Administration, Mean Sea Level Trend. http://tidesandcurrents.noaa.gov/sltrends/sltrends_states.shtml?region=fl (cited February, 2013).

NOAA, 2013e. National Oceanic and Atmospheric Administration, Tidal Bench Marks. http://www.co-ops.nos.noaa.gov/station_retrieve.shtml?type=Bench+Mark+Data+Sheets (cited February, 2013).

ÖnÖz, B., Bayazit, M., 1995. Best-fit distributions of largest available flood samples. Journal of Hydrology 167 (1-4), 195-208.

Park, J., Obeysekera, J., Irizarry, M., Barnes, J., Trimble, P., Park-Said, W., 2011. Storm surge projections and implications for water management in South Florida. Climatic Change, 109-128.

Parris, A., Bromirski, P., Burkett, V., Cayan, D., Culver, M., Hall, J., Horton, R., Knuuti, K., Moss, R., Obeysekera, J., Sallenger, A., Weiss, J., 2012. Global Sea Level Rise Scenarios for the US National Climate Assessment. NOAA Tech Memo OAR CPO-1. 37 pp. .

Pugh, D., 2004. Changing Sea Levels: effects of tides, weather and climate. Cambridge University Press.

Purvis, M.J., Bates, P.D., Hayes, C.M., 2008. A probabilistic methodology to estimate future coastal flood risk due to sea level rise. Coastal Engineering 55 (12), 1062-1073.

Ramsey, R., 2011. Lawmakers Approve Texas Windstorm Insurance Fix, The Texas Tribune. http://www.texastribune.org/texas-legislature/82nd-legislative-session/lawmakers-approve-texas-windstorm-insurance-fix/

Rao, A.R., Hamed, K.H., 2000. Flood Frequency Analysis. CRC Press, Inc.

Rego, J.L., Li, C., 2009. On the importance of the forward speed of hurricanes in storm surge forecasting: A numerical study. Geophys. Res. Lett. 36 (7), L07609.

Reiss, R.D., Thomas, M., 2007. Statistical Analysis of Extreme Values with Applications to Insurance, Finance, Hydrology and Other Fields, 3 ed. Birkhäuser-Verlag, Basel-Boston-Berlin.

Report, 2008. Hurricane Ike Impact Report. Foreword by Jack Colley, Chief, Texas Governor's Office of Homeland Security, Division of Emergency Management.

Shum, C.K., Kuo, C.-y., Guo, J.-y., 2008. Role of Antarctic ice mass balance in present-day sea-level change. Polar Science 2 (2), 149-161.

Sinclair, C.D., Spurr, B.D., Ahmad, M.I., 1990. Modified anderson darling test. Communications in Statistics - Theory and Methods 19 (10), 3677-3686.

Tebaldi, C., Strauss, B.H., Zervas, C.E., 2012. Modelling sea level rise impacts on storm surges along US coasts. Environmental Research Letters 7 (1), 14032-14042.

Teugels, J., Sundt, B., 2004. Encyclopedia of Actuarial Science. Wiley and Sons.

Turner, R., 1991. Tide gauge records, water level rise, and subsidence in the Northern Gulf of Mexico. Estuaries and Coasts 14 (2), 139-147.

Vermeer, M., Rahmstorf, S., 2009. Global sea level linked to global temperature. Proceedings of the National Academy of Sciences vol.106, 21527-21532.

Warner, N.N., Sterba-Boatwright, B., Tissot, P., Jeffress, G., 2012a. Estimated Increase in Inundation Probability with Confidence Intervals for Pensacola, Florida and Key West, Florida, Oceans, 2012, pp. 1-10.

Warner, N.N., Sterba-Boatwright, B., Tissot, P.E., Jeffress, G., 2012b. Estimated Increase in Inundation Probability with Confidence Intervals for Galveston, Texas, in: Spaulding, M.L. (Ed.), Estuarine and Coastal Modeling. American Society of Civil Engineers, pp. 528-541.

Warner, N.N., Tissot, P.E., 2012. Storm flooding sensitivity to sea level rise for Galveston Bay, Texas. Ocean Engineering 44 (0), 23-32.

Weaver, R.J., Slinn, D.N., 2010. Influence of bathymetric fluctuations on coastal storm surge. Coastal Engineering, 62-70.